The expression and function of human Anterior Gradient Homolog 3 in Prostate Cancer

Zur Erlangung des akademischen Grades eines

DOKTORS DER NATURWISSENSCHAFTEN

(Dr. rer. nat.)

der Fakultät für Chemie und Biowissenschaften
des Karlsruher Instituts für Technologie (KIT) – Universitätsbereich

genehmigte

DISSERTATION

von

Erald Shehu

aus Fier, Albanien

2013

Dekan: Prof. Dr. Peter Roesky
Referent: Prof. Dr. Andrew Cato
Koreferent: Prof. Dr. Jörg Kämper
Tag der mündlichen Prüfung: 20.12.2013

Ich erkläre, dass ich diese Dissertation selbständing angefertig habe. Ich habe nur die angegebenen Quellen und Hilfsmittel benutzt und wörtlich oder inhaltlich übernommene Stellen als solche gekennzeichnet.

I hereby declare that this dissertation is my own independent work. I have only used the given sources and materials and I have cited others' work appropriately.

Erald Shehu

Karlsruhe

06.11.2013

ZUSAMMENFASSUNG

Prostatakrebs ist weltweit eine der der am häufigsten zum Tode führenden Krebsarten bei Männern. Die hohe Mortalitätsrate ist das Resultat von Patienten mit aggressiven (z. B. schnell fortschreitend) Tumoren, die ein hohes Risiko der Metastasenbildung besitzen. Um die Sterberate zu reduzieren, haben sich Wissenschaftler darauf fokussiert die molekularen Mechanismen zu identifizieren und charakterisieren, die mit den Prozessen assoziiert sind, die die Progression von Prostatakrebs ermöglichen. Einer der Faktoren, die mit dem Fortschreiten der Krankheit in Verbindung stehen ist Anterior Gradient Homolog 3 (AGR3), ein Mitglied der Familie der Proteindisulfidisomerasen, die in die Proteinfaltung involviert sind. Die Funktion von AGR3 in der Tumorprogression ist bislang jedoch unbekannt und wurde daher in dieser Arbeit untersucht.

Analysen der AGR3 Expression in Prostatakrebspatienten zeigte eine hohe Expression in Proben mit einem Gleason Score von 8-10, was darauf hinweist, dass AGR3 mit der aggressiven Krankheit in Verbindung steht. Knockdown Experimente in Prostatakrebszelllinien unter Verwendung von shRNA Lentivirenkonstrukten oder die Überexpression unter Verwendung eines induzierbaren Überexpressionsystems zeigten, dass AGR3 einen positiven Einfluss auf die Zellproliferation hat. Darüber hinaus konnte gezeigt werden, dass AGR3 die Migration und Adhäsion von Prostatakrebszellen erhöht. Die Analyse von Daten aus genome-wide Genexpressionsanalysen, in denen Kontroll und AGR3-knockdown VCaP Prostatakrebszellen verglichen wurden, ergaben eine Hochregulation verschiedener Gene, die in extrazelluläre Matrix-Prozesse involviert sind, eingeschlossen Lumican, ein sekretorisches Leucin-reiches Glycoprotein, welches die Zellmigration hemmt. Anschließende knochdown-Studien zeigten, dass AGR3 seinen positiven Einfluss auf die VCaP Zellmigration zumindest teilweise durch die Suppression der Lumican-Expression ausübt. Zusätzlich zu diesen Prozessen könnte AGR3 eine wichtige Rolle während physiologischem Stress spielen, welchem Krebszellen in der Tumormikroumgebung gewöhnlich ausgesetzt sind. Das AGR3 Protein ist im Endoplasmatischen Retikulum von Prostatakrebszellen lokalisiert und ist während Endoplasmatischem

Retikulum-Stress hochreguliert. Die AGR3 Expression korrelierte positiv mit der erhöhten Expression des pro-survival Chaperons GRP78 im Endoplasmatischen Retikulum sowie einer erhöhten Zellviabilität.
Zusammengefasst identifizierten diese Ergebnisse AGR3 als ein Protein, welches die Prostatakrebsprogression durch eine Verstärkung von Wachstum, Viabilität und Migration von Tumorzellen positiv reguliert.

ABSTRACT

Prostate cancer is one of the leading causes of cancer-related death in males worldwide. The majority of mortality is incurred by patients with aggressive (i.e. rapidly progressing) tumors that carry a great risk of metastasis. To reduce mortality, research has focused on finding and characterizing the molecular events associated with processes that enable prostate cancer progression. One of the targets associated with the progression of the disease is Anterior Gradient homolog 3 (AGR3), a member of the protein disulfide isomerase family that is involved in protein folding. However the function of AGR3 in the tumor progression is not known and is therefore the object of the present study.

Analysis of AGR3 expression in prostate cancer patients revealed high levels of expression in samples with a Gleason score of 8-10, suggesting an association of AGR3 with aggressive disease. Knockdown experiments in prostate cancer cell lines using a shRNA lentiviral construct or overexpression using an inducible system revealed that AGR3 exerts a positive influence on cell proliferation. Furthermore, AGR3 was found to enhance prostate cancer cell migration and adhesion. Analysis of genome-wide gene expression data comparing control and AGR3-depleted VCaP prostate cancer cells revealed upregulation of several genes involved in extracellular matrix processes including Lumican, a secreted leucine-rich glycoprotein known to inhibit prostate cancer cell migration. Subsequently, knockdown studies showed that AGR3 exerts its positive influence on VCaP cell migration at least in part by suppressing Lumican expression. In addition to these processes, AGR3 may play an important role during the physiological stress commonly experienced by cancer cells in the tumor microenvironment. The AGR3 protein localizes in the endoplasmic reticulum of prostate cancer cells, and is upregulated during endoplasmic reticulum stress. AGR3 expression correlated positively with enhanced expression of pro-survival endoplasmic reticulum chaperone GRP78 as well as increased cell viability.

Taken together, these results identify AGR3 as a protein that positively regulates prostate cancer progression by increasing the growth, viability, and migration of the tumor cells.

TABLE OF CONTENTS

LIST OF FIGURES

LIST OF TABLES

ABBREVIATIONS

%	percentage
°C	degrees Celsius
[^{3}H]	Tritium
A	Alanine
ADT	Androgen Deprivation Therapy
AG1	Anterior gradient 1
AG2	Anterior gradient 2
AG3	Anterior gradient 3
AGR	Anterior gradient
AGR1	Anterior gradient homolog 1
AGR2	Anterior gradient homolog 2
AGR3	Anterior gradient homolog 3
AHR	Aryl hydrocarbon receptor
Akt	v-Akt murine thymoma viral oncogene homolog 1
APLP1	Amyloid-like protein 1
AR	Androgen Receptor
ATF6	Activating Transcription Factor 6
BCMP11	Breast Cancer Membrane Protein 11
BD	Becton Dickinson
bp	base pairs
Bq	Becquerel, SI unit of radioactivity
BSA	Bovine Serum Albumin
C	Cysteine
c-Myc	v-Myc myelocytomatosis viral oncogene homolog, avian
CCS	Charcoal stripped Calf Serum
cDNA	complementary Deoxyribonucleic acid
CG	Cement Gland
Chip-PCR	Chromatin-immunoprecipitation – Polymerase Chain Reaction
Ci	Curie, non-SI unit of radioactivity (3.7 x 10^10 decays/sec)
COL5A2	Collagen 5 subunit A2
CPM	Counts per minute
CRISP3	Cysteine-Rich Secretory Protein 3

CRPC	Castration Resistant Prostate Cancer
Ct	value at which exponential expression signal crosses a pre-defined threshold in qPCR
CUX1	Cut-like homeobox 1
CxxC	Cysteine - aminoacid – aminoacid – Cysteine
CxxS	Cysteine - aminoacid – aminoacid – Serine
D	Aspartic acid
dH_2O	distilled H_2O
DHT	Dihydrotestosterone
DMD	Dystrophin
DMSO	Dimethylsulfoxide
DNA	Deoxyribonucleic acid
dNTP	deoxyribonucleotide
Draq5	Draqulin 5, a DNA intercalator
DTT	Dithiothreitol
E	Glutamic acid
e.g.	Latin: gratia exempli, English: for example
ECL	Enhanced Chemofluorescence
ER	Endoplasmic reticulum
ERG	v-Ets erythroblastosis virus E26 oncogene related
ERK1/2	Extracellular regulated kinase 1/2
ERP18	Endoplasmic reticulum protein 18
ERα	Estrogen Receptor α
et al.	Latin: et alii., English: and others
EtOH	Ethanol
Ets	E26 transformation specific
Ezh2	Enhancer of zeste homolog 2
F	Phenylalanine
FCS	Fetal Calf Serum
FGF9	Fibroblast Growth Factor 9
FOXA1	Forkhead box A1
FOXA2	Forkhead box A2
g	gram

G	Glycine
GFP	Green fluorescent protein
GI	Gastrointestinal
GO	Gene Ontology
GOB-4	Expressed in goblet cells - 4
GSEA	Gene set enrichment analysis
h	hour
H	Histidine
H3K27	Histone 3 Lysine 27
HIF1A	Hypoxia inducible factor A1
I	Isoleucine
i.e.	Latin: id est., English: that is
IRE1	Inositol requiring 1
K	Lysine
KAL1	Kallmann syndrome 1
kDa	kilo-Dalton
KDSR	3-Ketodihydroshingosine reductase
L	Leucine
LHRH	Luteinizing hormone-releasing hormone
LOH	Loss of heterozygosity
LUM	Lumican
M	Molar
M	Methionine
MAS5	Affymetrix. Microarray Suite. Version 5.0.
mg	Milligram
min	minutes
ml	milliliter
mM	millimolar
mRNA	messenger Ribonucleic acid
Muc1	Mucin 1
Muc2	Mucin 2
N	Asparagine
n	Number of independent experiments

nAG	newt (A. maculatum) anterior gradient
ng	nano gram
Nkx3.1	Nirenberg Kim 3 homeobox 1
nm	nano meter
np77	cDNA encoding part of XAG2 (accession U82110)
ns	Not significant
p	short arm of a chromosome
P	Proline
PBS	Phosphate buffered saline
PCR	Polymerase chain reaction
PCR	Polymerase chain reaction
PDI	Protein Disulfide Isomerase
PIN	Prostatic intraepithelial neoplasia
pmol	pico molar
Prod1	cell surface molecule of the three finger protein superfamily
Pten	Phosphatase and tensin homolog
PVDF	Polyvinylidene fluoride
q	long arm of a chromosome
Q	Glutamine
qPCR	quantitative Polymerase chain reaction
R	Arginine
R1881	synthetic (stable) androgen
RNA	Ribonucleic acid
RNA-seq	mRNA sequencing
RPLP0	RibP0, gene encoding ribosomal protein
rpm	rotations per minute
S	Serine
SD	Standard deviation
SDS-PAGE	Sodium dodecyl sulfate - polyacrylamide gel electrophoresis
SEM	Standard error of the mean
shAGR3	cells stably expressing anti-AGR3 shRNA
shCon	cells stably expressing non-target shRNA
shRNA	short hairpin ribonucleic acid

siGFP	cells transfected with anti-GFP siRNA
siLUM	cell transfected with anti-Lumican siRNA
siRNA	short interfering ribonucleic acid
SMAD4	SMA and MAD related protein 4
SSH	Suppressive subtractive hybridization
sXBP1	spliced x-box binding protein 1
T	Threonine
TBq	terra Becquerel
TBS	Tris buffered saline
Tg	Thapsigargin
TLP19	Thioredoxin-like protein 19
Tm	Tunicamycin
Tmprss2	Transmembrane protease, serine 2
Tris	Tris (hydroxylmethyl) aminomethane
U	Units (arbitrary)
UPR	Unfolded protein response
UV	Ultraviolet
V	Valine
v	volume
vs.	versus
W	Tryptophan
w	weight
XAG1/2	Xenopus anterior gradient 1/2
Y	Tyrosine
ΔCt	gene expression, normalized to housekeeping gene in qPCR
ΔΔCt	difference in expression between samples for the same gene
µci	micro Curie
µg	microgram
µl	microliter

1. INTRODUCTION

1.1 Prostate cancer

Prostate cancer is one of the leading causes of cancer-related mortality in males worldwide [1]. The majority of this malignancy originates in the prostate epithelium where the two main cell types, basal and luminal (secretory), form superimposed cell layers separated from the surrounding stroma by a sheet of extracellular-matrix fibers known as the basement membrane. In healthy prostate tissue and precursor stages of prostate cancer known as PIN (prostatic intraepithelial neoplasia), cell proliferation remains confined to the epithelium. In prostate adenocarcinoma, abnormal cell growth leads to epithelium overpopulation with luminal cells that in the advanced stages invade through the basement membrane and migrate to distant sites in the body in a process known as metastasis. Patients with advanced disease incur the majority of mortality, and therefore, the underlying mechanisms that enable abnormal epithelial cell growth to become lethal are a main focus of prostate cancer research.

Luminal cell survival in the prostate epithelium is sustained by steroid androgens (e.g. testosterone or DHT, dihydrotestosterone). Androgens activate a member of the steroid nuclear receptor family (ligand-inducible transcription factor) known as AR (androgen receptor), which drives the expression of genes involved in cell proliferation and survival [2-5]. Androgen-dependent tumors are commonly treated with ADT (androgen deprivation therapy) by either reducing circulating androgens through chemical castration (e.g. with LHRH agonists, luteinizing hormone-releasing hormone), or by preventing androgen from binding to AR with antiandrogens (e.g. with flutamide). ADT reduces the number of luminal cells by 90% mainly through apoptosis, and leads to a period of tumor regression [6-8]. However, in the majority of patients, tumor growth resumes as CRPC (castration resistant prostate cancer), in which AR continues to play a crucial role though gain-of-function mutations, AR gene amplification, and upregulation of its

transcriptional co-activators [9-11]. CRPC patients develop metastasis in ~30% of cases and face high mortality [12]. The limited number of treatments for CRPC has lead to the search for additional molecular factors that enable prostate cancer progression.

1.2 Molecular features of prostate cancer progression

In addition to AR, which plays a role in the majority of prostate tumors, there are multiple events associated with progression of prostate cancer. Of these, the best-characterized examples include changes in expression of key tumor suppressors and oncogenes through chromosomal fragment deletions and amplifications, epigenetic alterations, and the formation of prostate-specific gene fusions [13]. Often, these alterations directly influence the activity of each other as well as the AR during prostate cancer progression.

The most common event associated with prostate cancer progression is loss of heterozygosity (LOH) at chromosome 10q23, which causes reduction of expression of the tumor suppressor protein Pten (phosphatase and tensin homolog) [14]. Reduced Pten activity enables cell survival largely through activation of the downstream Akt (v-akt murine thymoma viral oncogene homolog 1) pathway [15]. Recent evidence suggests that after Pten deactivation, the pro-survival signal emanating from Akt promotes CRPC by maintaining cell growth in the absence of AR mediated survival [16].

While sufficient to cause malignancy, deletion at chromosome 10q23 is typically not an isolated feature in most aggressive prostate cancers. Other oncogenic events, such as upregulation of the transcription factor c-Myc (v-myc myelocytomatosis viral oncogene homolog, avian), cooperate with reduced Pten activity to promote disease progression [17]. c-Myc is a potent transcription factor known to negatively regulate genes involved in cell cycle arrest, induce formation of PIN, and lead to invasive adenocarcinoma [18, 19]. Furthermore, upregulation of MYC is inversely correlated with (and possibly suppresses) the expression of tumor suppressor Nkx3.1 (Nirenberg Kim 3 homeobox 1) [20].

Nkx3.1 downregulation is an early event in prostate cancer progression present in up to 85% of PIN cases [21, 22]. The Nkx3.1 gene encodes an androgen regulated homeobox transcription factor, crucial to all stages of prostate development that drives epithelial secretory function and differentiation [23, 24]. Reduction of Nkx3.1 is brought about through several mechanisms, including frequent deletions at chromosome 8p21 and epigenetic suppression [23]. Nkx3.1 expression can be epigenetically suppressed through promoter methylation by the polycomb group gene Ezh2 (enhancer of zeste homolog 2) [25]. Ezh2 is a H3K27 (histone 3 lysine 27) methyltransferase frequently upregulated in aggressive prostate malignancy [26, 27]. Regulation of the Ezh2 expression is in turn mediated by ERG (v-Ets erythroblastosis virus E26 oncogene related), which forms part of one of the most common gene fusion events in prostate cancer [25]. ERG is member of the Ets (E26 transformation specific) family of transcription factors that forms a prostate-specific gene fusion with androgen regulated Tmprss2 (transmembrane protease, serine 2) in up to 50% of patients [28, 29]. The TMPRSS2-ERG protein product promotes a transcriptional program that reverses cell differentiation and promotes CRPC [30].

Even though these lesions reveal some of the most frequent mechanisms that promote malignancy and lead to CRPC, they are not exhaustive. The search for a comprehensive catalogue of the alterations occurring in prostate cancer was advanced through use of genome wide technologies such SSH (suppressive subtractive hybridization), microarray, and recently RNA-seq (mRNA sequencing). These technologies have confirmed all previously described lesions of prostate malignancy and revealed a new set of events that may influence tumor progression.

One of the most recently characterized genes implicated in prostate cancer progression is AGR2 (anterior gradient homolog 2) [31, 32]. Initially identified in an SSH screen comparing differential gene expression between benign and malignant patient samples, AGR2 was recently shown to be part of a core set of genes whose expression correlates strongly with CRCP [31, 33]. AGR2 is an AR-regulated gene that can promote cell growth, migration, and invasion in prostate cancer [32, 34, 35].

In *Homo sapiens*, AGR2 has two other homologues, namely AGR3 and AGR1 (anterior gradient homolog 3 and 1), which share 61% and 39% protein sequence homology respectively. AGR3 is also AR regulated and follows a similar pattern of expression to AGR2 during model organism development (e.g. *Xenopus laevis*) [36-40]. These shared attributes with AGR2 suggest a possible role for AGR3 in prostate cancer progression.

1.3 AGR genes are conserved and play a role in development and regeneration in amphibians

The AGR (anterior gradient) family was first described in the tetraploid *Xenopus laevis*, which has four AGR genes and their respective pseudoalleles (denoted as 1/2 or a/b), namely XAG1/2 (xenopus anterior gradient 1/2), AGR1(a/b), AGR2(a/b), and AGR3(a/b) (anterior gradient homolog 1, 2, and 3) [39, 41, 42]. AGR2 and AGR3 share the highest sequence homology at the mRNA level and reside in the same syntenic fragment in the genomes of most vertebrates indicating descent from a tandem gene duplication event [39, 43, 44]. Protein sequence homology reveals that XAG(1/2), AGR2(a/b) and AGR3(a/b) are closely related (>35%) suggesting the possibility of functional overlap [39].

		tandem gene duplication		
	ERP18 TLP19 AGR1	np77 AG1 XAG(1/2)	GOB-4 AG2 ARG2	BCMP11 AG3 AGR3
fish	✓	✓	✓	×
amphibian	✓	✓	✓	✓
reptiles	✓	×	✓	✓
birds	✓	×	✓	✓
mammals	✓	×	✓	✓

Table 1. AGR family conservation in vertebrates and their common synonyms. Gene synonyms were obtained from Xanbase (http://www.xenbase.org/). Species conservation analysis was adapted from [39]. "✓" and "×" denote presence or absence in the indicated vertebrate class. The shaded genes are closely related based on protein sequence homology.

One of the most remarkable functions of AGR genes was identified in the adult *A. maculatum* where an orthologue of XAG2, namely nAG (newt anterior gradient), mediates limb regeneration. nAG is expressed and secreted by gland cells of the wound healing epidermis after limb amputation where it promotes stem cell (i.e. blastema) proliferation and, through interaction with Prod 1, helps establish the correct identity of regenerating tissues [45-47]. AGR genes are thought to function similarly in *X. laevis*, which can regenerate tissues at specific stages (43-57) of development. During these stages, the XAG2, AGR2(a), and AGR3(a) transcripts are upregulated in larval stumps following limb amputation, indicating AGR gene involvement in amphibian appendage regeneration [39].

In addition to regeneration, the first AGR transcripts identified, XAG1 and XAG2 are expressed in *X. laevis* development [41]. XAG mRNA is initially found in the anterior ectoderm and is progressively restricted to the anterior-most segment where, when overexpressed, XAG2 (but not XAG1) is sufficient to induce formation of CG (cement gland, a mucus secreting ectoderm-derived organ) [38, 41]. Strong XAG(1/2), AGR2(a), and AGR3(a) expression is eventually detected in the developing CG as well as other ectoderm-derived organs such as Otic vesicles [41].

In higher vertebrates, the homolog of the XAG gene is deactivated through multiple in-frame stop codons (e.g. located through synteny on chromosome 2q37 in *H. sapiens*) (Table 1), suggesting that AGR function is likely to be mediated by AGR2 and AGR3, and possibly the distantly related AGR1 [39].

1.4 Expression and function of AGR homologs in mice

As in *X. laevis*, AGR (e.g. AGR2) gene expression is upregulated during mouse embryo development [48]. However, whereas AGR expression in *X. laevis* is found predominantly in ectoderm derived organs, AGR2 expression in adult mice is found in the endoderm-derived epithelia of lungs and GI (gastrointestinal) tract [49-52]. AGR2 expression occurs mainly in

mucin secreting epithelial cells where it is thought to induce cell differentiation (e.g. promote differentiation of mucous-secreting goblet cells in intestine or lung epithelia) [50, 52, 53]. Furthermore, suppression of AGR2 leads to perturbed mucin production caused in part by disruption of AGR2–dependent Muc1 (pancreatic cells) and Muc2 (murine intestine epithelium) (mucin 1 or 2) protein processing in the ER (endoplasmic reticulum) [51, 54]. Together, these findings suggest a two-fold function for AGR molecules in the maintenance of secretory cell homeostasis and secretory protein processing in the ER.

A similar function has been described in mammary gland development, where AGR2 suppression leads to disrupted lobuloalveolar morphology and reduction in milk protein expression [55]. Given its previously described role in ER protein folding, AGR2 expression is thought to be required during periods of increased protein production in differentiated secretory cells [55, 56].

Analogous to AGR2, the mRNA of AGR3 in pregnant mice increase steadily until its highest point at lactation [55]. However, AGR3 transcript levels are consistently lower than those of AGR2, suggesting a more prominent role for the latter in mammary gland development and milk protein production.

Taken together, these reports implicate AGR family genes in mammalian development, and suggest a role in differentiated secretory epithelial cell homeostasis and protein processing in the ER.

1.5 Structural features of AGR proteins

The AGR genes belong to the greater PDI (protein disulfide isomerase) family, members of which act as chaperones and isomerases of disulfide bonds during protein folding in the ER. Structurally, all three genes encode small proteins (~17kDa) with three main features: an N-terminus cleavable ER-leader sequence which targets the nascent peptide for co-translational translocation into the ER, a thioredoxin fold which houses the catalytic CxxC/S motif, and a C-terminus variant of the KDEL tag that mediates

retention in the ER. Localization in the ER has been demonstrated for all three proteins and is thought to depend on the extent of homology between their respective ER-retention signals with the classic KDEL motif [56-59]. The crystal structures of AGR1 (2K8V), AGR2 (2LNS), and AGR3 (3PH9) have confirmed the presence of the predicted thioredoxin-like fold for each protein [35, 60]. Within this fold, the AGR1 protein sequence bears the classic Cxx***C*** motif instead of the Cxx***S*** present in AGR2 and AGR3, suggesting reduced isomerase function of the latter proteins when compared to AGR1 [61].

```
hAGR1      -METRPRLGAT-CLLGFSFL--------------LLVISSDGHNGLGKGFGDHIHWRT-L
hAGR2      -MEKIP-VSAFLLLVALSYTLARDTTVKPGAKKDTKDSRPKLPQTLSRGWGDQLIWTQTY
hAGR3      MMLHSA-LGLCLLLVTVSSNLA-----------IAIKKEKRPPQTLSRGWGDDITWVQTY
            *     :.    *: .*                        : *.:*:**.: *

hAGR1      EDGKKEAAASGLPLMVIIHKSWCGACKALKPKFAESTEISELS-HNFVMVNLEDEEEPKD
hAGR2      EEALYKSKTSNKPLMIIHHLDECPHSQALKKVFAENKEIQKLA-EQFVLLNLVY--ETTD
hAGR3      EEGLFYAQKSKKPLMVIHHLEDCQYSQALKKVFAQNEEIQEMAQNKFIMLNLMH--ETTD
           *:.   :  *  ***:* * . *  .:***  **:. **.::: .:*:::**    * .*

hAGR1      EDFSPDGGYIPRILFLDPSGKVHPEIINENGNPSYKYFYVSAEQVVQGMKEAQERLTGDA
hAGR2      KHLSPDGQYVPRIMFVDPSLTVRADITGRYSNRLYAYEPADTALLLDNMKKALKLLKTEL
hAGR3      KNLSPDGQYVPRIMFVDPSLTVRADIAGRYSNRLYTYEPRDLPLLIENMKKALRLIQSEL
           :.:**** *:***:*:*** .*: :*  . .*  * *   .   ::: **:* . :  :

hAGR1      FRKKHLEDEL
hAGR2      ----------
hAGR3      ----------
```

Figure 1. Protein sequence alignment of *H. sapiens* (h) AGR1, AGR2, and AGR3.
Protein sequences were aligned with Clustalw2 algorithm.
(*Green*) – N-terminal signaling peptide. The right-most highlighted amino acid represents the putative cleavage site predicted by submitting the matching accessions (hAGR1, NP_056997, hAGR2, NP_006399, hAGR3, NP_789783) to (http://www.cbs.dtu.dk/services/SignalP/).
(*Blue*) – Putative catalytic motif CxxC/S.
(*Orange*) – peptide binding loop.
(*Purple*) – C-terminal variant of the ER-retention tag.

In addition, a region of AGR2 between amino acids 104-111, termed the peptide-binding loop, is able to interact with tumor suppressor protein Reptin [62]. A similar region is present in both AGR3 and AGR1 (Figure 1, orange region), but respective peptides from the homologous (but not identical) region failed to bind Reptin [62]. Nevertheless, the conservation of this region is thought to constitute a potential client-docking site for all AGR family members.

AGR2 has recently been shown to dimerize through an interaction stabilized by an intermolecular salt bridge between E60 and K64 [35, 62]. In

AGR3, the equivalent position of AGR2-K64 is occupied by a tyrosine residue, which reduces the likelihood of a stable AGR3 homodimer, but does not exclude the possibility of an AGR2-AGR3/1 heterodimer. Given the high degree of similarity between AGR2 and AGR3, it possible that they share other binding partners, and by extension, overlap in function and regulation.

1.6 Transcriptional regulation of AGR genes in H. sapiens

Upregulation of AGR2 has been detected frequently in cancers. As a result, various studies have found diverse mechanisms of AGR2 transcript regulation.

Several transcription factors involved in development, such as SMAD4 (SMA and MAD related protein 4), ERK1/2 (extracellular regulated kinase 1/2), and the AHR (aryl hydrocarbon receptor) regulate AGR2 expression in *H. sapiens* [54, 63, 64]. Importantly, AHR-mediated AGR2 expression was demonstrated under etoposide-induced (DNA-damage) implying AGR2 promoter regulation during cellular stress [63].

gene	biological process	transcription factor	supporting literature
AGR2	steroid hormone response	ERα	Vanderlaag et al., 2010; Hrstka et al., 2010
		AR	Zhang et al., 2005; Bu et al., 2011; Bu et al., 2013
	cellular differentiation	FOXA1	Zheng et al., 2006; Zhang et al., 2010
		FOXA2	-
		AHR	Ambolet-Camoit et al., 2010
		SMAD4	Norris et al., 2012
		ERK1/2	Zweitzig et al., 2007
	cellular stress	HIF1A	Hong et al., 2013
		ATF6	Higa et al., 2011
AGR3	steroid hormone response	ERα	Al Saleh et al., 2011
		AR	Bu et al., 2013

Table 2. Transcription factors regulating AGR2 and AGR3 expression in *H. sapiens.* A survey of AGR2 and AGR3 literature with focus on experimentally determined (i.e. reporter gene assays and quantitative PCR) transcription factors that regulate AGR gene expression. Although there is considerable overlap between the processes listed, an effort has been made to group transcription factors based on their most common, prominent, or better-studied function.

Other types of cellular stress, such as those induced by lack of nutrients, hypoxia, or accumulation of misfolded proteins in the ER (i.e. ER stress) have all been shown to regulate the AGR2 promoter [31, 56, 64].

During ER stress, AGR2 expression depends on transcription factor ATF6 (activating transcription factor 6) and the activity of ER-membrane kinase IRE1 (inositol-requiring 1), which acts through sXBP1 (spliced x-box binding protein 1), an IRE1-dependent transcription factor [56]. Cellular stress induced by hypoxia can also regulate the AGR2 promoter in a HIF1A-dependent (hypoxia-inducible factor 1A) manner in glioblastoma cells, suggesting a possible role in the preservation of cell viability [65]. Together, these reports indicate frequent upregulation of AGR2 in cellular stress conditions commonly associated with the tumor microenvironment and its possible involvement in the processes that relieve them.

AGR2 expression in cancer occurs even in the absence of simulation by developmental pathways or stress. In breast and prostate cancer cells, AGR2 expression is mediated by steroid nuclear receptors such as ER and AR, respectively, though the latter requires *de novo* protein synthesis to achieve AGR2 expression, given that treatment with cycloheximide (a *de novo* protein synthesis inhibitor) can block its upregulation during androgen stimulation [31, 32, 37, 66]. Binding of ERα (estrogen receptor α) and AR to cognate sites is mediated by the transcription factor FOXA1 (forkhead box A1) [67, 68]. Two separate reports have shown FOXA1 and FOXA2 (forkhead box A2, a close homolog), activity on the promoter of AGR2, though the significance of this interaction in nuclear-receptor mediated transcription of AGR2 has not been investigated [40, 69].

As with AGR2, the AGR3 promoter is regulated by a variety of nuclear receptors activated by their respective ligands [37, 70]. In prostate cancer cell lines such as LNCaP, DUCaP, and 22Rv.1, the expression of AGR3 can be induced by androgen, estrogen (E_2), and progesterone in an AR-dependent manner [37]. In contrast to AGR2 however, AR-mediated AGR3 upregulation is not hindered by pre-treatment of cells with cyclohexamide, indicating direct transcriptional regulation by AR [37]. The same study used Chip-PCR (chromatin immunoprecipitation coupled to polymerase chain reaction) in DUCaP cells to confirm AR occupancy at a previously identified binding site in the first intron of the AGR3 gene. In addition, AR binding sites can be readily identified within 25kb of the AGR3 transcription start site of LNCaP cells (Figure 2). Despite subtle differences, these reports suggest similar hormone-

dependent regulation of both AGR2 and AGR3 promoters. However, these two genes are not always expressed together, indicating the existence of mutually exclusive regulation.

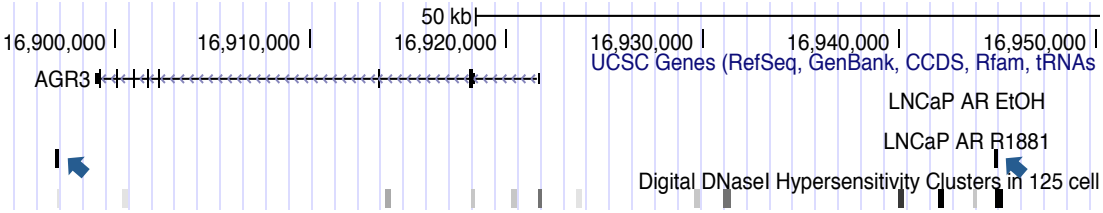

Figure 2. AR binding sites on the distal promoter of the AGR3 gene of LNCaP cells. Public chip-seq datasets [30] were processed on the main Galaxy server (https://main.g2.bx.psu.edu) and visualized using the University of California, Santa-Cruz (UCSC) genome browser website (http://genome-euro.ucsc.edu). AR binding sites are indicated by blue arrows with 25kb of the AGR3 transcription start site. DNaseI hypersensitive regions are mapped on the bottom-most track.

1.7 Functions of AGR2 and AGR3 in cancer

In cancer, AGR2 is the most frequently upregulated member of the AGR family. Studies of patient survival and AGR2 expression have found either enhanced or poor outcome in patients with high AGR2 expression in their biopsy, suggesting that the relationship of this protein with cancer is complex [71-77]. As a result, there have been many studies investigating its role in various cancers, with most findings converging on three main AGR2 functions: cell growth and transformation, metastasis, and resistance to endocrine and chemotherapy.

Functional studies using various *in vitro* growth and migration assays, as well as *in vivo* xenografts in mice have helped clarify the properties of AGR2 in cancer. The ability of AGR2 to transform cells was first described in NIH3T3 (mouse embryonic fibroblasts) cells, in which AGR2 expression was sufficient to both promote enhanced growth of NIH3T3 xenografts in nude mice and dramatically enhance anchorage independent cell growth in soft agar assays [78]. Subsequently, *in vitro* studies using human cancer cell lines found that AGR2 expression is sufficient to increase cell growth, colony formation, and anchorage independent growth [66, 79-81]. However, a

previous study using Rama 37 (non-metastatic rat mammary cells) overexpressing AGR2 *in vivo* did not find a pronounced effect on xenograft tumor growth, but instead reported enhanced metastasis to the lungs [82]. Similar AGR2 behavior was reported in prostate cancer cells where AGR2 overexpression leads to a decrease in cell proliferation and colony formation *in vitro*, reduced tumor growth *in vivo*, but enhanced cell migration and invasion *in vitro* [32, 69].

Given that different cancers progress through distinct mechanisms it is possible that the reported AGR2 phenotype differences could be caused by the variety of cell types used to investigate its function (i.e. primary tumor or metastasis derived) and their tissue of origin (i.e. breast, ovarian, or prostate cancer). It is possible that different tumor cells exhibit only a portion of the wide range of AGR2 properties, which could in part explain the observed discrepancy between AGR2 expression and patient survival.

AGR2 can affect patient survival by playing a role in tumor resistance to endocrine therapy. Tamoxifen is an antagonist of the ERα used in treatment of breast cancer, which results in initial tumor regression, usually followed by relapse with a tamoxifen-resistant phenotype sustained by tamoxifen-induced and ERα mediated gene expression. AGR2 is one of the few known genes upregulated after both estradiol and tamoxifen treatment, in an ERα dependent manner [80]. MCF7 cells treated with tamoxifen display increased survival in the presence of AGR2, suggesting a role for this protein in tamoxifen resistance of breast tumors [80]. Another aspect of AGR2 tumor biology is its ability to promote tumor cell survival after various cellular insults. Early on, AGR2 was shown to suppress the activation of tumor suppressor p53 (tumor protein 53kDa) after UV (ultra violet) radiation in H1299 cells (human non-small cell lung carcinoma) [79]. Another study showed that suppression of AGR2 in pancreatic cells (Mpanc-96) sensitized them to treatment with gemcitabine, a nucleoside chemotherapeutic reagent [83]. These findings, together with the extensive evidence linking AGR2 expression to cancer cell survival, suggest a role for AGR2 in resistance to therapy.

Currently, the only functional study of AGR3 points to role in chemotherapeutic resistance analogous to that of AGR2. AGR3 overexpression in ovarian cancer cells results in enhanced resistance to

cisplatin treatment *in vivo* [57]. However, in serous borderline ovarian tumor (an ovarian cancer primary tumor subtype), AGR3 expression correlates with increased cell differentiation and better prognosis, suggesting cell type specific functions during tumor progression [84]. In ovarian cancer, the expression of AGR2 and AGR3 overlaps in mucinous primary tumors, but follows no discernable overlapping pattern in serous, clear cell, and endometrial subtypes. Query of public databases (https://www.nextbio.com), showed that in most tissues AGR3 expression is found in epithelia of digestive and respiratory system in a pattern similar to that of AGR2. Furthermore, like AGR2, AGR3 is expressed in breast cancer patients and cell lines (i.e. T47D) where it correlates strongly with ERα status [43]. A similar correlation between ER and AGR3 expression has not been detected in ovarian cancer, a finding which could possibly be explained by a recently reported gene fusion event between the 3' end of CUX1 (cut-like homeobox 1, chromosome 7q22) and the proximal promoter region of AGR3 (chromosome 7p21) in uterine leiomyoma [57]. This fusion event may adversely affect AGR3 regulation in uterine cancers and uncouple AGR2 and AGR3 expression. Over the course of the present study, AGR3 expression was detected throughout prostate cancer progression [85]. However, the function of AGR3 in prostate cancer remains unknown.

2. AIM

AGR2 and AGR3 are conserved homologs of AGR and XAG genes in *X. laevis*, which play a crucial role in development and regeneration. These genes lie adjacent to each other on chromosome 7p21, share a high degree of sequence homology, and are similarly regulated by hormone activated steroid receptors. The proteins of both AGR2 and AGR3 enter the endoplasmic reticulum where they can either be retained, or follow the secretory pathway to secretion. The role of AGR2 in cancer, especially that of the prostate, has been well characterized. To date, little is known about the tumor biology of AGR3.

This project aims to identify the role of AGR3 in prostate cancer. To accomplish this, first the influence of AGR3 in cell growth will be investigated in several prostate cancer cell lines. The ability of AGR3 to influence the spread of prostate tumor cells will be investigated using relevant assays. Furthermore, to provide a comprehensive view on AGR3 function, the influence of AGR3 in prostate cancer cell survival under stress will also be evaluated.

3. MATERIALS AND METHODS

3.1 Materials

3.1.a Chemicals and consumables

reagent	supplier
Agarose	Peqlab, Erlangen
Ampicillin	Roth, Karlsruhe
Bovine Serum Albumine (BSA)	PAA Laboratories GmbH, Pasching
Bacto-Agar	Otto Nordwald GmbH, Hamburg
Bacto-petri dishes	Greiner Labortechnik, Nürtingen
Bacto-Trypton	Roth, Karlsruhe
Bacto-yeast extract	Roth, Karlsruhe
n-buthanol	Roth, Karlsruhe
Celltiter-Blue	Promega, Mannheim
Chloroform	Merck, Darmstadt
Collagen I	Sigma-Aldrich, Taufkirchen
Crystal violet	Lighting Powder Company, INC.,
Desoxy-nucleoside-triphosphate (dNTPs)	Roche, Mannheim
DiI cell labeling solution	Life Technologies, Karlsruhe
Dimethylsuloxide (DMSO)	Fluka, Neu Ulm
Dithiothreitol (DTT)	Gibco, Invitrogen, Karlsruhe
DNA Marker 1 Kb	PeqLab, Erlangen
ECL (western blotting detection)	Amersham Pharmacia Biotech, Freiburg
Ethylenediamine Tetraacetic Acid (EDTA)	Roth, Karlsruhe
Ethanol (EtOH)	Roth, Karlsruhe
Ethidium Bromide	Roth, Karlsruhe
Fibronectin	Sigma-Aldrich, Taufkirchen
FBS (Fetal Bovine Serum)	Gibco, Invitrogen, Karlsruhe

G418 (Geneticin)	Sigma-Aldrich, Taufkirchen
Glycylglycerine	Roth, Karlsruhe
Glycine	Roth, Karlsruhe
Glycogen	Peqlab, Erlangen
Hydrogen Chloride (HCl)	Roth, Karlsruhe
Hexadimethrine Bromide	Sigma-Aldrich, Taufkirchen
Insta-Gel Plus (Scintillation Counting)	PerkinElmer, Waltham, USA
Isopropanol	Roth, Karlsruhe
Magnesium Chloride ($MgCl_2$)	Roth, Karlsruhe
Magnesium Sulfate ($MgSO_4$)	Roth, Karlsruhe
Methanol (MeOH)	Roth, Karlsruhe
ß-mercaptoethanol	Roth, Karlsruhe
Milk powder	Saliter, Obergünzburg
Phenol	Roth, Karlsruhe
peqGold RNA Pure	Peqlab, Erlangen
Plasmid Maxiprep Kit	Qiagen, Düsseldorf
Phosphate Buffered Saline	Gibco, Invitrogen, Karlsruhe
Potassium Chloride	Merck, Darmstadt
Poly-L-lysine	Sigma-Aldrich, Taufkirchen
Rotiphorese® Gel30 (37.5:1)	Roth, Karlsruhe
RPMI medium 1640	Gibco, Invitrogen, Karlsruhe
Protein Marker	PeqLab Erlangen
Puromycin	Calbiochem, Bad Soben
Sodium Acetate	Roth, Karlsruhe
Sodium Chloride	Roth, Karlsruhe
Sodium Dodecyl Sulphate (SDS)	Roth, Karlsruhe
Sodium Hydroxide	Roth, Karlsruhe
Sodium N-lauryl sarcosinate (Sarkosyl)	Sigma-Aldrich, Taufkirchen
StrataClean resin	Stratagene, Amsterdam
SYBR-Green Mix	Qiagen, hilden
Tetramethyl ethylene	Roth, Karlsruhe

diamine (TEMED)	
Thapsigargin	Life Technologies, Karlsruhe
5'-[^{3}H]-thymidine	Hartman Analytic, Braunschweig
Tris-base	Roth, Karlsruhe
Tris-HCl	Roth, Karlsruhe
Triton-X-100	Sigma-Aldrich, Taufkirchen
Trypsin 0,025% with EDTA	Gibco, Invitrogen, Karlsruhe
Tunicamycin	Sigma, Steinheim
Tween 20	Roth, Karlsruhe

3.1.b Cell lines

3.1.b.1 Bacteria

The bacteria used to express plasmid DNA in high quantity were DH5α with the following phenotype:
fhuA2 lac(del)U169 phoA glnV44 Φ80' lacZ(del)M15 gyrA96 recA1 relA1 endA1 thi-1 hsdR17

3.1.b.2 Eukaryotic cell lines

prostate cell lines

PNT2: Human prostate epithelial cell line immortalized by transfection with the SV40 genome, and express the large T antigen. These cells express cytokeratines 8, 18 and 19 which are consistent with a luminal cell phenotype. Cytokeratin 14, a marker of the basal phenotype is not present.

BPH-1: Human epithelial cells derived from a 68 year old male with benign prostate hyperplasia immortalized with SV40 large T antigen. They express cytokeratines 8 and 18 (luminal epithelial cell phenotype).

prostate cancer cell lines

22Rv.1: Human cell line derived from a prostate carcinoma xenograft (CWR22) that was serially propagated in nude mice after castration-induced regression and relapse of the parental, androgen dependent CWR22 xenograft.

DUCaP: Prostate cancer cell line established from the dura matter metastatic lesion of the autopsy of a patient with hormone refractory prostate cancer. These cells express the androgen receptor and cytokeratin 18 suggesting a luminal phenotype. This cell line produces tumors in nude mice.

VCaP: Prostate cancer cell line established from the vertebral metastatic lesion of a patient with hormone refractory prostate cancer. These cells expression cytokeratines 18 and the androgen receptor suggesting a luminal cell phenotype. These cells express the TMPRSS2-ERG gene fusion, form tumors, and generate predominantly osteoblastic bone metastasis.

LNCaP: Androgen dependent human cancer cell line derived fro ma needle aspiration biopsy of the left supraclavicular lymph node of a 50 year old Caucasian male with confirmed prostate metastatic cancer.

LNCaP_abl: These cells are a subclone of the LNCaP cell line that was generated by continuously passaging in RPMI 1640 in 10% charcoal-stripped fetal calf serum (CCS), with the aim of obtaining an androgen independent cell line.

PC-3: Prostate cancer cell line established from bone metastasis, with functional and morphologic characteristics of poorly differentiated adenocarcinoma. PC-3 cells lack the androgen receptor, and do not respond to androgen treatment. In mice, these cells are highly tumorigenic and result in mainly osteolytic bone metastasis.

DU145: Human prostate cancer cell line derived from dura matter metastatic lesion. These cells do not express the androgen receptor. In mice these cells are less tumorigenic and have lower metastatic potential than PC-3 cells

other cell lines

T47D: Human breast cancer cell line derived from the ductal carcinoma of a 54 year old female patient. These cells were used as a positive control in western blotting experiments owing to their abundant expression of AGR3.

3.1.c Oligonucleotides

3.1.c.1 Oligonucleotides for PCR

ß-actin:

forward: 5’ CTC CTG AGC GCA AGT ACT CC 3’
reverse: 5’ GTC ACC TTC ACC GTT GTT CCA GT 3’

AGR3:

forward: 5’ GCA ATA AAA AAG GAA AAG AGG CC 3’
reverse: 5’ GGG CAA ATA CTT TCT TTA GTG CTT GA 3’

3.1.c.2 Oligonucleotides for qPCR

AGR3:

forward: 5’ CCA GAA TAC ATT TCC AAC AAG AGC A 3’
reverse: 5’ GAC GAG TAA GAG GCA GAG ACC 3’

RPLP0 (RibPO):

forward: 5’ GAA GGC TGT GGT GCT GAT GG 3’
reverse: 5’ CCG GAT ATGAGG CAG CAG 3’

DMD:

forward: 5’ TGA TAC GGG ACG AAC AGG GA 3’

reverse: 5’ ATG TTA CTG CCC CCA AAG GAT G 3’

LUM:

forward: 5’ CCA CAC CAC AAG ATC CCC AC 3’

reverse: 5’ CCA CCA ATC AAT GCC AGG AAG A 3’

KAL1:

forward: 5’ TTC ACT GCC CCC AGC AAA CA 3’

reverse: 5’ CAT CCG TAG TCT TTC TCC GCT TC 3’

COL5A2:

forward: 5’ GGTGTA CGA GGC AGT GTA GGA 3’

reverse: 5’ CTG GGT GCT TTT TCG AGC CA 3’

APLP1:

forward: 5’ GCG TCA TGGC CCT TAT CAA CG 3’

reverse: 5’ GTG TCT GCA TCC TTG GAA TCT GGA 3’

GRP78:

forward: 5’ GGT GCT GAT GTC CCT CTG TC 3’

reverse: 5’ TTG GAG GTG AGC TGG TTC TT 3’

3.1.c.3 anti-Lumican siRNA

The siRNA oligonucleotide used to knockdown Lumican expression was purchased from Sigma-Aldrich (Taufkirchen, Germany). The catalogue number is SASI_Hs01_00221304 (Mission siRNA). (sequence available upon request).

3.1.d Enzymes

BamHI-HF, and XhoI restriction enzymes were purchased from New England Biolabs (Frankfurt, Germany). All other enzymes, (e.g. DNase, RNase, polymerases, and reverse transcriptases) were purchased from Promega (Mannheim, Germany). Specific information for each enzyme is provided in the following sections, which describe their use.

3.1.e Plasmids

pcDNA3.1 and pcDNA3.1-AGR3:

Stable AGR3 expression was induced by transfection a pcDNA3.1 vector (G418 and ampicillin resistance cassettes) that includes the AGR3 cDNA. Transfection of the original pcDNA3.1 vector was carried out to generate control cells.

shAGR3 lentiviral packaged pLKO.1-puro vectors:

To generate cells with a stable knockdown of AGR3, vectors containing shRNA sequences in pLKO.1-puro vectors (puromycin resistance cassette) targeting AGR3 were purchased from the MISSION shRNA line of products (Sigma-Aldrich). Three different sequences against AGR3 were used to generate separate subclones (sequences available upon request):
Sasi_Hs01_00094948 – shRNA #1
Sasi_Hs01_00094949 – shRNA #2
Sasi_Hs01_00094950 – shRNA #3
SHC002V – non-target shRNA control particles

pNEB-X1-AG3:

22Rv.1 cells with a stable transfection of the Rheo activator/receptor plasmid (pNEB-R1, New England Biolabs) were transfected with pNEB-X1-hygro plasmid (hygromycin resistance cassette, New England Biolabs) expressing AGR3 cDNA under the control of the Rheo activator/receptor.

3.1.f Buffers

1x Laemmli electrophoresis buffer

Tris	25 mM
Glycine	192 mM
SDS	0.1 % w/v

10x transfer buffer – western blotting

Tris-base	58.1 g
Glycin	29.3 g
Methanol	20%

diluted 1:10 in dH_2O to make 1x TBS

Laemmli 2x sample buffer

SDS	4%
ß-mercaptoethanol	10%
Glycerol	20%
bromophenol blue	0.004%
Tris-HCl	125 mM

TBS 10x (concentrated TBS)

Tris-HCl	24.23 g
NaCl	80.06 g
dH_2O	final volume 1 L
pH	7.6

diluted 1:10 in dH_2O to make 1x TBS

1x LB-medium (1 liter in dH_2O)

Trypton	10 g
NaCl	10 g
Yeast extract	5.0 g

50x TAE buffer

Tris-Base	40 mM
EDTA	1 mM
Glacial Acetic Acid	20 mM
pH	8.9

diluted 1:50 in dH_2O to make 1x TAE

3.1.g Antibodies

For western blotting each antibody was diluted in the indicated amounts and buffer and incubated with membranes for 1 h at room temperature or up to 24 h at 4°C. After each primary antibody incubation, the membrane were washed 3 times in 1xTBST and incubated for 1 h at room temperature with secondary antibody. Subsequently, the membranes were washed 3 additional times with 1x TBS-T before further processing.

primary antibodies

antibody	type	in 10 ml	in 1x - TBS	catalog #	supplier
AGR3	mouse monoclonal	5.0 µg	5% w/v Milk, 5% v/v FBS, 0.1% v/v Tween20	ab82400	Abcam
ß-actin	mouse monoclonal	2.0 µg	5% w/v Milk, 5% v/v FBS, 0.1% v/v Tween20	sc-8432	Santa Cruz
α-Tubulin	mouse monoclonal	2.0 µg	5% w/v Milk, 5% v/v FBS, 0.1% v/v Tween20	sc-8035	Santa Cruz
GRP78	goat polyclonal	3.3 µg	5% w/v Milk, 5% v/v FBS, 0.1% v/v Tween20	sc-1050	Santa Cruz
PDI	mouse monoclonal	5.0 µg	5% w/v Milk, 0.1% v/v Tween20	ER staining kit	Invitrogen
Lumican	mouse polyclonal	4.0 µg	5% w/v BSA, 0.1% v/v Tween20	ab70191	Abcam

secondary antibodies

antibody	type	in 10 ml	solvent	catalog #	supplier
anti-mouse	polyclonal, rabbit, HRP conjugated	1.0 µg	1 x TBS, 5% w/v Milk, 5% v/v FBS, 0.1% v/v Tween20	P016102-2	Dako Diagnostika GmbH

anti-goat	polyclonal, rabbit, HRP conjugated	1.0 µg	1 x TBS, 5% w/v Milk, 5% v/v FBS, 0.1% v/v Tween20	P044901-2	Dako Diagnostika GmbH
Alexa Fluor 488 anti-mouse	rabit polyclonal	2.5 µg	1x PBS, 10% v/v FBS	A11059	Life Technologies
Alexa Fluor546 anti-Goat	rabit polyclonal	2.5 µg	1x PBS, 10% v/v FBS	A11078	Life Technologies

3.1.h Equipment

Equipment	**supplier**
Sterile cell cuture CO_2 incubator	Labotect, Göttingen
Centrifuge (5417R)	Eppendorf, Hamburg
Liquid Scintillation Counter	Wallac ADL, Freiburg
Tomec Cell Harvester	Wallac ADL, Freiburg
Thermocycler (PTC 200)	MJ Research, Watertown
SetpOne Plus thermocycler (qPCR)	Applied Biosystems, Darmstadt
Waving platform shaker (Polymax 1040)	Heidolph Instruments, Schwabach
Biological safety cabinet (EN12469)	ThermoScientific

3.2 Methods

3.2.a Cloning methods

3.2.a.1 Phenol:Chloroform extraction of RNA

RNA samples were extracted from eukaryotic cells by using the peqGOLD RNA Extraction kit (Qiagen, Hilden, Germany), which is based on the phenol: chloroform RNA extraction method. For all experiments, between

1 and 3 x 10^5 cells were lysed with 1 ml peqGOLD solution over 5 min at room temperature. Cell lysates were supplemented with 200 µl of chloroform and vortex-mixed to ensure a homogeneous solution prior to 5 min of incubation at 4°C and subsequent centrifugation for 10 min at 12.000 rpm at 4°C to separate protein, DNA, and RNA containing phases. The soluble RNA trapped in the aqueous (upper) phase was supplemented with 1:50 (v/v) glycogen (carrier molecule, to enhance RNA precipitation) and precipitated with a 1:1 (v/v) isopropanol over 15 min incubation at 4°C. Precipitated RNA was then pelleted by centrifuging for 10 min at 12'000 rpm at 4°C. The pellet was washed of residual isopropanol with 1 ml of 75% ethanol. After air-drying, the pellet was dissolved in 20-50 µl RNase-free water, and incubated 10 min at 37°C and an additional 5 min at 60°C, before measuring concentration, and storing at -80°C.

3.2.a.2 Nucleic acid quantification

Nucleic acid samples were quantified by using a Nanodrop ND-1000 spectrophotometer (Thermo Scientific, Dreich, Germany) by measuring absorbance at 260, 280 and 230 nm. Samples were considered pure when the absorbance ratio of 260/280 nm produced values greater than 1.85 for DNA or 2.0 for RNA.

3.2.a.3 cDNA synthesis

Before cDNA synthesis, contaminant genomic DNA was digested using 1 unit of DNase I, and 1 µl of (20-40 units/µl) RNAse inhibitor for 30 min at 37°C for every 1 µg of RNA. The DNase digestion reaction was stopped with 2 µl of (0.5 M) EDTA and supplemented with 200 ng of random primer, which was allowed to anneal for 5 min at 70°C. Subsequently, 20 µl dNTP (10 mM), 200 units of M-MLV Reverse Transcriptase, and 4µl of 5x buffer were added and allowed to react in a thermocycler with an initial step of 10 min at 25°C, followed by 60 min at 42°C, and a final extension step of 10 min at 70°C. In

parallel, identical control reactions were carried out with 1 µg of RNA in the absence of M-MLV Reverse Transcriptase. After completion, each cDNA reaction was made to a final volume 250 µl using nuclease-free dH_2O. 4 µl of each resulting cDNA sample and matching control (reaction without M-MLV reverse transcriptase) was used as template in control PCR reactions supplemented with 0.5 µl of (10 mM) dNTP, 10 pmol of each forward and reverse ß-actin primers, 1.25 units of GoTaq polymerase, 4 µL of 5x Green GoTaq reaction buffer, and made to a final volume of 20 µl using dH_2O. In a thermocycler, reactions were subjected to an initial denaturation step of 2 min at 95°C before 30 cycles of: 30 sec denaturing at 95°C, 40 sec annealing at 55°C, and 45 sec extension at 72°C. After a final extension step of 10 min at 72°C, PCR products from each reaction were visualized on a 2% agarose gel (ß-actin band at 298 bp). All reagents were purchased from Promega, Mannheim, Germany.

3.2.a.4 Polymerase chain reaction (PCR)

PCR reaction (used to detect AGR3 mRNA in prostate cancer cell lines) was carried out using 4 µl of cDNA sample from each cell line, supplemented with 0.5 µl of (10 mM) dNTP, 10 pmol of each forward and reverse AGR3 specific primers, 1.25 units of GoTaq polymerase, 4 µL of 5x Green GoTaq reaction buffer, and made to a final volume of 20 µl using dH_2O. In a thermocycler, reactions were subjected to an initial denaturation step of 2 min at 95°C before 30 cycles of: 30 sec denaturing at 95°C, 40 sec annealing at 55°C, and 45 sec extension at 72°C. After a final extension step of 10 min at 72°C, PCR products from each reaction were visualized on a 2% agarose gel (AGR3 band at 99 bp). All reagents were purchased from Promega, Mannheim, Germany.

3.2.a.5 Quantitative polymerase chain reaction (qPCR)

Quantitative PCR reactions were carried out by supplementing 4 µl of template cDNA with 10 pmol of each forward and reverse primers, 10 µl of 1X SYBR green mix (Promega, Mannheim, Germany), made to a final volume of 20 µl with dH_2O. In parallel, a control reaction was carried out in the absence of cDNA template (volume compensated with dH_2O). This reaction was run in StepOnePlus (Life Technologies, Carlsbad, California) using this program: a holding stage of 95°C for 15 min, a two-step cycling stage of 95°C for 15 sec, then 60°C for 30 sec, followed by a melting curve with a starting temperature of 60°C increased in 0.5°C increments until a 95°C final step of 15 sec. Relative mRNA expression was calculated using the ΔΔCt method: 2^(ΔCt gene – ΔCt RPLP0).

3.2.a.6 Nucleic acid separation by gel electrophoresis

2% agarose gels were prepared to resolve the PCR products of both ß-actin and AGR3 PCR amplification reactions. Agarose was dissolved in 1x TAE buffer (0.04 M Tris pH 7.2, 0.02 sodium acetate, and 1 mM EDTA). Before casting, the melted agarose solution was added ethidium bromide to a final concentration of 0.4 mg / ml and allowed to set at room temperature in horizontal gel chambers. The same 1x TAE buffer was used to submerge the agarose gel, before loading PCR reaction samples into wells. To estimate PCR product size, a peqGOLD DNA-leiter (0.5 mg DNA / ml) was loaded in parallel to samples. Electrophoresis was carried out at 120 V.

3.2.a.7 Extraction of DNA fragment from agarose gel

The peqGOLD gel extraction kit (peqLab Biotechnology GmbH, Erlangen, Germany) was used to extract DNA fragments from agarose. After agarose gel electrophoresis at 120 V separated DNA fragments were visualized under UV light and required bands excised. The gel slice was dissolved at 55°C in binding buffer (XP2) and the DNA captured by adding to a HiBind DNA spin column and centrifuging at 10000 rpm for 1 min (centrifuge 5415D, Eppendorf). The column was washed once with 300 µl of XP2 buffer,

and twice more with 600 µl of SPW buffer (80% ethanol). After 3 min incubation, the column was dried by centrifugation for 1 min at 10000 rpm prior to the final elution step carried out by adding 30 – 50 µl of dH_2O to the column and centrifuging for 1 min at 5000 rpm.

3.2.a.8 DNA fragment digestion

To clone the AGR3 cDNA from a pcDNA3.1-AGR3 plasmid into the pNEBR-X1 plasmid of the inducible expression system, 1 µg of each plasmid was separately digested with 10 units of each BamHI and XHoI (New England Biolabs, Ipswich, Massachusetts), in reactions with final concentrations of 1x Buffer #2 and 1x BSA for 1 h at 37°C. The reaction contents were supplemented with 10 µl of 5x GoTaq green reaction buffer before loading into 2% agarose gel. After adequate separation, the AGR3 or open pNEBR-X1 fragments were isolated from the agarose gel as described in 2.2.a.4, and the resulting DNA dilutions were used in a ligation reaction. An insert: plasmid ratio of 1:5 was used in each ligation reaction carried out by adding 1 unit of T4 DNA ligase in T4 DNA ligase buffer (50 mM Tric-HCl pH 7.5, 10 mM $MgCl_2$, 10 mM DTT, 1 mM ATP, and 25 µg/ml BSA) in a final volume of 20 µl for 4 h at 16°C. The reaction was stopped by incubating its contents at 65°C for 10 min.

3.2.a.9 Bacteria transformation with DNA plasmids

50 µl of competent DH5α bacteria were incubated with 5 µl of ligation reaction content from 2.2.a5 for 30 min on ice before heating to 42°C for 45 sec, placing 2 min on ice, and suspending in 1 ml of sterile SOC (0.5% yeast extract, 2% Tryptone, 10 mM NaCl, 2.5 mM KCl, 10 mM $MgCl_2$, 10 mM $MgSO_4$, and 20 mM of Glucose) medium. The resulting bacteria suspension was mixed for 30 min at 37°C and pelleted by spinning for 5 min at 3200 rpm before removing 900 µL of the supernatant. The bacteria pellet was resuspended in the remaining 100 µl of medium and streaked on a selective plate (1:1000 v/v LB-ampicillin) before incubation over night at 37°C.

3.2.a.10 Plasmid DNA purification (small scale, mini preps)

Small-scale purification of plasmid DNA was carried out with a modified protocol of the Qiagen Plasmid Maxi Kit (Qiagen, Hilden, Germany). 1 ml of cultured bacteria was pelleted at 12000 rpm for 30 sec at 4°C and re-suspended and incubated for 5 min at RT in 100 µl of buffer P1 (10 mM EDTA, 50 mM Tris-HCl pH 8.0, and 400 mg/ml RNase A). The bacteria suspension was added 200 µl of buffer P2 (200 mM NaOH and 1% SDS), mixed gently, and allowed to lyse over 5 min at 4°C. 200 µl of buffer P3 (3 M Na Acetate, pH 8.8) was used to neutralize the lysate for an additional 5 min at 4°C. Precipitated debris were separated from the lysate by centrifugation at 12000 rpm for 15 min at 4°C and transferred to new container. Thereafter, the DNA in the lysate was precipitated 70% isopropanol, pelleted for 10 min at 12000 rpm, washed of isopropanol in 500 µl of 80% EtOH twice, and re-dissolved in 20-50 µL of dH_2O.

3.2.a.11 Plasmid DNA purification (large-scale, maxi preps)

Large-scale plasmid DNA purification was carried out using the Qiagen Plasmid Maxi Kit according to the manufacturers instructions. Cultured bacteria were pelleted by centrifuging at 6000 rpm for 30 min at 4°C and resuspended in 10 ml of buffer P1 (including RNase) for 10 min. Alkaline lysis was carried out for 10 min at 4°C by adding and mixing 10 ml of lysis buffer P2. The reaction was stopped (pH neutralized) by adding 10 ml of buffer P3. Subsequently, separation of cellular debris and lysate was carried out by centrifuging the resulting mixture at 4000 rpm at 4°C for 30 min. The supernatant was applied to a Qiagen Tip 500 (a anion-exchange resin column) previously equilibrated with 15 ml of QBT buffer (700 mM NaCl, 50 mM MOPS pH 7.0, 15% isopropanol (v/v), 0.15%, and 0.15% (v/v) Triton X-100). After the volume of the lysate flowed through, the column was washed twice with 30 ml of QC buffer (1 M NaCl, 50 mM MOPS pH 7.0, and 15% (v/v) isopropanol). DNA was eluted by applying 15 ml of buffer QF (125 mM NaCl,

50mM Tris-HCl pH 8.5, and 15% (v/v) isopropanol) and precipitated by adding 11 ml of isopropanol prior to a 10 min incubation on at 4°C. The plasmid DNA was pelleted by centrifuging for at 4000 rpm for 30 min at 4°C, washed twice with 80% ethanol, air dried, and dissolved in dH_2O.

3.2.b Cell culture and transfection methods

3.2.b.1 Bacterial cell culture

Freshly transformed bacteria or were streaked on selection plates (LB, 0.15% (w/v) agar, and 0.1% (v/v) agar), and colonies were allowed to form over night at 37°C. Bacteria colonies, or previously cultured bacteria were picked and applied to a suitable volume of LB medium with 0.1% (v/v) ampicillin, and allowed to grow overnight at 37°C while shaking at 180 rpm. The resulting culture was then collected and pelleted before lysis and purification.

3.2.b.2 Mammalian cell culture

All mammalian (adherent) cells were cultured in a humidified incubator at (95% humidity), at 37°C, and 5% CO_2 (Forma Scientific Labortech GmbH, Göttingen, Germany). Cellstar culture vessels of different formats were used throughout this study as needed (Greiner Bio-One, Frickenhausen, Germany). Cells were considered confluent when visually estimated to have covered 75% of the culture vessel growth area. At this point, cells were passaged by removing the culture medium, washing once with 1 x PBS, applying an appropriate amount of 1 x Trypsin solution with 0.25% (v/v) EDTA (Gibco – Life Technologies, Carlsbad, California) for 2-5 min at 37°C, deactivating the trypsin with 10 ml of 10% (v/v) RPMI 1640 medium, and plating a fraction of the resulting cell suspension new cell culture dishes as required. All cell lines used were cultured in 10% FBS (v/v) RPMI 1640 medium. For long-term

storage, 2-5 million mammalian cells were suspended in 10% DMSO (v/v) FBS, and allowed to thaw at -80°C for 1 day

3.2.b.3 Transfection of plasmid DNA (FuGene)

Cells in log-growth phase were transfected with FuGene and plasmid DNA according to the manufacturers instructions. Typically, each well of a 6-well plate format was transfected with a solution of 2% plasmid DNA (w/v) of serum free RPMI 1640 medium (100 µl) supplemented with 6% (v/v) of FuGene HD reagent pre-incubated for 15 min to allow complexing of DNA to the components of FuGene HD. Depending on the application, 24 – 72 h were allowed to elapse prior to cell use.

3.2.b.4 Transfection of siRNA (HiPerfect)

Prior to each experiment cells were seeded in numbers that allowed for log-growth phase on the day of transfection. SiRNA transfection was typically carried out in 6-well plates. For each well, 1-2 x 10^5 cells growing in 1.9 ml of normal growth medium (RPMI 1640 and 10% (v/v) FBS) were transfected with a 100 µl mixture of serum free RPMI 1640 medium, containing 6 µl of HiPerfect transfection reagent (Qiagen, Hilden, Germany), and 5 µl of a 20 µM stock solution of siRNA. The mixture was applied to each well drop wise. The final concentration of siRNA in each well was 50 nM in a final growth medium volume of 2 ml. For those transfections carried out in 6 cm and 10 cm plates the relevant cell numbers and transfection mixtures are given below.

Format	**6-well**	**6 cm**	**10 cm**
volume of stock (20 µM siRNA) in µl	5	7.5	17.5
serum free medium (µl)	100	150	350
HiPerfect reagent volume (µl)	6.0	9.0	21.0
# of cells seeded	1.0-2.0 x 10^5	4.0 x 10^5	1.5-2.0 x 10^6

3.2.b.5 Transduction of shRNA (lentiviral mediated)

Transduction of VCaP cells with lentiviral particles packaging vectors with anti-AGR3 shRNA sequences was carried out to generate cells with a stable gene knockdown. According to the manufactures instructions, a 5 day protocol was followed. 0.5-1.0 x 10^4 cells were seeded in 96-well plate wells and allowed grow under normal growth conditions for 1 day. To enhance lentiviral transduction, the cell medium was replaced with 110 µl of normal growth medium containing 8 µg/ml of hexadimethrine bromide in addition to a volume of lentiviral particles containing either of three different anti-AGR3 or a control shRNA sequence. The multiplicity of infection (MOI) was maintained at 2 (i.e. 2 particles per cell). After 24 h of transduction, the medium was replaced with 100 µl of normal growth medium and cells allowed to recover for an additional day. Thereafter, normal growth medium with 1 µg/ml or puromycin was applied to cells for selection before expansion of stable transfectants to larger cell culture dish formats.

3.2.b.6 [^{3}H]-thymidine incorporation, short-term proliferation assay

1 x 10^3 cells were seeded in quadruplicate on two 96 well plates. One plate was incubated in normal incubation conditions (90% humidity, 5%CO_2, 37°C) for 1h. 20 µL of Celltiter-Blue reagent (Promega) per well was subsequently applied for each well to indirectly quantify the number of cells in each well. After another hour of incubation the plate was read at 580 nm with a FluoroStar Optima (BMG Labtechnologies) spectrophotometer (excitation: 540nm, gain: 1200). These values were used to normalize the results obtained by the thymidine incorporation proliferation assay. Each well of the second 96-well plate was supplemented with 1µCi (~37kBq) of 5'-[^{3}H]-thymidine (Hartman Analytic, MT-846). Cells were allowed to incorporate the thymidine under normal cell culture conditions. After 12 h, the thymidine-containing medium was removed, and 40µL of trypsin was added to each well. After a further 30 min of incubation under normal cell culture conditions,

the cells were harvested with a Tomtec cell harvester (Wallac-ADL) onto a filter mat (Perkin Elmer), which was subsequently soaked in Insta-Gel Plus liquid scintillation counting cocktail (Perkin Elmer) and read on a liquid scintillation counter (1450 Microbeta, Wallac Jet).

3.2.b.7 Celltiter-Blue, long-term proliferation assay

1 x 10^3 cells were seeded in triplicate in 96-well plates and incubated under normal growth conditions. 1, 24, 72, and 120 h after seeding, cells were supplemented with 20 µl of Celltiter-Blue reagent which was allowed to metabolize for 1 h prior to reading the converted dye signal at 580 nm with a FluoroStar Optima (BMG Labtechnologies) spectrophotometer (excitation: 540nm, gain: 1200). Values from 24, 72, and 120 h were normalized to those obtained at 1 h after seeding at the beginning of the experiment.

3.2.b.8 Celltiter-Blue, viability assay

1 x 10^3 cells were seeded in quadruplicate in 96 well cell culture plates, and treated with either EtOH or 0.5 µM thapsigargin for 12 and 36 h. At each of these time points, 20 µl of Celltiter-Blue reagent was added to the cells and allowed to metabolize over 1 h in normal growth conditions before measuring fluorescence at 580 nm with a FluoroStar Optima (BMG Labtechnologies) spectrophotometer (excitation: 540nm, gain: 1200). % viability was calculated by dividing the fluorescence values of Tg treated cells to matching values of EtOH treated cells at each time point.

3.2.b.9 Determination of protein localization by Immunofluorescence confocal microscopy

For immunofluorescence, cells were cultured in Lab-Tek II Chamber Slide 8-well units (VWR International, Bruchsal, Germany) pre-coated for 24 h

at 37°C with a 100 µl of 1µg/ml fibronectin in 1 x PBS (Sigma-Aldrich, Taufkirchen, Germany). Each well was washed once with 300 µl of 1 x PBS prior to seeding 5 x 10^4 cells and incubating under normal growth conditions. After 24 h, the growth medium was then removed, and the cells washed once with 1 x PBS, prior to fixing at room temperature with 300 µl of 4% (v/v) PFA (paraformaldehyde). After 5 min, cells were washed 3 times with 1 x PBS and permibilized with 300 µl of 1 x PBS – 0.2 % (v/v) Triton X-100 solution for 5 min at room temperature. Cells were then washed twice with 1 x PBS and blocked for 10 min at room temperature with a 1 x PBS with 10% (v/v) FBS solution. The same blocking solution was supplemented with a 0.2% (w/v) concentration of primary antibody and used for staining with both GRP78 (Santa Cruz, California, USA), and AGR3 antibodies (Abcam, Cambridge, UK). Draq5 was diluted in 1 x PBS with 10% (v/v) FBS solution (blocking solution) at a final concentration of 10 µM and was used to stain the DNA in nuclei. Primary antibody and nuclear staining was carried out over 1 h at room temperature. Cells were then washed 3 x with 1 x PBS, and incubated with secondary antibodies. Alexa Fluor 488 Rabbit anti-Mouse (targeting AGR3) and 546 Rabbit anti-Goat (targeting GRP78) antibodies were diluted in the same blocking solution to final concentrations of 0.25 µg/ml and used in a volume of 200 µl. After incubating for 1 h at room temperature shielded from light, cells were washed 3 x with 1 x PBS, dried, and covered with PVA (polyvinyl alcohol) solution before being covered with a glass coverslip (Erie Scientific, Portsmouth, US). Immunofluorescence was visualized using a Zeiss LSM510 confocal microscope operated through the LSM LSe115 image examiner software.

3.2.b.10 Endoplasmic Reticulum stress induction

Endoplasmic reticulum stress was induced in 3 x 10^5 cells in log-growth phase by applying either 0.5 µM of Tg (thapsigargin, Life Technologies, Karlsruhe) Tg, 0.5 µM of Tm (tunicamycin, Sigma-Aldrich), 1 mM DTT (dithiothreitol, Roth, Karlsruhe), or 1 µM H_2O_2 in a final volume of 2 ml of

normal growth medium (10 % (v/v) FBS in RPMI 1640). Control cells were treated with an equal volume of EtOH, DMSO (Fluka, Neu-Ulm), or dH_2O as control for Tg, Tm, and DTT / H_2O_2 respectively. In every experiment, stressed cells in suspension were collected and included in all further analysis.

3.2.b.11 Cell adhesion assay

Prior to the adhesion assay, 96-well plates were coated with 100 µl of fibronectin (5 µg/ml) or Collagen I (10 µg/ml) serum free RPMI 1640 solution for 1 h at 37°C. Wells were then washed 2 times with 1x PBS to remove unbound substrate and blocked with 100 µl of a 10 mg/ml heat-denatured (65°C, 1 h) BSA solution for 30 min at 37°C. The blocking solution was then removed and the wells washed two times with 1 x PBS prior to assaying for substrate specific adhesion. Substrate specific adhesion was assayed by seeding 3 x 10^4 cells suspended in serum-free medium in quadruplicate in fibronectin or Collagen I (coated, and BSA-blocked (10 mg/ml, heat denatured) cell culture media under normal growth conditions (37°C, 5% CO_2, and 95% humidity). Unhindered cell adhesion was estimated by seeding the same number of cells, suspended in normal growth medium (10% FBS (v/v) RPMI 1640) in uncoated wells. 1 h after seeding, cells were washed 3 times with 1 x PBS and fixed with 100% methanol for 5 min at room temperature. After fixation, the methanol was removed, and the cells were air-dried in a fume hood prior to staining with 0.1% w/v crystal violet solution for 30 min at room temperature with gentle shaking. Subsequently, cells were washed with water and the plate allowed to dry at room temperature. The dye trapped in cells was extracted with 100 µl of 10% v/v acetic acid and quantified by measuring absorbance at 595 nm. Substrate specificity (i.e. specific adhesion to either fibronectin or collagen I is reported by the signal from substrate-coated wells as a percentage from uncoated (i.e. unhindered adherence) wells.

3.2.b.12 Chemotactic migration (modified Boyden chamber) assay

Cell migration was assayed using an HTS FluoroBlok multiwell insert system (Becton, Dickinson Biosciences). Prior to seeding in inserts, every 1 x 10^5 cells were labeled by incubating at 37°C with 1 ml of serum free RPMI 1640 containing 1 µM Vybrant DiI live-cell labeling dye (Invitrogen, Eugene, Oregon). After 20 min, cells were washed once with serum free RPMI 1640 and resuspended to a concentration of 2 x 10^5 / ml. To estimate the actual number of cells in suspension, 100 µl from each labeled-cell sample was seeded in a 96-well plate and the number of cells estimated by measuring their signal using a spectrophotometer (FLUOstar OPTIMA, BMG, excitation 520 nm, emission 580 nm, gain 2000, scan matrix 3 x 3). These (input) values were used to normalize migration values and therefore minimize the impact of cell counting error on subsequent migration values. To avoid bubbles below the FluoroBlok membrane, the lower chambers of each well were added 750 µl of chemo attractant (10% FBS in RPMI 1640) first. Subsequently, the upper chambers were filled with 500 µl (~1.0 x 10^5 stained cells) of labeled cell suspension. Each experimental condition was seeded in quadruplicate, and the FluoroBlok insert was incubated in normal growth conditions over 36 h to allow cells to migrate to the bottom chamber. Cell migration was estimated by measuring fluorescence of the cells on the bottom of the FluoroBlok membrane by exciting at 520 nm and reading at 580 nm in a 4 x 4 matrix at gain 2000.

3.2.b.13 Generation of (AGR3) conditioned media

To maximize accumulation of AGR3 protein in the medium, AGR3 inducible 22Rv.1 cells were first pre-induced for 24 h with 5 µM Ponasterone in normal growth medium (10% FBS v/v, in RPMI 1640), then washed once with 1 x PBS before being grown for a further 24 h in serum-free medium with 5 µM Ponasterone A. The same procedure was repeated in the absence of

Ponasterone A to generate serum free medium lacking AGR3 as control. This control serum-free medium was then supplemented with either EtOH or 5 µM Ponasterone A to generate control media. Both control media (with EtOH or just Ponasterone A) and AGR3 conditioned media were supplemented with 10% FBS prior to use.

3.2.c Protein methods

3.2.c.1 Preparation of protein samples from cell lysates

Before lysis, cells were washed once with 1 x PBS and resuspended in a defined volume 1 x PBS prior to estimating cell concentration by counting with a hemocytometer (Fuchs Rosenthal, 0.200mm depth). After the number of cells to be lysed was calculated, cells were pelleted at 1200 rpm for no more than 3 min and the residual supernatant removed. A second centrifugation step of 1 min at 1200 rpm was carried out to remove all suspension solution from the vessel walls, and therefore ensure no additional unwanted volume in lysed cells. The pellet was then suspended in 2 x protein sample buffer (Tris-HCl 160 nM, 4% v/v SDS, 20% v/v Glycerol, 4% v/v 2-ß-mercaptoethanol, and 0.01 w/v bromophenol blue). The volume of sample buffer used was calculated to lyse 4 x 10^4 cells with 1 µl of 2 x sample buffer.

3.2.c.2 Separation of proteins by SDS-PAGE

Gels of either 0.75 or 1 mm thickness were cast using the Mini-PROTEAN 3 system (Bio-Rad, Munich, Germany). For most experiments, a 12 % polyacrylamide separating gel was cast using a mixture of 2.2 ml of dH_2O, 3 ml of 37% w/v acrylamide mix, 1.9 ml of 1.5 M Tris-HCl, 75 µl of 10% w/v SDS, 75 µl of 10% w/v APS (ammonium persulfate), and 5 µl of TEMED (N,N,N',N'-tetramethylethylenediamine). After polymerization, an appropriate volume of stacking gel (2.75 ml of dH_2O, 0.65 ml of 37% w/v acrylamide mix,

0.5 ml of 1.5 M Tris-HCl, 40 µl of 10% w/v SDS, 40 µl of 10% w/v APS (ammonium persulfate), and 4 µl of TEMED (N,N,N',N'-tetramethylethylenediamine) was cast over the polymerized separating gel, and shaped using 10-well or 15-well combs (Bio-Rad, Munich, Germany) of appropriate thickness. Electrophoresis was carried out with an appropriate volume of 1x Laemmli buffer (for 10x, 30.0 g of Tris-base, 144.0 g Glycine, 10.0 g SDS dissolved in 1 l of dH_2O, and diluted 1:10 also in dH_2O), and constant 22.5 mA / 1 mm thick gel over 1.5 h, or until the dye front eluted off the bottom of the vertically set gel.

3.2.c.3 Immunobloting of proteins (Western blot)

SDS-PAGE resolved proteins were transferred to methanol-activated PVDF (polyvinylidene fluoride, Millipore, Schwalbach, Germany) membranes prior to immunobloting. Transfers were performed using a Mini Trans-Blot electrophoretic transfer cell (Bio-Rad, Munich, Germany) in transfer buffer consisting of (for 10x) 58.1 g of Tris-base, 29.3 g of Glycin, dissolved in dH_2O, diluted 1:10 in dH_2O and supplemented with 20% v/v methanol, and a constant 115 V at 4°C with constant mixing for 1.5-2 h. An alternative overnight transfer (8-16 h) used the same blotting buffer and a constant 40 V at room temperature.

After transfer completion, the membrane was blocked with appropriate blocking solution for 30 min – 1 h with gentle shaking, and subsequently incubated with primary antibody diluted in blocking solution for 1 h, or over night at 4°C. The membrane was then washed 3 times for 10 min each in washing buffer 1x TBS-T which was diluted 1:10 from 10x TBS (24.0 g of Tris-base, 80 g of NaCl, and pH 7.6) and supplemented with 0.1% Tween 20 detergent. Secondary antibody was carried out for 30 min to 1 h using the same blocking buffer as the primary antibodies with gentle shaking. Subsequently, the membrane was washed 3 times for 10 min in 1x TBS-T, and incubated with ECL (enhancer of chemioluminescence, Amersham,

Braunschweig, Germany) solution for 1 min, prior to exposure on Fuji Super RX 18x24 film (Ernst Christiansen GmbH, Planegg, Germany).

3.2.c.4 Visualization of blotted proteins on membrane (staining with Coomassie blue)

To visualize blotted proteins, PVDF membranes were stained with coomassie blue solution (45% v/v methanol, 10% v/v acetic acid, 0.01% w/v coomassie blue) for 30 min – 1 h at room temperature with gentle shaking. Subsequently, excess dye was washed off the membrane by incubating for 30 min periods at room temperature with gentle shaking in destaining solution (45% v/v methanol, 10% v/v acetic acid). After adequate destaining, the membrane was rinsed with dH_2O.

3.2.d Bioinformatics methods

3.2.d.1 Gene set enrichment analysis

Gene set enrichment analysis (GSEA) was conducted to analyze the patterns of differentially expressed genes. GSEA is a computational method that determines whether the differential expression of groups of genes between two different conditions is statistically significant (http://www.broad.mit.edu/gsea). Here, differences in the expression of a priori defined gene sets (i.e. a biological pathway) was identified by using GSEA. Enrichment of GO gene sets (gene ontology), which consists of groups of genes annotated by the same GO terms in the Molecular Signature Database (MSigDB) were analyzed against a fold-change ranked list of 1022 genes. Due to the size of the gene list, all GO sets with less than 5 or more than 500 genes were excluded from analysis. Enrichment was computed by evaluating statistical significance against 1000 random permutations.

3.2.d.2 Chip-seq data analysis: read processing and peak calling

Chip-seq data of LNCaP cells treated with either EtOH or 10nM R1881 were obtained from [30] in fastq format. These files were uploaded on the main galaxy project server (https://usegalaxy.org/) and first quality filtered using the "filter by quality" tool, by discarding all reads where the quality of 90% of reads was lower than 20. Reads were then mapped on hg19 (human genome version 19) using bowtie, and the resulting "SAM" format file was converted into the "BAM" format using Samtools 0.1.18. MACS (model based analysis of chip-seq) was used to identify binding sites, and the resulting BED file was converted to GFF format prior to visualizing peaks on the UCSC (University of California Santa Cruz) genome browser website.

3.2.d.3 Graphing software and Statistics

Throughout this study, statistical analysis was carried out using a students t-test unless otherwise specified. Data was visualized in graphs generated using the R environment (3.0.1), with the ggplot2 graphing package (0.9.3.1). Heatmaps were generated using the MEV (multi-experiment viewer) version 4.8.

4. RESULTS

4.1 AGR3 expression is elevated in late-stage PCa patients and the VCaP cell line

One of the unmet challenges of prostate cancer is the ability to distinguish between indolent and aggressive disease. Currently, aggressive prostate cancer diagnosis relies in part on the estimated Gleason score, which rates aggressiveness based on deviation from healthy prostate tissue morphology on a scale of 1 (indolent) to 10 (most aggressive). Early recognition of aggressive disease requires better characterization of supporting molecular mechanisms. Recent studies have revealed several disregulated genes in prostate cancer whose expression correlates positively with an aggressive disease phenotype [86-88]. AGR3 was recently detected as part of a set of genes upregulated in prostate cancer [85]. The present study sought to confirm AGR3 upregulation in prostate cancer, and to determine whether AGR3 expression correlates with aggressive disease.

AGR3 gene expression values and matching Gleason scores were obtained from the Oncomine database, which is a repository of genome-wide gene expression values and associated clinical metadata (e.g. Gleason score) of cancer patients. Any datasets (i.e. group of patient data) lacking normal tissue samples, necessary to confirm AGR3 upregulation in prostate cancer, were excluded from analysis. Within each dataset, patient samples were subdivided into normal (healthy prostate), Gleason 1-7 (low – intermediate disease), and Gleason 8-10 (aggressive disease) categories. Datasets with fewer than 5 samples in any of these categories were deemed to contain an insufficient number of datapoints to establish a trend, and were omitted. AGR3 expression values were plotted against these three categories in the remaining datasets (Figure 3A), and statistical significance of differences estimated using a one-tailed t-test.

In both datasets tested, AGR3 expression in Gleason 1-7 and Gleason 8-10 samples was significantly higher than in normal samples, confirming the

previous observations of AGR3 upregulation in prostate cancer [85]. The Taylor, *et al*. dataset showed significant difference between Gleason 1-7 and 8-10 categories, with the latter containing the highest expression values of AGR3. Similarly, Vanaja, *et al*. contained the highest AGR3 expression values in the Gleason 8-10 category, but yielded only a near-significant difference (p=0.094) in the Gleason 1-7 v.s. 8-10 comparison. Together, these results confirm a previous report of AGR3 upregulation in prostate cancer, and suggest a possible association between AGR3 mRNA expression and aggressive (Gleason 8-10) disease.

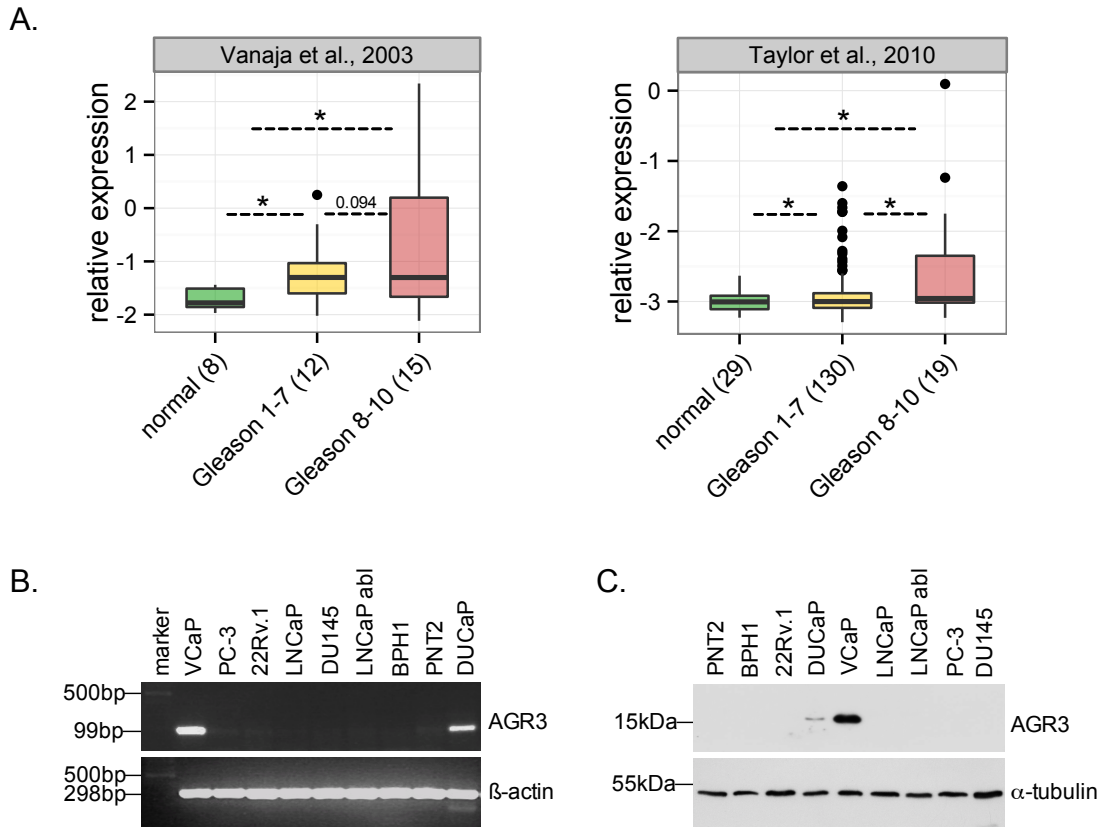

Figure 3. AGR3 expression in prostate cancer patients cell lines.
(A) Log_2 transformed, median centered AGR3 expression values obtained from two Oncomine datasets (www.oncomine.org, studies [89] and [13]) were plotted against normal, low-moderate (1-7), and high (8-10) Gleason scores. Bracketed numbers in the x-axis labels indicate the number of patient samples in each category. The horizontal line within the box indicates the median value. The upper and lower limits of the box indicate the bottom of the 1st and 3rd quartiles (q1 and q3). The vertical lines indicate standard deviation, while round dots above and below each box indicate outliers calculated as follows: below the box = q1 – 1.5(q3-q1), and above the box = q3 + 1.5(q3-q1). A one-tailed t-test was used to evaluate

significant differences between patient categories (* $p<0.05$).
(B) AGR3 mRNA expression in a panel of PCa cell lines was estimated by PCR (polymerase chain reaction) in cDNA samples reverse transcribed from total RNA using AGR3 primers and ß-actin specific primers as control.
(C) AGR3 protein expression in a panel of PCa cell lines was estimated by immunobloting whole-cell lysates with AGR3 and α-tubulin antibody as control.

To study AGR3 in prostate cancer, AGR3 expression was first determined at the mRNA level using PCR in cDNA reverse transcribed from total RNA extracted from a panel of prostate cancer cell lines, as well as BPH1 (benign prostatic hyperplasia derived) and PNT2 (normal prostate epithelium derived) cell lines. (Figure 3B). The highest level of AGR3 mRNA was detected in both DuCaP and VCaP cells, while no expression could be detected in any of the other cell lines. To confirm this result, AGR3 protein expression was examined in whole-cell lysates from the same panel of cell lines by immunobloting with either AGR3 or α-tubulin antibody as control. AGR3 protein expression was detected in VCaP, and faintly in DUCaP cells, confirming expression results obtained at the mRNA level. The VCaP cell line was chosen for further knockdown studies because of higher AGR3 expression at both protein and mRNA level.

4.2 Endogenous AGR3 enhances VCaP cell proliferation

The most distinct feature of prostate malignancy is increased cell proliferation in the epithelium. To determine whether AGR3 influences prostate cancer cell proliferation, its expression was suppressed in VCaP cells using lentiviral-mediated transduction of expression vectors containing an anti-AGR3 shRNA sequence. Three different shAGR3 sequences were used to generate stable AGR3-knockdown in VCaP cells (lanes 4-6, Figure 4B), while a non-target shRNA sequence was used to generate control cells (lanes 1-3, Figure 4B). Suppression of AGR3 protein was confirmed by immunobloting whole-cell lysates of these 6 clones with either AGR3 or ß-actin antibody as control (Figure 4B). The effect of AGR3 on prostate cancer

cell proliferation was determined using the [^{3}H]-thymidine incorporation assay, which measures cell proliferation indirectly by estimating the amount of new DNA synthesis.

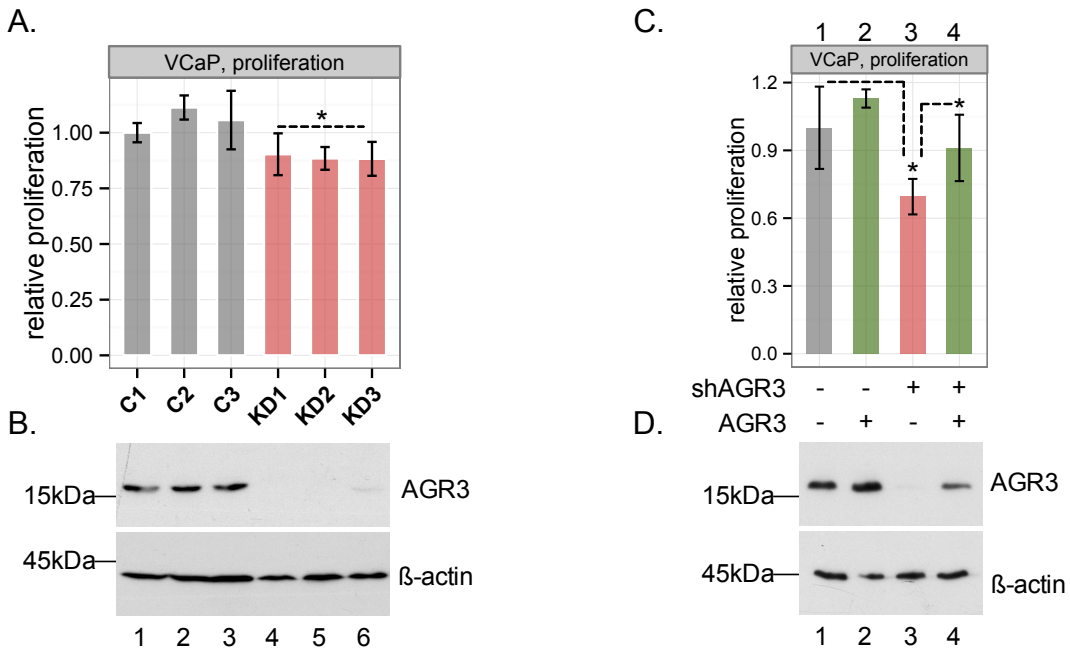

Figure 4. AGR3 enhances VCaP cell proliferation.
(A) AGR3 influence on VCaP cell proliferation. Stable control (C1-3) and AGR3-knockdown (KD1-3) clones were allowed to proliferate in the presence 1µCi (~37kBq) of 5'-[^{3}H] thymidine (specific activity of 20-30 Ci (0.74-1.11 TBq)/mmol). After 12 h, cells were harvested on a filter matt that was soaked in scintillation counting cocktail and the CPM (counts per minute) read on a scintillation beta counter. To minimize cell counting and seeding errors, the number of cells seeded at the beginning of the experiment was determined by incubating for 1 h with Celltiter-Blue reagent followed by quantification with a spectrophotometer (excitation/emission 560/590 nm). CPM values were normalized to Celltiter-Blue fluorescence values, and significance was estimated using a one-tailed t-test. (* $p<0.05$, ns = not significant, mean ± SD, n = 3)
(B) AGR3 protein expression in VCaP cells used in (A). Whole-cell lysates from three control clones (lanes 1-3), obtained using a non-target shCon sequence, and three AGR3-knockdown clones (lanes 4-6), each generated from a unique anti-AGR3 shRNA sequence, were immunoblotted with AGR3 and ß-actin antibody as control.
(C) To rescue the effect observed in (A), AGR3 expression was restored in AGR3-knockdown cells by stably transfecting with AGR3 cDNA (lane 4) or empty vector (lane 3) as control. Control VCaP cells, stably expressing a non-target shRNA sequence, were also transfected with empty vector (lane 1) or AGR3 cDNA (lane 2). Proliferation of these cells was determined using the conditions described in (A). Significance was estimated using a one-tailed t-test. (* $p<0.05$, ns = not significant, mean ± SD, n = 3)
(D) AGR3 expression was determined from whole-cell lysates of cells generated in (C) by

immunobloting with either AGR3 or ß-actin antibody as control.

In this assay, cells are exposed to [^{3}H]-thymidine (a tritium labeled nucleotide), which is incorporated into newly synthesized DNA rendering it quantifiable by measuring radioactivity with a beta scintillation counter. Control and AGR3-knockdown VCaP cells were incubated with 1 µCi (~37kBq) of 5'-[^{3}H]-thymidine for 12 h before determining the amount of [^{3}H]-thymidine incorporated. These same cells were also incubated with 20 µl of Celltiter-Blue reagent for 1 h. The Celltiter-Blue reagent (resazurin) is metabolized by viable cells to resorufin, which fluoresces at 590 nm and indicates the number of viable cells present. Proliferation was determined by normalizing DNA radioactivity measured in CPM (counts per minute) to the fluorescence at 590 nm (Celltiter-Blue measurement) obtained at the beginning of the experiment. This assay revealed reduced cell proliferation in cells with a stable AGR3-knockdown when compared to controls, indicating that endogenous AGR3 sustains prostate cancer cell proliferation (Figure 4A).

To confirm this result, the ability of AGR3 to rescue the reduced proliferation resulting from its suppression was tested by restoring AGR3 expression in the AGR3-knockdown VCaP cells. After transfecting with an AGR3 cDNA-containing vector (lanes 2 and 4, Figure 3D) or empty vector as control (lanes 1 and 3, Figure 3D), AGR3 protein expression was determined in whole-cell lysates by immunobloting with either AGR3 or ß-actin antibody as control. To determine proliferation of these cells, the [^{3}H]-thymidine incorporation assay was used as previously described. Restoring AGR3 expression in AGR3-knockdown cells resulted in significantly increased proliferation when compared to controls (compare 3 and 4 in Figure 4C). In addition, cells with a stable knockdown of AGR3 also showed significantly decreased proliferation (compare 1 and 3 in Figure 4C). However, overexpression AGR3 beyond endogenous levels did not significantly increase proliferation (compare 1 and 2 in Figure 4C), suggesting that near-endogenous AGR3 levels are sufficient to enhance proliferation in VCaP cells. Together, these experiments suggest a positive role for AGR3 in prostate cancer cell proliferation.

4.3 Overexpression of AGR3 enhances prostate cancer cell proliferation

To determine whether the effect of AGR3 on cell growth is limited to VCaP cells, AGR3 protein was stably expressed in three different AGR3-negative prostate cancer cell lines, namely 22Rv.1, LNCaP, and PC-3. To estimate AGR3 expression, whole-cell lysates from control (C1 and C2) and AGR3-expressing cells (#1 and #2) were immunoblotted with either AGR3 or ß-actin antibody for each cell line (Figure 5A, 5C, 5E). [^{3}H]-thymidine incorporation proliferation assays revealed that in these cells moderate AGR3 levels enhanced cell proliferation, but high expression of AGR3 either did not alter (LNCaP and PC-3 cells, #2 in Figure 5D and 5F), or reversed this effect (22Rv.1 cells, #2 in Figure 5B). These results indicate a positive influence of AGR3 on cell proliferation and suggest that this effect is not cell-type specific. However, since not all clones showed increased proliferation, this result may also stem from differences between individual clones (i.e. clonal variation). Alternatively, given that proliferation was reduced or unchanged only in clones with high AGR3 expression, this effect may be due to forced expression of artificially high amounts of AGR3.

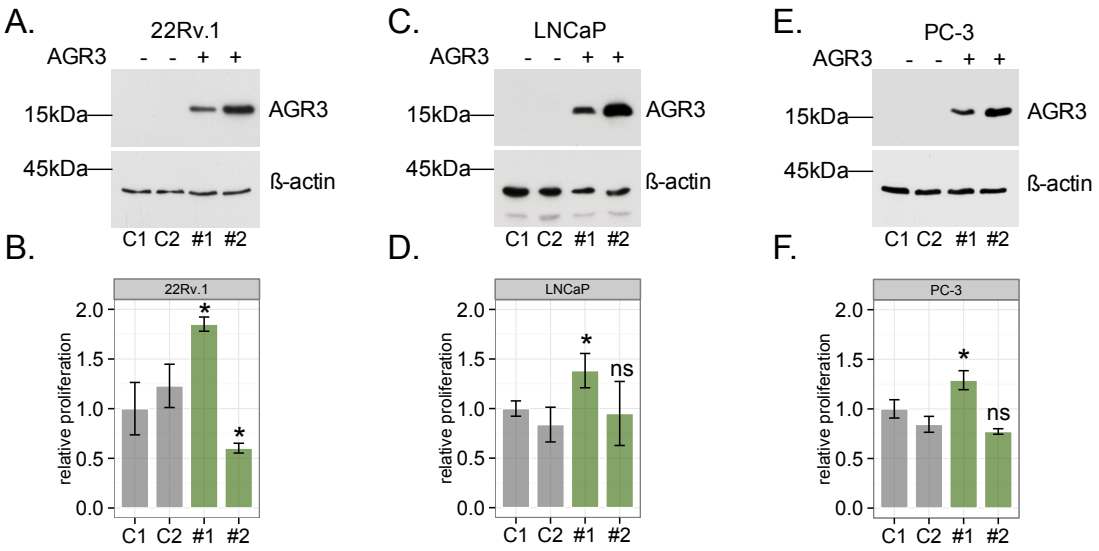

Figure 5. AGR3 enhances proliferation in 22Rv.1, LNCaP, and PC-3 cells.
(A) AGR3 protein expression in 22Rv.1, LNCaP **(C)**, and PC-3 **(E)** cells was detected in two control (C1 and C2) and two AGR3-expressing (A1 and A2) clones by immunoblotting whole-cell lysaes with AGR3 or ß-actin antibody as control.
(B) Proliferation of control, low, and high AGR3-expressing 22Rv.1, LNCaP **(D)**, or PC-3 **(F)** clones was estimated as described previously (Figure 4B). Briefly, 10^3 cells were incubated with either 100 µl of normal growth medium containing 1 µCi (~37kBq) for 12 h, or with 100 µl and 20 µl of Celltiter-Blue reagent for 1 h under nomral gorwth conditions. CPM values from the [^{3}H]-thymidine incorporation were nomralized to 595 nm fluoresence values from metabolized Celltiter-Blue reagent. Significance was computed by comparing each AGR3 expression clone (low and high) with the two control clones, using a one-tailed t-test. (* $p<0.05$, ns = not significant, mean ± SD, n = 3)

To address these possibilities, 22Rv.1 cells were used to generate a cell system in which AGR3 expression is inducible. One of the main advantages of the inducible system is the ability to compare gene expression within a similar genetic background (i.e. in the same clone). To generate the inducible system, cells were first transfected with the Rheo activator/receptor (pNEB-R1 plasmid) and selected with using G418. Cells with stable pNEB-R1 expression were isolated and transfected with the pNEBR-X1 Hygro plasmid, which expresses the AGR3 mRNA under the control of the Rheo activator/receptor. Stable expressers were selected by growing cells in hygromycin B. Once both plasmids were stably expressed, AGR3 expression was induced by stimulating the Rheo activator/receptor with Ponasterone A, an Ecdysone steroid hormone analog that regulates metamorphosis in *Drosophila melanogaster* [90].

One Control and three AGR3 inducible clones (A, B, and C), differing in their maximal AGR3 expression level, were isolated and characterized by treating with either 5 µM of Ponasterone A (to achieve maximal expression) or EtOH as control. AGR3 protein expression was monitored with western blotting every 24 h for 6 days after induction (Figure 6A-D). AGR3 expression in T47D was used as a reference to compare maximal AGR3 protein expression between clones. After application of 5 µM Ponasterone A, Clone A yielded the highest level of AGR3 expression, followed by clone B, and then clone C which expressed AGR3 at only moderate levels. Maximal expression was detected 48 h after treatment and steadily declined over the next 96 h (Figure 6A). As expected, treatment of the Control clone with Ponasterone A, or treatment of any clone with EtOH, did not result in AGR3 expression.

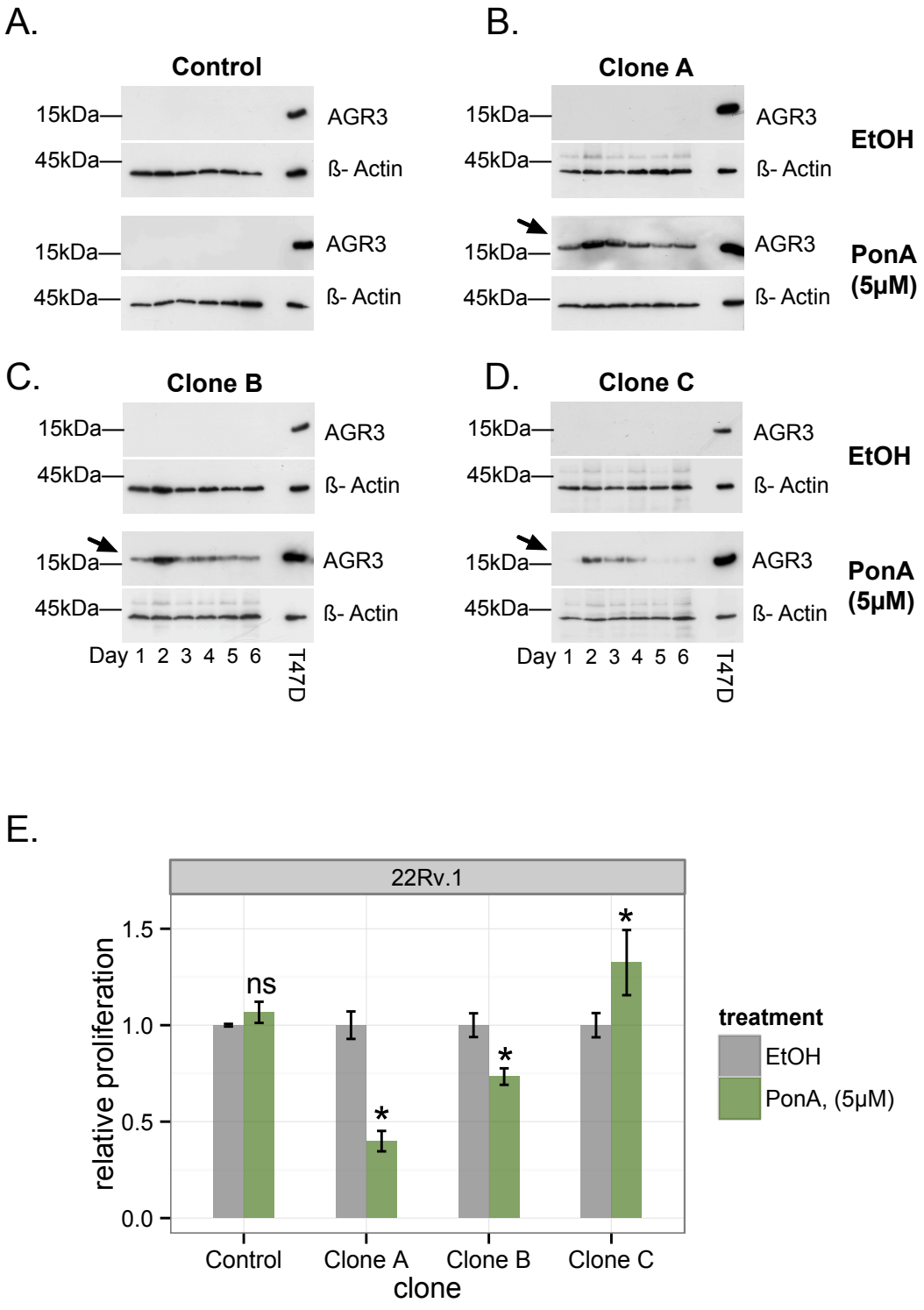

Figure 6. Inducible AGR3 overexpression in 22Rv.1 cells leads to contrasting effects on growth dependent on AGR3 expression level.

(A) Characterization of 22Rv.1 cells with inducible AGR3 expression. In AGR3 inducible 22Rv.1 cells, AGR3 expression was induced by activating the stably expressed Rheo activator/receptor with either 5 µM Ponasterone A. An equal amount of EtOH was applied as control. AGR3 expression was monitored at the protein level by obtaining whole-cell lysates every 24 h over 6 days, and immunobloting with AGR3 and ß-actin antibodies as control. A

constant amount of T47D breast cancer cell lysate, which express high levels of endogenous AGR3, was included as a reference to compare maximal AGR3 expression between inducible 22Rv.1 clones.
(B) Expression level determines the effect of AGR3 on 22Rv.1 cell proliferation. The proliferation of Control, and Clones A-C was measured by pre-treating 1 x 10^3 cells for 24 h with 5 µM of Ponasterone A or EtOH as control in normal cell culture growth medium before supplementing with 1 µCi of 5'- [^{3}H]-thymidine for 12 h or 20 µl of Celltiter-blue reagent for 1h. Proliferation values were computed by normalizing CPM counts to absorbance at 595 nm for each sample. Significance was estimated using a one-tailed t-test. (* $p<0.05$, ns = not significant, mean ± SD, n = 3).

To estimate the effect of AGR3 expression on proliferation using the inducible system, an equal number of cells from Control and AGR3-inducible clones (A, B, and C) were treated with either 5 µM Ponasterone A or an equal volume of EtOH as control under normal growth conditions for 24 h before carrying out a 12 h [^{3}H]-thymidine incorporation assay. Proliferation of the Control clone was not affected by the application of Ponasterone A indicating the absence of any pleiotropic effects from ligand application (Figure 6B). Proliferation of clones A and B (high expressers) was reduced, while proliferation of clone C (moderate expresser) was enhanced. Moreover, Clone A, which expresses the highest amount of AGR3 upon induction, also showed the greatest reduction in proliferation. Together, these results provide additional evidence of the positive effect of AGR3 on prostate cancer cell proliferation, and indicate that the reduction of proliferation observed may be due to artificially high levels of expression.

Another aspect of the inducible system is the ability to tune the expression of the gene of interest by changing the amount of inducing ligand (Ponasterone A) applied. To show that moderate AGR3 levels enhance proliferation in a clone independent manner, different levels of AGR3 expression were induced by pre-treating Control and Clone A cells with either 0.5, 1, 2.5 and 5 µM of Ponasterone A or EtOH as control over 24 h. To monitor expression level, a fraction of cells from each treatment was used to generate whole-cell lysates immunoblotted with AGR3 or ß-actin antibody as control (Figures 7A and 7B).

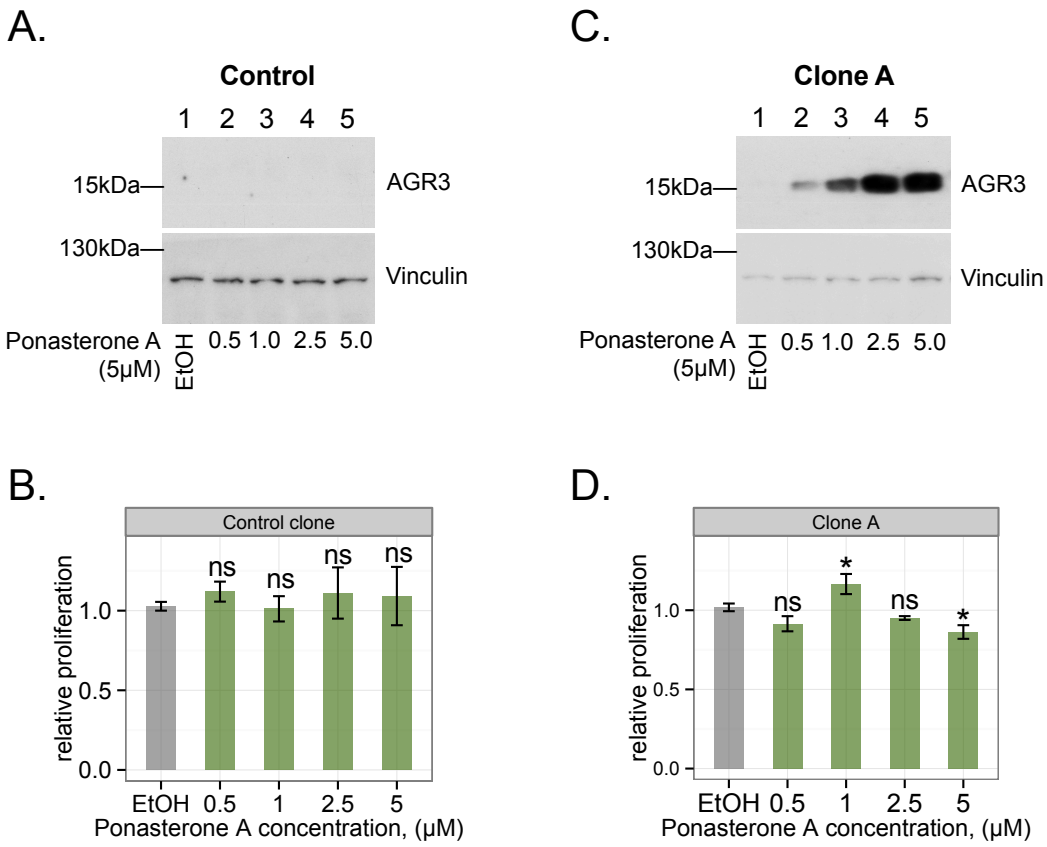

Figure 7. Modulating AGR3 expression levels alters 22Rv.1 cell proliferation.
(A) Whole-cell lysates obtained from Control and Clone A cells treated with a range of Ponasterone A concentrations (0.5, 1, 2.5, and 5 μM) or EtOH as control for 24 h were immunoblotted with either AGR3 or Vinculin antibody as loading control.
(B) Control and Clone A cells pre-treated for 24 h with a range of Ponasterone A concentrations (0.5, 1, 2.5, and 5 μM) or EtOH were used to carry out a [^{3}H]-thymidine proliferation assay. Briefly, 1 x 10^3 cells were grown in normal growth medium supplemented with either 1 μCi of [^{3}H]-thymidine for 12 h or 20 μl of Celltiter-Blue reagent for 1 h. Proliferation values were computed by normalizing CPM counts to absorbance at 595 nm for each sample. Significance was estimated using a one-tailed t-test. (* $p<0.05$, ns = not significant, mean ± SD, n = 3).

AGR3 expression was lowest at 0.5 μM of Ponasterone A, and increased gradually to maximal levels when induced with 5 μM of ligand. No AGR3 expression could be detected in Control cells treated with Ponasterone A, or any cells treated with EtOH. To measure proliferation of the pre-induced cells, a [^{3}H]-thymidine incorporation assay was carried out for 12 h. Ponasterone A treatment did not affect proliferation at 0.5 or 2.5 μM, decreased proliferation at 5 μM, but enhanced it at 1 μM of ligand (Figure 7D),

confirming that AGR3 enhances proliferation, and demonstrating that induction of abnormally high amounts of this protein abrogates and even reverses this effect.

To further confirm this effect, an alternative long-term assay was used to measure cell proliferation in the AGR3-inducible 22Rv.1 cell system. In the Celltiter-Blue proliferation assay, conversion of the fluorescent reagent resazurin into to resorufin by metabolically active cells provides an indirect means of estimating cell number. The conversion rate of this reaction correlates linearly with the number of cells resazurin is exposed to, and indirectly reveals cell proliferation. Inducible Clones A, B and C, as well as the Control clone were treated with 5 µM Ponasterone A or EtOH as control and used in a long-term proliferation assay carried by sampling at 1, 3, and 5 days after induction.

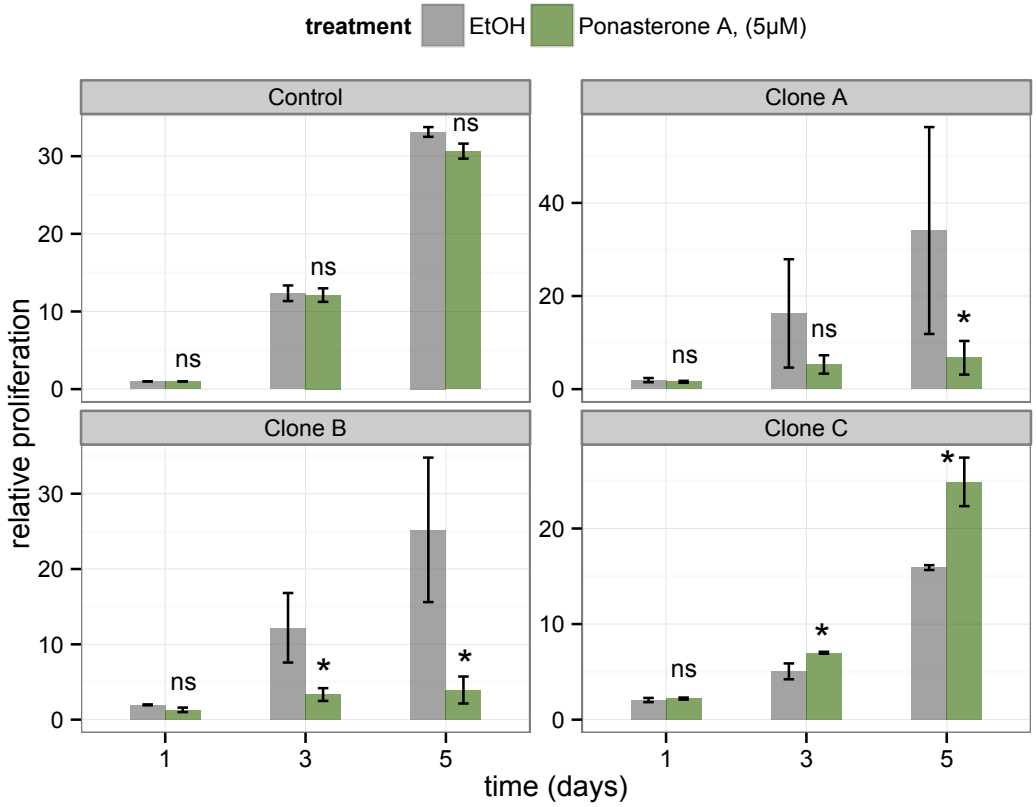

Figure 8. Long-term effect of AGR3 expression in inducible 22Rv.1 cells.
1 x 10^3 cells were treated with 5 µM of Ponasterone A or EtOH as control, and incubated under normal growth conditions. 1, 24, 72, and 120 h after seeding, cells were supplemented

with 20 µl of Celltiter-Blue reagent which was allowed to metabolize for 1 h prior to reading the converted dye signal at 595 nm with a spectrophotometer. Values from 24, 72, and 120 h were normalized to those obtained at 1 h after seeding at the beginning of the experiment. Significance was estimated using a one-tailed t-test. (* $p<0.05$, ns = not significant, mean ± SD, n = 3).

In this assay, Clones A and B showed dramatically reduced proliferation by day 5, while Clone C showed significantly increased proliferation confirming previous results obtained using the [^{3}H]-thymidine based assay (Figure 8). The Control clone did not show any significant differences between EtOH and Ponasterone A treatments suggesting no adverse effects from long term exposure to ligand.

Together, the results of the [^{3}H]-thymidine incorporation and Celltiter-Blue assays indicate a positive role for AGR3 in prostate cancer cell proliferation. In subsequent experiments, only 22Rv.1 cells stably expressing proliferation-enhancing levels of AGR3 were used.

4.4 Secreted AGR3 enhances prostate cancer cell proliferation

The AGR3 protein contains an N-terminal signal peptide that targets it for secretion. Its close homolog, AGR2, has a similar signal peptide and is secreted to the extracellular space where it participates in a diverse set of functions [59]. For example, extracellular nAG, an AGR2 homolog in adult *A. maculatum*, is able to induce proliferation of blastema cells in culture, while extracellular *H. sapiens* AGR2 plays a role in adhesion and migration [35, 46, 78, 82]. Given the extracellular roles of AGR gene homologs, this study sought to find out whether AGR3 is also a secreted protein, and if so, whether extracellular AGR3 contributes to prostate cancer cell proliferation.

To find out whether AGR3 is a secreted protein, 22Rv.1 cells were transiently transfected with either empty or AGR3 cDNA-containing vector. Untransfected 22Rv.1 cells were included as an additional control. After 24 h of transfection, medium was collected and medium protein and matching whole-cell lysate samples were immunoblotted with AGR3 and ß-actin

antibody as control. Empty vector and untransfected control cells displayed no detectable AGR3 protein, which was detected only in the lysate and medium of cells transfected with the AGR3 cDNA-containing vector (Figure 9A). The presence of this protein in the medium suggests that, similar to AGR2, AGR3 is also a secreted protein.

AGR3-conditioned medium was generated and used to study the role of extracellular AGR3 in prostate cancer cell proliferation. The amount of AGR3 in AGR3-conditioned media was optimized using in 22Rv.1 inducible cells. AGR3 expression was induced in Clone A 22Rv.1 cells (AGR3 inducible) using a range of different (0.1, 0.5, 1.0, 2.5, 5.0 μM) Ponasterone A concentrations or EtOH as control. Secreted protein samples were obtained by precipitating medium proteins with 10 μl of Strataclean resin, and eluting with Laemmli buffer. Together with corresponding whole-cell lysates, these samples were immunoblotted with AGR3 and α-tubulin as control. Similarly obtained secreted and whole-cell lysate T47D samples were included to compare the amount of secreted AGR3 protein to that secreted by T47D. Induction of AGR3 protein was detected in cells treated with 2.5 and 5 μM Ponasterone A, and secretion was observed for the same set of samples (Figure 9B). The highest level of secreted AGR3 protein was observed in cells treated with 5 μM Ponasterone A (Figure 9B). Together, these results indicated that induction of AGR3 protein in Clone A cells with 5 μM Ponasterone A for 24 h was optimal to generate AGR3-conditioned medium.

To find out whether secreted AGR3 protein plays a role in proliferation, AGR3-conditioned and control media were generated using AGR3-inducible 22Rv.1 cells. Clone A cells were pre-induced for 24 h with 5 μM Ponasterone A in 10% FBS v/v (fetal bovine serum) growth medium to generate an initial amount of AGR3 expression. These cells, were then washed with 1xPBS (phosphate buffered saline) to remove any residual FBS and grown for a further 24 h in serum-free medium with 5 μM Ponasterone A to induce additional AGR3 expression and secretion (3), or without as control. The latter medium, which did not include Ponasterone A, and therefore contained no secreted AGR3, was used to generate control media (1 and 2) by adding either EtOH or 5 μM of Ponasterone A respectively (Figure 9C).

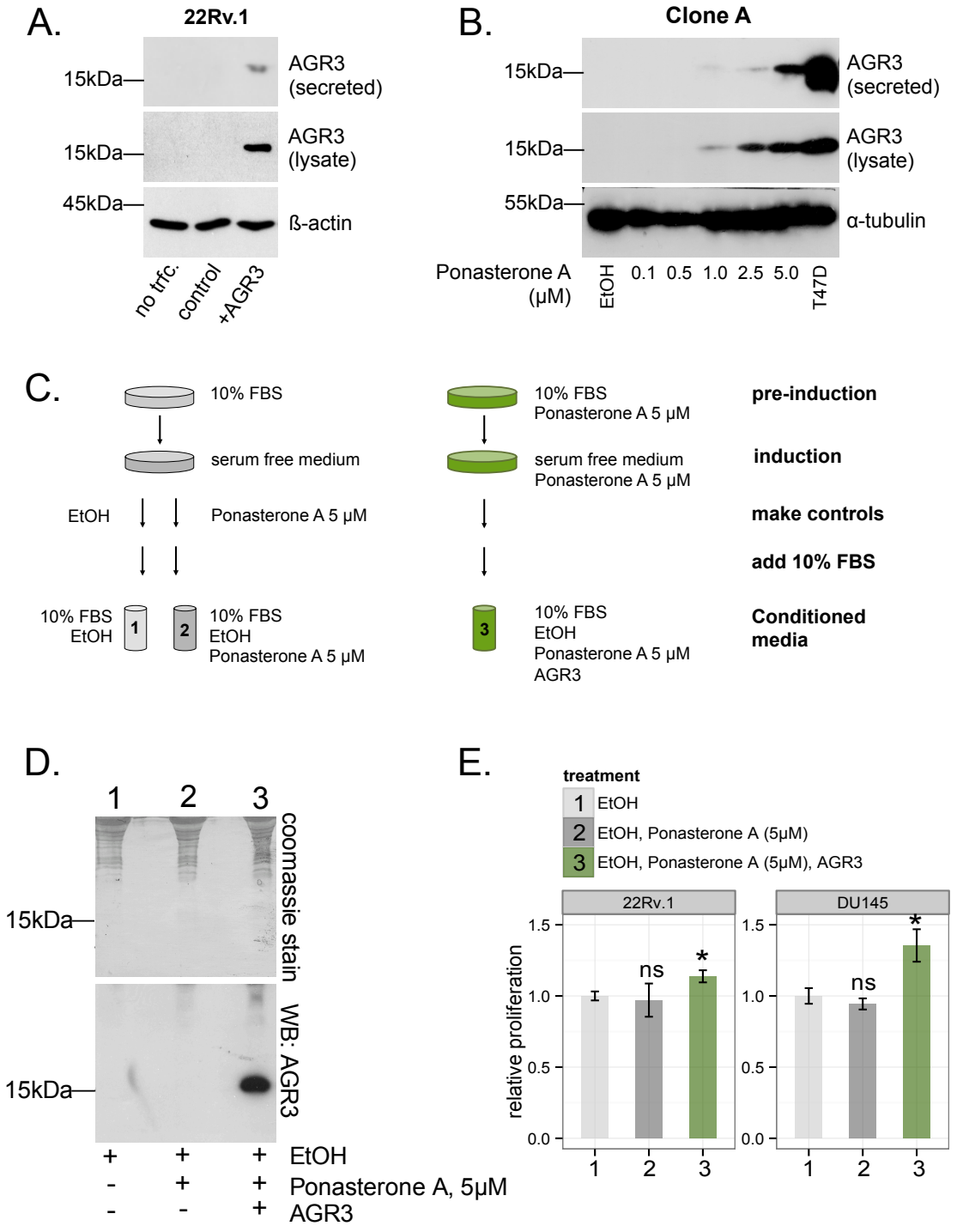

Figure 9. Secreted AGR3 has a moderate effect on prostate cancer cell growth.
(A) AGR3 protein is secreted by prostate cancer cells. 22Rv.1 cells were transiently transfected for 24 h with empty or AGR3 cDNA as control. An additional sample of non-transfected (no trfc.) cells was included as control. After 24 h, medium protein samples were obtained by precipitating medium proteins Strataclean resin followed by elution in Laemmli sample buffer. Secreted and whole-cell lysate protein samples were immunoblotted with

AGR3 and ß-actin antibody as control.
(B) Optimization of AGR3 protein concentration in conditioned media. AGR3-inducible Clone A (22Rv.1) cells were treated for 24 h with a range of Ponasterone A concentrations (0.1, 0.5, 1, 2.5, and 5 µM) or EtOH as control. Secreted protein samples were obtained by precipitating medium proteins using Strataclean resin followed by elution in Laemmli sample buffer. Secreted and whole-cell lysate protein samples were immunoblotted with AGR3 and α-tubulin antibody as control. T47D secreted or whole-cell lysate protein samples were immunoblotted in parallel as positive control.
(C) The strategy used to generate control (1 and 2) and AGR3-conditioned media (3). To maximize accumulation of AGR3 protein in the medium, Clone A 22Rv.1 cells were first pre-induced for 24 h with or without 5 µM Ponasterone in normal growth medium (includes 10% v/v FBS). Cells were then washed once with 1 x PBS and grown for a further 24 h in serum-free medium with or without 5 µM Ponasterone A. Serum-free medium without Ponasterone A, and therefore without AGR3, was supplemented with EtOH or 5 µM Ponasterone A to generate control media 1 and 2 respectively.
(D) Detection of AGR3 protein in conditioned media. Medium proteins in media 1, 2, and 3 were detected as described in (A). Medium and matching whole-cell lysate protein samples were immunoblotted with AGR3 antibody as control. After AGR3 detection, proteins trapped on the PVDF membrane were stained with coomassie blue dye to show equal loading of samples.
(E) 22Rv.1 Control clone (non-inducible) and DU145 cells were grown using conditioned media 1, 2, and 3 for 48 h prior to a 12 h [^{3}H]-thymidine incorporation based proliferation assay carried as described previously. Significance was estimated using a one-tailed t-test. (* $p<0.05$, ns = not significant, mean ± SD, n = 3).

To confirm AGR3 presence in the medium, secreted protein samples from media 1-3 were obtained by precipitating medium proteins with Strataclean resin, and eluting in Laemmli sample buffer. Subsequently, these samples were immunoblotted with AGR3 antibody. As expected, AGR3 was readily detected in medium 3, but not in control media 1 and 2 (Figure 9D).

Conditioned media 1-3 where used to grow Control clone 22Rv.1 cells that do not express AGR3 after Ponasterone A application. To rule out any influence of endogenous cellular AGR3, DU145 prostate cancer cells, which have no detectable AGR3 expression at the protein level, were also included in this experiment. After 48 h of growth in either control (1 and 2) or AGR3-conditioned (3) media, 22Rv.1 and DU145 cells reseeded for a [^{3}H]-thymidine incorporation proliferation assay. Proliferation was calculated by normalizing CPM values obtained after an additional 12 h of growth in conditioned media 1-3 supplemented with 1µCi of 5'-[^{3}H]-thymidine to fluorescent values measured at 590 nm (Celltiter-Blue) obtained at the beginning of the [^{3}H]-thymidine treatment. Proliferation of Control clone 22Rv.1 cells was slightly

but significantly increased after growth in AGR3-conditioned medium (Figure 9E). Furthermore, AGR3-negative DU145 cells showed a more pronounced increase in proliferation after treatment with AGR3 conditioned media, suggesting that a portion of AGR3-mediated increase in cell proliferation may be attributable to secreted AGR3 protein. Together, these results confirm secretion of a fraction of AGR3 protein, which may play a role in prostate cancer cell proliferation.

4.5 AGR3 expression modulates migration and adhesion of prostate cancer cells

In addition to increased proliferation, cancer cells adhere to substrate and have a higher tendency to migrate than non-cancer cells. Since AGR3 expression was found to correlate with advanced prostate cancer (Gleason scores 8-10) in which cells commonly spread beyond their tissue of origin, a possible role of AGR3 was hypothesized in cell migration.

Migration of previously generated AGR3 knockdown clones (see Figure 4B) was assessed using the Boyden chamber assay, in which cells seeded on the upper chamber of a two a two-chamber setup migrate across a separating membrane toward a chemo attractant present in the lower chamber. In this iteration of the Boyden chamber assay, cell migration was tracked by measuring the fluorescence of cells stained with Vybrant DiI (a non-toxic lipophilic cell-membrane dye used to stain live cells) on the lower-chamber facing side of the membrane using a spectrophotometer. To reach the lower chamber, cells sense the normal growth medium (chemo attractant) and then traverse the membrane through 8 µm (diameter) pores.

In this experiment, stained cells were suspended in serum-free medium and allowed to migrate toward normal cell growth medium (containing 10% v/v FBS) over 36 h under normal cell growth conditions. The amount of stained cells detected on the lower-chamber facing side of the membrane was visually inspected using a fluorescent microscope, and then quantified by

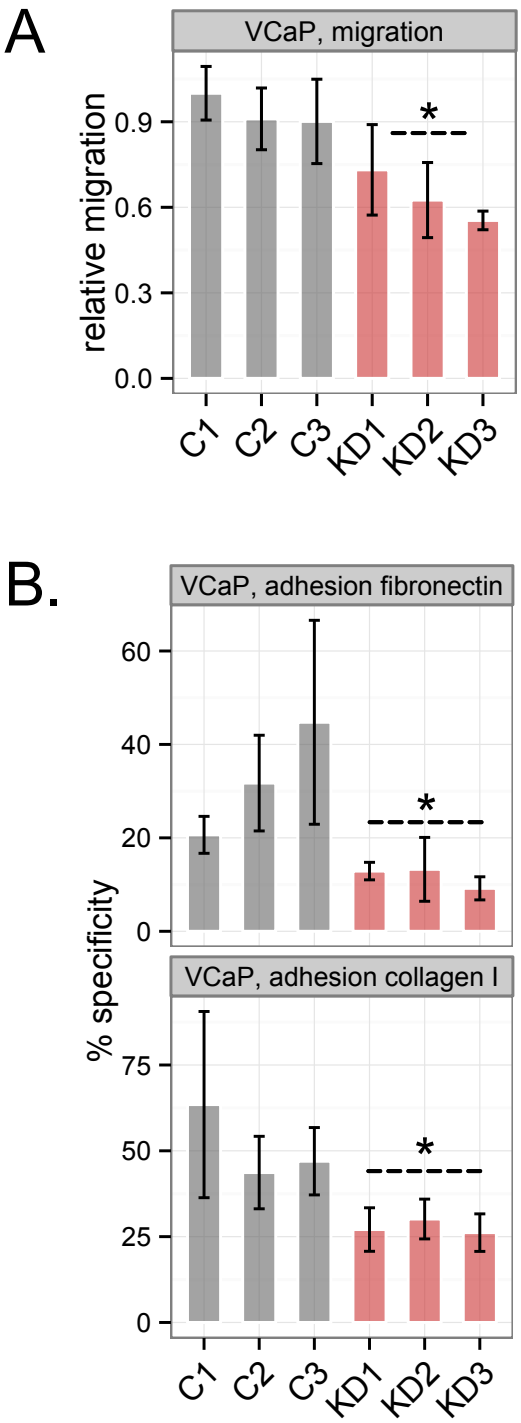

Figure 10. AGR3 affects the migration and adhesion of VCaP cells.
(A) Migration of control (C1-3) and AGR3-knockdown (KD1-3) VCaP cells. Vybrant DiI stained cells were seeded in quadruplicate in the upper chamber of 24-well BD cell culture inserts (Boyden chambers). Cells were allowed to migrate for 36 h toward growth medium supplemented with 10% v/v FBS. The number of migrated cells was estimated by measuring fluorescence at 495 nm. Significant differences were estimated using a one-tailed t-test. (* $p<0.05$, mean ± SD, ns = not significant, n = 3)
(B) Substrate specific adhesion of control (C1-3) and AGR3-knockdown (KD1-3) VCaP cells. Control or AGR3-knockdown cells were suspended in serum free medium and seeded in fibronectin or Collagen I coated cell culture plates under normal growth conditions. Unhindered binding was measured by seeding the same number of cells, suspended in normal growth medium in uncoated wells. 1 h after seeding, cells were fixed with methanol, and stained with crystal violet. The dye trapped in cells was extracted with acetic acid and quantified by measuring absorbance at 595 nm. Substrate-specific adhesion (i.e. substrate specificity) was determined by expressing substrate coated adhesion values as a percentage of unhindered adhesion values. (* $p<0.05$, mean ± SD, ns = not significant, n = 3)

measuring and averaging fluorescence at 9 different locations arranged in a 3 x 3 matrix in each well. The fluorescence of cells remaining in the upper chamber is blocked from detection by the membrane, and does not contribute to the detected signal. To minimize error due to cell seeding, the fluorescence of a sample of stained cell suspension from each clone was quantified at the beginning of every experiment, and used subsequently to normalize migration values. In this experiment the number of cells migrating to the bottom chamber for VCaP cells with a stable AGR3 knockdown (KD1-3)

was lower than that of controls (C1-3), indicating decreased VCaP cell migration in the absence of AGR3 (Figure 10A).

Cell migration depends on efficient reorganization of cell adhesion, a process that includes cell-substrate (extracellular matrix) interactions [91]. To determine whether reduced migration was associated with altered cell adhesion, the same VCaP cells, with or without a stable AGR3 knockdown, were assayed for their ability to adhere to extracellular matrix substrate proteins such as fibronectin and collagen I. Substrate affinity was estimated by plating cells in collagen I or fibronectin coated culture dishes blocked with heat denatured BSA to prevent any direct adhesion of cells to plastic. Cells were suspended in either serum-free medium and seeded in substrate-coated wells, or normal growth medium and seeded in uncoated wells to estimate unhindered adhesion rates. Unattached cells were removed by washing with 1xPBS prior to fixing with methanol and staining with crystal violet dye. The trapped crystal violet was subsequently extracted with acetic acid from attached cells and quantified by measuring absorbance at 595 nm. Substrate specific adhesion (i.e. to collagen I or fibronectin) was quantified by amount of cells attached to substrate-coated wells (specific adhesion) expressed as a percentage of cells attached to uncoated wells (unhindered adhesion). Compared to controls, AGR3-depleted VCaP cells showed reduced binding to both fibronectin and collagen I, indicating impaired cell interaction with key components of the extracellular matrix (Figure 10B, upper and lower chart).

Together, these results indicate that AGR3 may play a role in prostate cancer cell migration by modulating cell adhesion.

4.6. AGR3 suppression results in increased Lumican mRNA expression

To characterize the mechanism of action of AGR3, data from a genome-wide gene expression experiment comparing control and AGR3-depleted VCaP cells was analyzed. AGR3 suppression in previously generated control and AGR3-knockdown VCaP clones was confirmed at the protein level by immunobloting whole cell lysates with AGR3 or α-tubulin as control, and at the mRNA level through qPCR (quantitative polymerase chain

reaction) with cDNA template reverse transcribed from total RNA obtained from the same cells (Figure 11A).

Subsequently, total RNA samples from a *single sample* of each shCon and shAGR3 were extracted, reverse transcribed to cDNA, and applied to Human Genome U133 Plus 2.0 array chips by Dr. L. Klein-Hitpass (Universität Duisburg-Essen, Essen, Germany) who used the MAS 5.0 (Affymetrix® Microarray Software suite 5.0) software to generate gene expression values and associated detection p-values, as well as fold-change differences between this pair of samples. Given that only one sample was analyzed from shCon and shAGR3 cells, the list differentially regulated genes was filtered on the basis of detection and expression fold-change p values (caption, Figure 11B) produced by the MAS 5.0 software that compares probe sets (11 pairs of 25-nucleotide long match and mismatch oligomers) for each gene.

Furthermore, reduction in experimental noise was sought by excluding from analysis a minority of genes with expression values below 330 units in both samples (over 15 genes were selected for qPCR validation and 330 is the lowest expression value of a successfully validated difference in gene expression). The remaining 1022 (out of 3240) genes were arranged according to phenotype (i.e. “upregulated” and “downregulated” after AGR3 suppression), ranked based on expression fold-change values (shAGR3 vs. shCon), and visualized in red-yellow (expression value) and red-green (fold-change) heatmaps (Figure 11B).

To extract biological information on AGR3 function, the ranked 1022 gene list established in the previous step (Figure 11B) was used to compute GO (gene ontology) gene set enrichment analysis using the GSEA 2.0 (gene set enrichment analysis) desktop software. GSEA computes enrichment based on the distribution of genes from a gene set (e.g. a GO gene set) along a ranked gene list (here the 1022 genes) [92]. GO gene set enrichment was determined according to p value. The gene list in Figure 11B contained 21 significantly enriched GO gene sets (p values of less than 0.05) that broadly describe changes in developmental, neurological, and extracellular matrix related processes (Figure 11C).

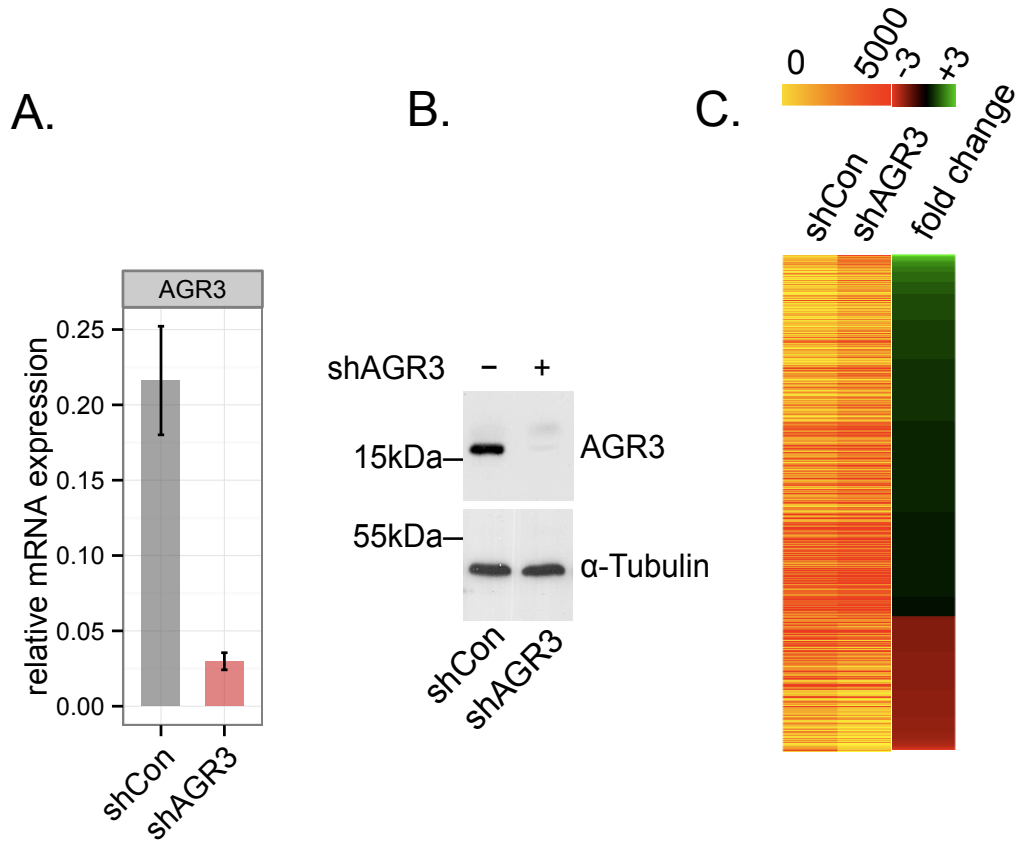

D.

GO gene set	p value
system development	0.002
nervous system development	0.003
proteinaceous extracellular matrix	0.004
signal transduction	0.007
extracellular matrix	0.007
system process	0.015
neurological system process	0.020
anatomical structure development	0.022
receptor binding	0.022
multicellular organismal development	0.024
intracellular signaling cascade	0.025
kinase binding	0.032
extracellular matrix part	0.033
tissue development	0.037
response to external stimulus	0.045
extracellular region	0.046
nucleolus	0.046
substrate specific transporter activity	0.046
protein kinase binding	0.047
extracellular region part	0.047
epidermis development	0.048

Figure 21. Genome-wide expression analysis of AGR3 knockdown in VCaP cells reveals overrepresentation of extracellular matrix and developmental processes.
(A) AGR3 mRNA expression of control (shCon) and AGR3-knockdown (shAGR3) cells used in genome-wide expression analysis experiment. Relative AGR3 mRNA expression was determined using qPCR in cDNA reverse transcribed from the total RNA of control and AGR3-knockdown cells. (mean ± SD, n = 3)
(B) Whole cell lysates from control or AGR3-depleted VCaP cells used in genome-wide expression analysis experiment were immunoblotted with AGR3 and α-tubulin as control.
(C) Genome wide-gene expression changes as a result of AGR3 depletion in VCaP cells. A Human Genome U133 Plus 2.0 Array chip was used hybridize cDNA reverse transcribed from RNA of control and AGR3-knockdown VCaP cells after 48 h of growth in medium supplemented with 3% v/v (charcoal-stripped calf serum) and EtOH for 24 h. This treatment was performed as part of an experiment designed to investigate androgen regulation in VCaP cells. Probe intensities were converted to expression values, fold-change ratios, and associated change p-values using the MAS5 algorithm implementation of the Affymetrix software suite. Genes with a detection p-value less than 0.05 in both samples were included in this analysis. After carrying out the shAGR3 treatment vs. shCon comparison, all genes with fold-change p-values greater than 0.0001 were excluded from further analysis. In addition, a minority of genes with signal values below 330 units in both samples, deemed to be too low to bear biological significance, were removed from the fold-change ranked list of genes. The 330 cutoff value was determined after qPCR validation of over 15 genes. 330 is the lowest microarray derived expression value of a successfully validated difference in gene expression using qPCR. The remaining 1022 out of 3240 genes were ranked according to fold change on the shAGR3 v.s. shCon comparison and visualized on a red-green heatmap, while matching raw gene expression values were visualized on the adjacent red-yellow heatmap.
(D) GSEA was carried out using the GO term set (category 5 on the MSigDB) of the fold-change ranked list of genes from (B). GSEA was performed against a background of 1000 random GO term (gene sets) permutations using a weighted statistic. In addition, all GO terms with less than 5 or more than 500 genes were omitted from analysis. P-values in red text indicate terms enriched in downregulated genes of the shAGR3 v.s. shCon comparison. Terms highlighted with a gray background were used to carry out leading-edge analysis (i.e. find the top genes driving the enrichment of these terms, see Figure 12A).

Given that processes involving the extracellular matrix are related to cell migration and adhesion, the present study focused on the 5 extracellular matrix related GO gene sets which were investigated further using GSEA “leading edge” analysis. This analysis helps determine which genes are overrepresented (frequently present) within the group of 5 enriched extracellular matrix GO gene sets [92], and are therefore likely to be involved in these processes in the present study.

A.

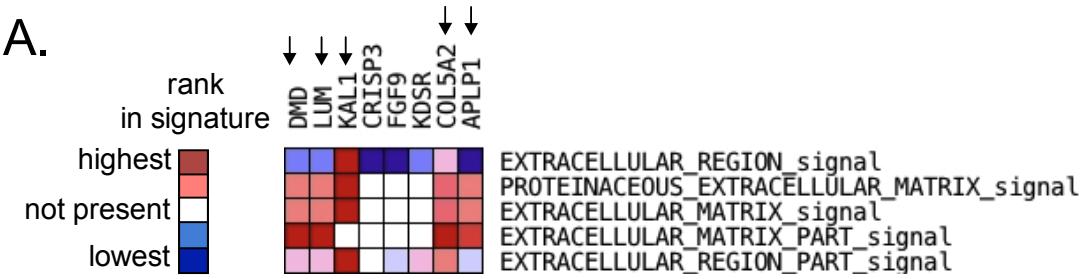

B.

		raw signal	
gene	fold change	shCon	shAGR3
KAL1	2.46	308	736
COL5A2	1.62	336	640
DMD	1.51	338	540
LUM	1.51	14166	22187
APLP1	1.41	930	1094

C.

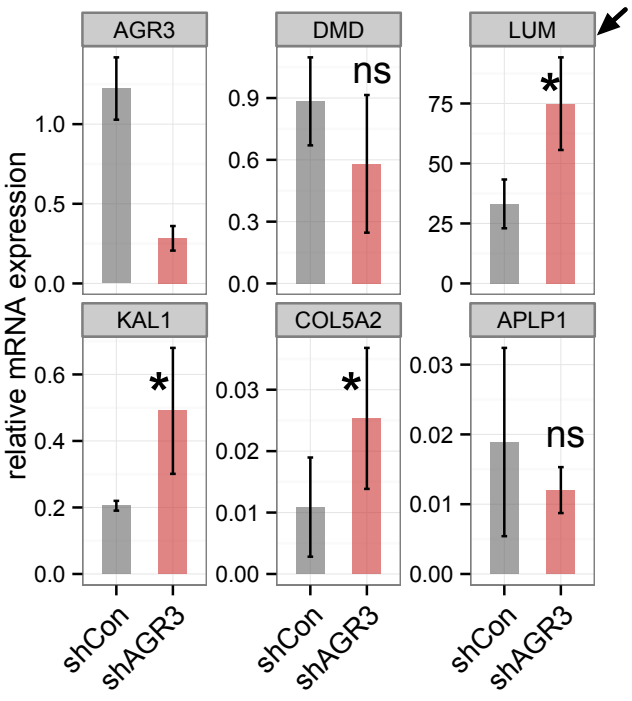

Figure 12. Leading edge analysis and qPCR reveal upregulation of Lumican in AGR3 depleted VCaP cells.

(A) Leading edge analysis of five AGR3-depletion enriched GO terms involved in extracellular matrix homeostasis (highlighted in Figure 11C). In the heatmap, white colour indicates absence from GO term. Red colour intensity indicates high rank (high fold change) within GO term, while blue colour intensity indicates low rank (low fold change). A white cell indicates an absent gene in signature. Arrows indicate genes selected for validation with qPCR.

(B) Gene expression and fold-change values (shAGR3 v.s. shCon) for the 5 overrepresented genes in the leading edges of significantly enriched extracellular matrix related GO gene sets. These fold-change and expression values were calculated by MAS 5.0 when comparing equivalent probe pair intensities in the HG U133 Plus 2.0 array chips for matching probe sets of shAGR3 and shCon samples.
(C) AGR3, DMD, LUM, KAL1, COL5A2, and APLP1 mRNA expression was assessed by reverse transcribing total RNA from triplicate samples of three different shCon (C1-3) and shAGR3 (KD1-3) VCaP clones into cDNA followed by qPCR analysis with AGR3, DMD, LUM, KAL1, COL5A2, APLP1, and RibP0 specific primers. Relative gene expressions were averaged from three different experiments before estimating statistical significance. (* $p<0.05$, mean ± SD, ns = not significant, n = 3)

Leading edge analysis determined a group of genes responsible for the enrichment of the 5 extracellular matrix related GO gene sets. Of these genes, only DMD (Dystrophin), LUM (Lumican), KAL1 (Kallmann syndrome 1), COL5A2 (Collagen V, subunit A2), and APLP1 (Amyloid-like protein 1) were part of almost all 5 gene sets analyzed (e.g. CRSIP3 is *not* present in all gene sets, Figure 12A), and therefore the expression of these 5 genes was considered further.

In the microarray experiment, all 5 of these genes are upregulated in VCaP cells with a stable AGR3 knockdown (Figure 12B). To confirm this result, expression of these 5 genes, and AGR3 as control, was investigated in control and AGR3-depleted VCaP cells by carrying out qPCR with cDNA reverse transcribed from total RNA in triplicate. This analysis confirmed stable AGR3 suppression, and revealed that Lumican, COL5A2, and KAL1, but not DMD or APLP1 were upregulated in shAGR3 VCaP cells (Figure 12C). In addition, Lumican upregulation determined with qPCR was found to be higher than that reported by the microarray experiment, and highest among the genes tested.

Overall, this analysis reveals AGR3 involvement in a diverse set of functions that include extracellular matrix processes, and a link between AGR3 and Lumican gene expression.

4.7. AGR3 affects VCaP cell migration in part by modulating Lumican expression

Lumican is a secreted SLRP (small leucine-rich proteoglycan) implicated in cancer cell migration and adhesion [93-96]. In prostate cancer, external Lumican protein was shown to inhibit migration of LNCaP, PC-3, and DU145 cells [97].

In the present study, AGR3 knockdown lead to Lumican mRNA upregulation, and a decrease in cell migration and adhesion. Together, these data suggest the possibility that AGR3 influences VCaP cell migration and adhesion by modulating Lumican expression. To test this hypothesis, the effect of Lumican on VCaP cell migration and adhesion was investigated in control and AGR3-depleted VCaP cells by transiently suppressing Lumican expression with siRNA.

The expression of AGR3 and Lumican was determined in control and AGR3-depleted cells transfected for 72 h with either siLUM (anti-Lumican siRNA) or siGFP as control before assaying cell migration and adhesion. Total RNA and matching whole-cell lysate samples confirmed knockdown of the AGR3 and Lumican genes at both mRNA and protein level (Figure 13A and B). In addition, these experiments confirmed the previously observed (Figure 12C) upregulation in Lumican expression in AGR3-depleted cells (Figure 13A, right chart, lane 3 and lane 1) at both mRNA (Figure 13A) and protein level (Figure 13B).

To determine the effect of Lumican on VCaP cell migration, after 72 h of siRNA transfection, cells were stained with Vybrant DiI and platted in the upper chamber of BD cell culture insert wells. Normal growth medium containing 10% v/v FBS was used as chemo attractant in the lower chambers. Consistent with the previous results (Figure 10B), AGR3-knockdown VCaP cells showed reduced migration compared to control cells (Figure 13C, compare lane 3 with lane 1). Upon treatment with siLUM, migration of AGR3-knockdown cells was significantly enhanced compared to the same cells treated with siGFP (Figure 13C, compare lane 4 with lane 3). Migration of these cells was no longer significantly different from siGFP-treated control cells (Figure 13C, compare lane 4 with lane 1), suggesting that suppression of

Lumican in AGR3-knockdown cells reverses the loss of migration due to AGR3 suppression. Together, these results suggest that AGR3 suppression affects VCaP cell migration in part by inducing upregulation of Lumican.

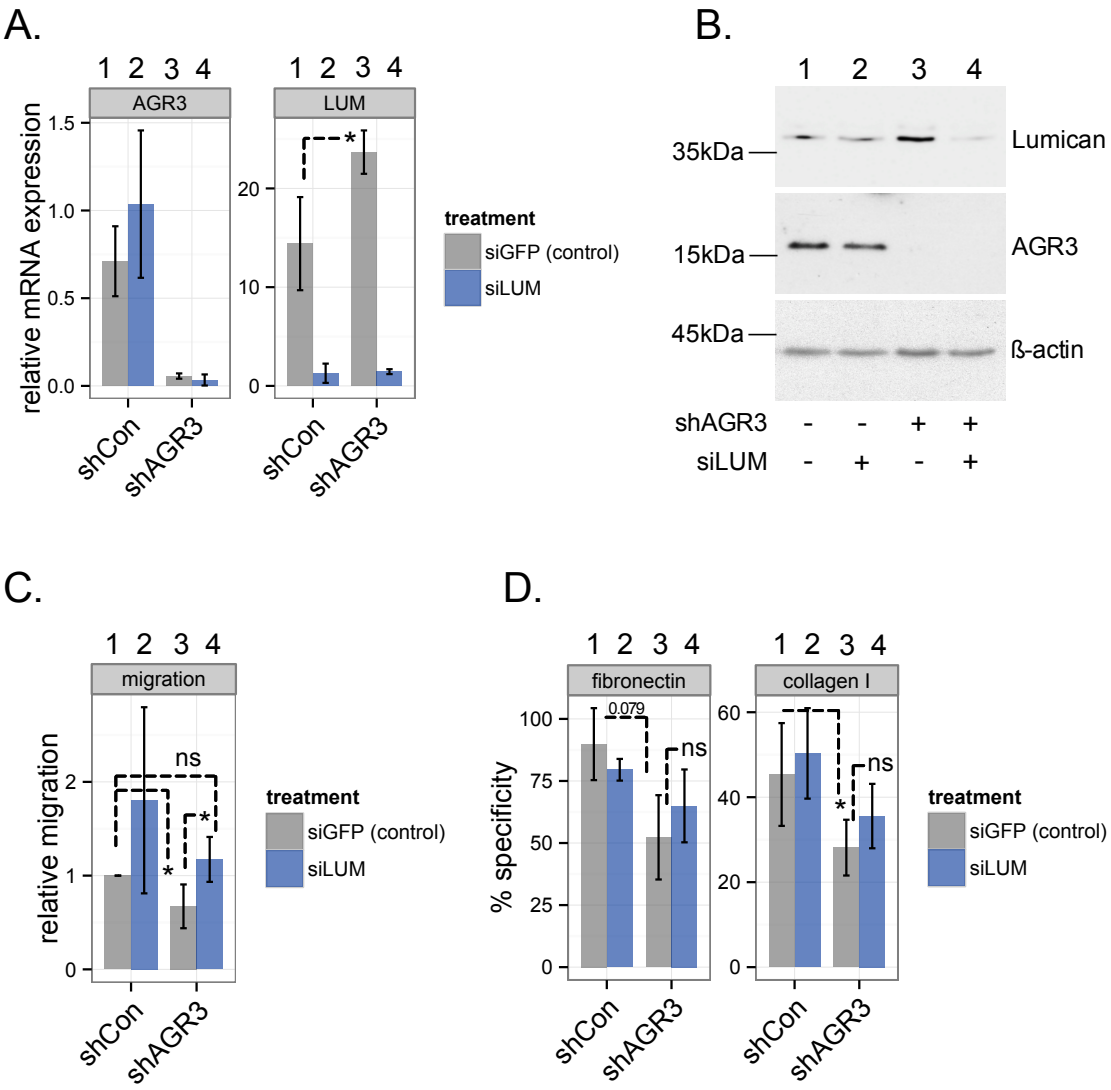

Figure 13. AGR3 affects VCaP cell migration in part by modulating lumican expression.
(A) After 72 h of transfection with either siLUM or siGFP as control, total RNA collected from control (shCon) and AGR3 knockdown (shAGR3) cells was reverse transcribed to cDNA, which was used as template in qPCR reactions with AGR3, LUM, and ribosomal protein RibP0 specific primers. Relative gene expression was computed for each gene against RibP0 values. These charts represents the average of 3 independent experiments. (* $p<0.05$, mean ± SD, ns = not significant, n = 3)
(B) Transient knockdown of Lumican protein in control and AGR3-knockdown VCaP cells. Control (shCon) and AGR3-knockdown (shAGR3) VCaP cells were transfected with 120 pmol of either anti-Lumican siRNA (siLUM) or anti-GFP (siGFP) as control. After 72 h, whole-cell lysates obtained from the transfected cells immunoblotted with Lumican, AGR3, and ß-actin antibody as control.
(C) Migration of control and AGR3-knockdown cells pre-treated for 72 h with siLUM or siGFP was carried by staining cells with DiI dye and allowing them to migrate for 36h toward 10% v/v

FBS as described previously (Figure 10A). Significant differences were estimated using a one-tailed t-test. (* $p<0.05$, mean ± SD, ns = not significant, n = 3)
(D) Substrate specific adhesion of control and AGR3-knockdown cells pre-treated for 72 h with siLUM or siGFP as control was carried out in fibronectin or Collagen I coated over 1 h as described previously (Figure 10B). A one-tailed t-test was used to evaluate significant differences between different treatments. (* $p<0.05$, mean ± SEM, n = not significant, n = 3)

Given the previously described role of Lumican in cell adhesion, the possibility that reduced cell adhesion after AGR3 suppression (Figure 10C) depends on Lumican upregulation was considered next. Cell-substrate affinity was measured by seeding control and AGR3-knockdown cells pre-treated with either siLUM or siGFP for 72 h in fibronectin or collagen I coated culture dishes. Consistent with previous results (Figure 10C), AGR3 suppression resulted in reduced adhesion in AGR3-knockdown (shAGR3) cells compared to control cells (Figure 13D, compare lane 3 and lane 1 in fibronectin, significance of 0.074, and collagen I charts). However, no significant difference in adhesion was observed when comparing either siLUM to siGFP treated cells (Figure 13D, lane 4 and lane 3 in fibronectin and collagen I charts), suggesting that suppressing Lumican expression does not significantly reverse the reduction of cell adhesion to the substrates.

Taken together, these results suggest that after AGR3 suppression, reduced migration, but not adhesion, depends in part on the upregulation of Lumican expression.

To determine if the link between Lumican and AGR3 is limited to VCaP cells, Lumican gene expression was investigated at the mRNA level in control and AGR3 expressing 22Rv.1 cells. Triplicate cDNA reverse transcribed from total RNA sample was used as a template in qPCR reactions together with AGR3, Lumican, and RibP0 (ribosomal protein) specific primers as control. Consistent with AGR3 behavior in VCaP cells, Lumican mRNA expression was reduced in 22Rv.1 cells expressing AGR3 (Figure 14A).

To determine if AGR3 expression in 22Rv.1 cells leads to effects consistent with those established in VCaP cells, the migration and adhesion of control and AGR3-expressing 22Rv.1 cells was determined next. Migration, assayed as described previously in Figure 10A, was increased in 22Rv.1 cells expressing AGR3 (Figure 14B). Adhesion assays, carried out as described in

Figure 10B, showed increased adhesion of AGR3-expressing 22Rv.1 cells to fibronectin, but not collagen I (Figure 14C)

Overall, these results suggest that AGR3 can influence both adhesion and migration of prostate cancer cells, the latter of which depends at least in part on AGR3-mediated changes in Lumican expression.

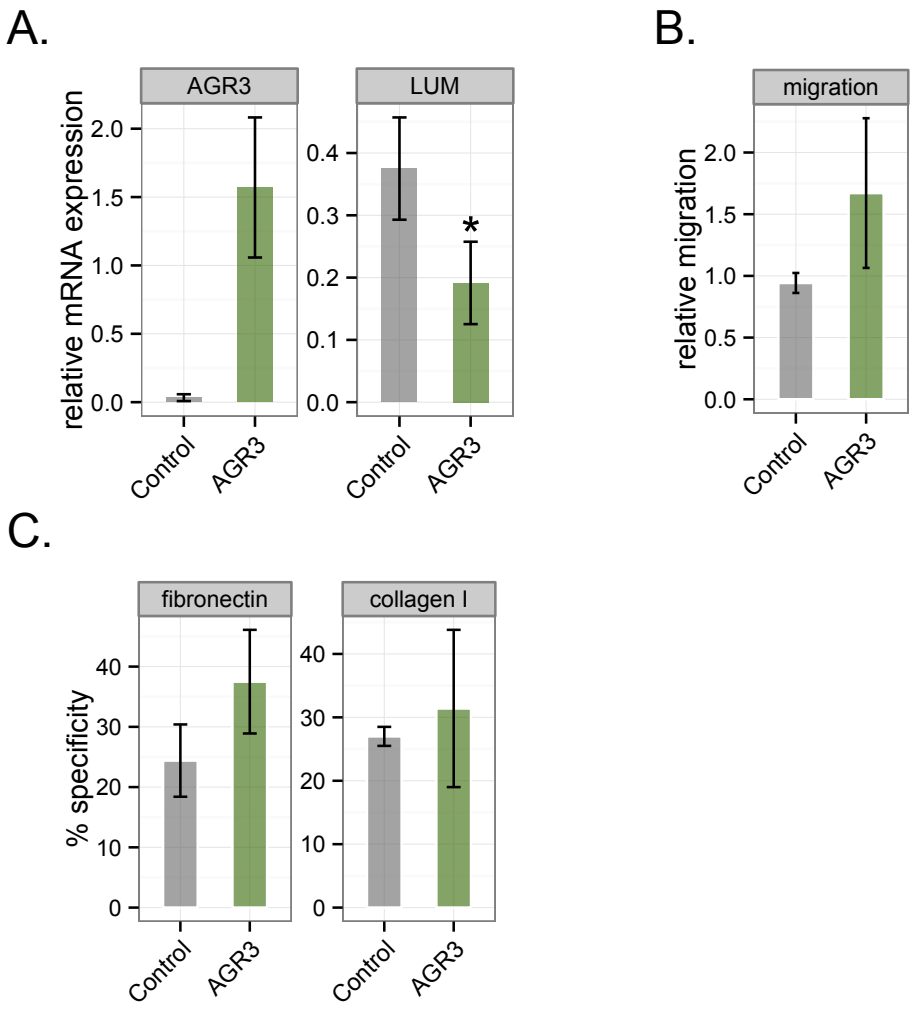

Figure 14. Overexpression of AGR3 in 22Rv.1 cells is associated with reduced Lumican mRNA expression and enhanced migration and adhesion.
(A) AGR3 and LUM mRNA expression in either control or AGR3 overexpressing 22Rv.1 cells. Triplicate total RNA samples from control or AGR3 expressing 22Rv.1 cells were reverse transcribed into cDNA and used as template in qPCR reactions with AGR3, LUM, or RibP0 specific primers. Relative AGR3 and LUM expression against RibP0 (* $p<0.05$, mean + SD, ns = not significant, n = 3)
(B) Migration of control or AGR3 expressing 22Rv.1 cells was carried out over 36 h as described previously (Figure 10A), in 24-well BD cell culture inserts (Boyden chambers) over 36 h using 10% v/v FBS as chemo attractant. The amount of fluorescent migrant cells was quantified using a spectrophotometer (excitation/emission 550/495 nm). (n = 2)
(C) Substrate specific adhesion of control and AGR3 expressing 22Rv.1 cells was carried out as described previously (Figure 10B) in fibronectin and Collagen I coated 96-well plates, over

1 h under normal growth conditions. Substrate-specific adhesion is reported as % specificity, which is the signal of cells in coated wells expressed as a percentage of the signal from the same sample seeded in uncoated wells. (n = 2)

4.8 AGR3 is upregulated during ER stress

In addition to enhanced proliferation and migration, tumor cells are characterized by their increased capacity to survive physiological stress (i.e. hypoxia and nutrient starvation). Under these conditions, survival depends in part on enhanced ER (endoplasmic reticulum) activity, which ensures the correct processing of up to one-third of all proteins [98].

The key constituents of the ER are molecular chaperones, which can simultaneously act as crucial regulators of survival signaling and direct effectors of protein folding. Molecular chaperones aid protein folding in the ER through a variety of mechanisms that include folding quality control and correct disulfide bond formation. The latter function is carried out by members of the PDI (protein disulfide isomerase) superfamily, which are molecular chaperones able to interact with the cystine moieties of other proteins through their thioredoxin-like protein folds. AGR3 is one of the smallest members of the PDI superfamily, with only one thioredoxin-like fold confirmed recently by the solution of its crystal structure [60]. The possible involvement of AGR3 in the cellular response to physiological stress has not been investigated.

A typical consequence of physiological stress is accumulation of misfolded proteins in the ER lumen (a condition known as ER stress), to which cells react by upregulating the expression of several classes of molecular chaperones, including members of the PDI superfamily [56, 99]. To determine whether AGR3 expression is also upregulated during ER stress, AGR3 expression was monitored in VCaP cells exposed to three different ER stress inducing reagents.

ER stress was induced by treating VCaP cells with Tg (thapsigargin, 0.5 µM), Tm (tunicamycin, 0.5 µg/ml), DTT (dithiothreitol, 1 mM), or 1 µM H_2O_2 and their respective solvents (EtOH, DMSO (dimethylsulfoxide), and dH_2O respectively) as control. Each of these reagents targets a crucial step in

ER protein maturation, such as disruption of ER Ca^{2+} homeostasis (Tg), N-linked glycosylation (Tm), and perturbation of reductive (DTT) and oxidative (H_2O_2) reactions, and they all result in accumulation of misfolded proteins in the ER leading to ER stress. To determine the extent of ER stress induced by each treatment, the expression of GRP78 (glucose regulated protein 78 kDa, an ER-resident chaperone sensitive to ER stress) was also monitored at the protein level. Whole-cell lysates obtained after 12 and 24 h treatment with Tg, Tm, or DTT, and after 24 h with EtOH, DMSO, dH_2O, and H_2O_2 were immunoblotted with AGR3, GRP78 and ß-actin antibodies as control. The protein level of AGR3 was increased in all treatments (Tg, Tm, DTT, and H_2O_2) to an extent consistent with the amount of ER stress induced, as indicated by the upregulation of GRP78 (Figures 15A and B).

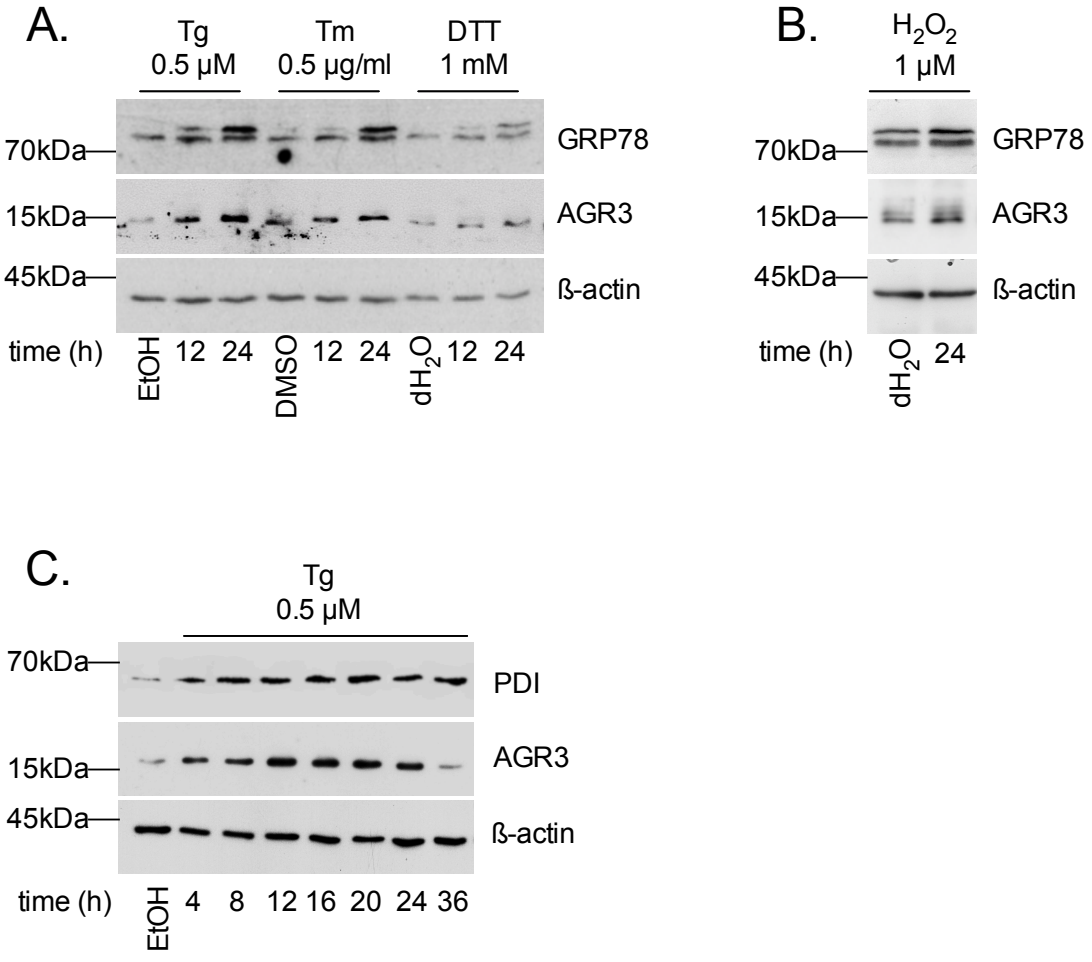

Figure 15. AGR3 is upregulated during ER stress.
(A) Expression of AGR3 after treatment with three different ER stress-inducing reagents. Whole-cell lysates of VCaP cells treated for 12 and 24 h with 0.5 µM thapsigargin (Tg), 0.5 µg/ml tunicamycin (Tm), 1mM DTT, or H_2O_2, and for 24 h with EtOH, DMSO, or dH_2O as control respectively, were immunoblotted with AGR3, GRP78, and ß-actin antibody as control.
(B) Expression of AGR3 protein after treatment with 1 µM of H_2O_2 for 24 h. Whole-cell lysates obtained after 24 h of H_2O_2 or dH_2O treatment as control were immunoblotted with AGR3, GRP78, and ß-actin antibody as control.
(C) Comparison of the expression pattern of AGR3 and PDI during 36 h of ER stress. VCaP cells were treated for 36 h with 0.5 µM Tg or EtOH as control, and whole-cell lysates collected every 4 h for 24 h and at 36 after Tg treatment, as well as after 36 h of EtOH treatment. Whole-cell lysates were immunoblotted with AGR3, PDI, and ß-Actin as control.

To further characterize the pattern of AGR3 expression during ER stress, a time course experiment was carried out in which whole-cell lysate samples were collected every 4 h for 24 h and at 36 h after treatment with 0.5 µM Tg, or after a 36 h treatment with EtOH as control. Tg treatment was chosen because it gave the most pronounced effect of AGR3 upregulation. To further characterize expression during ER stress, AGR3 upregulation was compared to the upregulation of PDI, which is both the founding member of the PDI superfamily and another marker of ER stress [100]. Whole cell lysates collected at the indicated points were immunoblotted with AGR3, PDI, and ß-actin antibody as control. Expression of both AGR3 and PDI protein reached maximum expression at 12 h after treatment. However, while PDI expression remained high even at 36 h of Tg exposure, the expression of AGR3 protein began to attenuate after 24 h and returned to basal levels by 36 h of treatment, suggesting an alternate mechanism of regulation during ER stress (Figure 15B).

Together, these results demonstrate that, similar to other molecular chaperones, AGR3 is upregulated during ER stress.

4.9. AGR3 is present in the endoplasmic reticulum of prostate cancer cells

Molecular chaperones meant to deal with the accumulation of misfolded proteins during ER stress are typically found in the ER lumen (e.g.

GRP78 and PDI). AGR3 contains an N-terminal ER-targeting signal, and an atypical C-terminal ER-retention tetrapeptide motif (QSEL). Despite the unusual sequence, the C-terminal motif of AGR3 was shown to be active in mediating ER localization in Hela cells (cervical cancer) [101]. Moreover, endogenous AGR3 has been detected in the ER of MCF7 breast cancer cells [57]. Together, these findings indicate that at least a portion of AGR3 protein localizes to the ER.

To determine if AGR3 could play a role during ER stress in prostate cancer cells, the present study sought to first confirm its localization in the ER of prostate cancer cells using immunofluorescence. To reach maximal AGR3 expression, VCaP cells were treated with 0.5 µM Tg for 12 h or EtOH as control. Cells were then fixed and permibilized prior to detecting AGR3 and GPR78 protein with specific antibodies, or staining nuclei with Draq5 (a DNA intercalator). In both EtOH and Tg (Figure 16A) treated VCaP cells, the AGR3 signal (Figure 16A, I and V, red colour) was predominantly detected around the nuclei. A similar localization pattern was detected for GRP78 (Figure 16A, II and VI, green colour). Merging of these signals revealed yellow coloured regions (Figure 16A, IV and VIII), which indicate at least a partial overlap between AGR3 and GRP78 protein, and suggest the presence of an ER-resident AGR3 protein fraction.

To confirm this result in an additional prostate cancer cell line, control or AGR3-expressing (stable) 22Rv.1 cells were also treated with either 0.5 µM Tg or EtOH as control for 12 h before incubation with AGR3 and GPR78 specific antibodies, as well as Draq5. A pattern of nuclear-adjacent signal similar to that observed for endogenous AGR3 in VCaP cells was detected for AGR3 and GRP78 in both EtOH and Tg treated 22Rv.1 cells (Figure 16B, IX and XIII, red colour / X and XIV, green colour respectively). Merging of these signals revealed a large degree of overlap between AGR3 and GRP78 proteins (Figure 16B, XII and XVI, yellow colour), which provides further evidence of AGR3 localization in the ER.

These results confirm the presence ER localization of endogenous AGR3 protein in VCaP cells, and indicate the establishment of such a fraction of overexpressed AGR3 in the ER of 22Rv.1 cells.

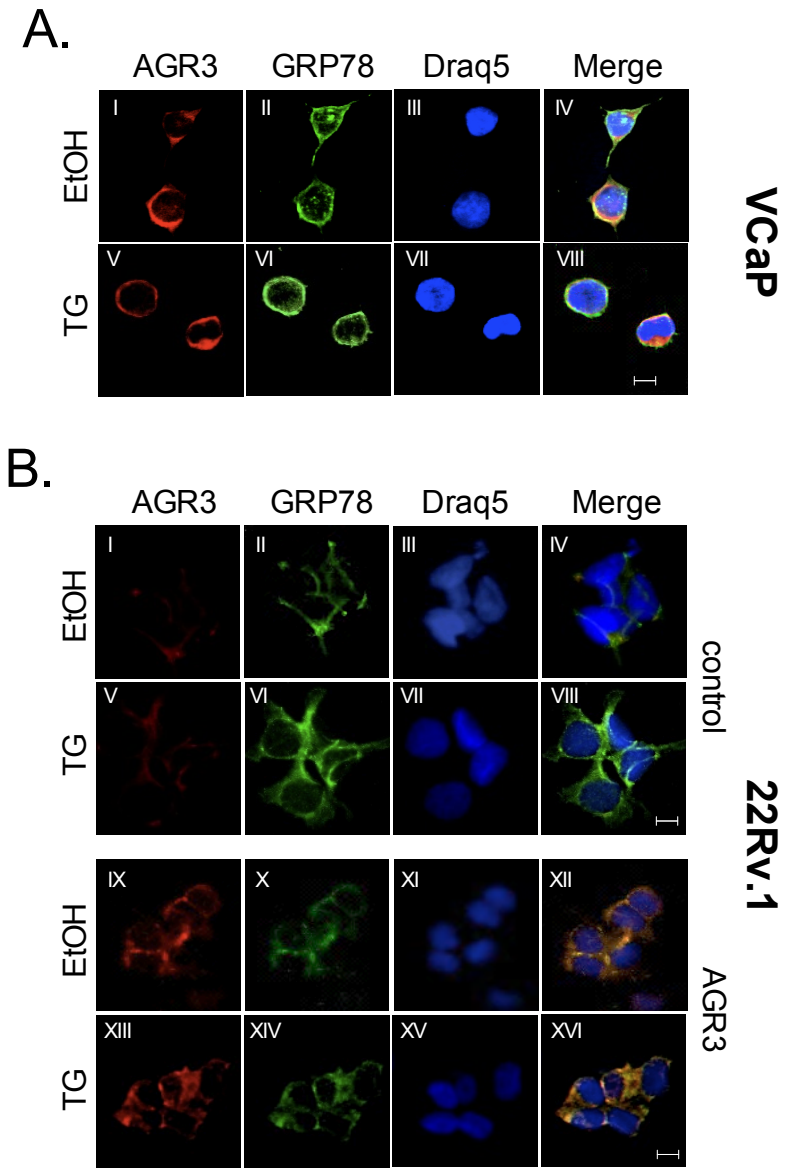

Figure 16. AGR3 is located in the endoplasmic reticulum of prostate cancer cells.
Immunofluorescence analysis of the subcellular localization of AGR3 in VCaP and AGR3-transfected 22Rv.1 cells.
(A) Confocal images (40x magnification) of VCaP cells treated with EtOH (upper panel) or 0.5 µM Tg (lower panel) for 12 h, and fixed with 4% v/v paraformaldehyde. AGR3 protein is shown in red (I and V), GRP78 protein, used here as a marker for the endoplasmic reticulum is shown in green (II and VI), while nuclei stained with Draq5 are shown in blue (III and VII). Merging of these three channels (IV and VIII) results in yellow colour (IV and VIII), which indicates overlap between AGR3 and GRP78 protein. The bar indicates 5 µm of length.
(B) Confocal images of control (I – VIII), and AGR3-expresing (IX – XVI) 22Rv.1 cells treated with either EtOH (upper panels, I – IV, and IX – XIII) or 0.5 µM Tg (lower panels, V – VIII, and XIII – XVI) for 12 h, and fixed with 4% v/v paraformaldehyde. AGR3 protein is shown in red (I, V, IX, and XIII), GRP78 protein is shown in green (II, VI, X, XIV), while nuclei stained with Draq5 are shown in blue (III, VII, XI, XV). Merging of these three channels results in yellow colour (IV, VIII, XII, XVI), which indicates overlap between AGR3 and GRP78 protein.

All images were acquired with a Zeiss LSM510 confocal microscope using the LSM LSell5 Image examiner software (Lecia Microsystems). The bar indicates 5 μm of length.

4.10 AGR3 enhances the expression of GRP78 during ER stress.

Upregulation of molecular chaperones is a key requirement of enhanced protein folding capacity during ER stress. In addition, cells activate a set of signaling pathways known as the UPR (unfolded protein response), which can execute either survival or apoptotic signaling, depending on the severity and persistence of ER stress.

In the ER, UPR signaling and protein folding integrate in the activity of GRP78. In the absence of ER stress, GRP78 binds to and inactivates ER membrane-resident stress sensors which lie directly upstream of the UPR [102]. During ER stress, unfolded and misfolded polypeptides competitively titrate the GRP78 chaperone away from complexes with ER membrane-sensors, leading to activation of the UPR and its downstream targets. Therefore GRP78, itself an upregulated molecular chaperone during ER stress, is a key indicator of the efficiency of cellular response to the accumulation of unfolded proteins.

To determine the effect of AGR3 on prostate cancer cell stress response, the level of GRP78 expression was monitored during ER stress in control and AGR3-knockdown VCaP cells treated with 0.5 μM Tg for 12 and 36 h or for 36 h with EtOH as control. Total RNA collected at these time points was reverse transcribed into cDNA, which was used to monitor GRP78 expression. Suppression of AGR3 levels did not alter the basal level of GRP78 mRNA. However, upon ER stress, GRP78 induction was lower in AGR3-knockdown (shAGR3) cells than control (shCon) cells, reaching significance at 36 h, and suggesting that absence of AGR3 leads to attenuated GRP78 upregulation during ER stress (Figure 17A).

To confirm this effect at the protein level, VCaP cells were similarly treated for 12, 24, and 36 h with 0.5 μM Tg or for 36 h with EtOH as control.

Whole-cell lysates obtained at these time points were immunoblotted with AGR3, GRP78, and ß-actin antibody as control. Consistent with results at the mRNA level, the basal GRP78 protein expression was not altered by suppression of AGR3. However, upon ER stress, GRP78 protein levels were lower in shAGR3 than shCon cells, especially at 24 and 36 h after treatment (Figure 17B).

To determine whether this effect was limited to VCaP cells, ER stress was similarly induced over 12 and 36 h with 0.5 µM Tg in AGR3-overexpressing 22Rv.1 cells, and GRP78 was monitored at the mRNA and protein level.

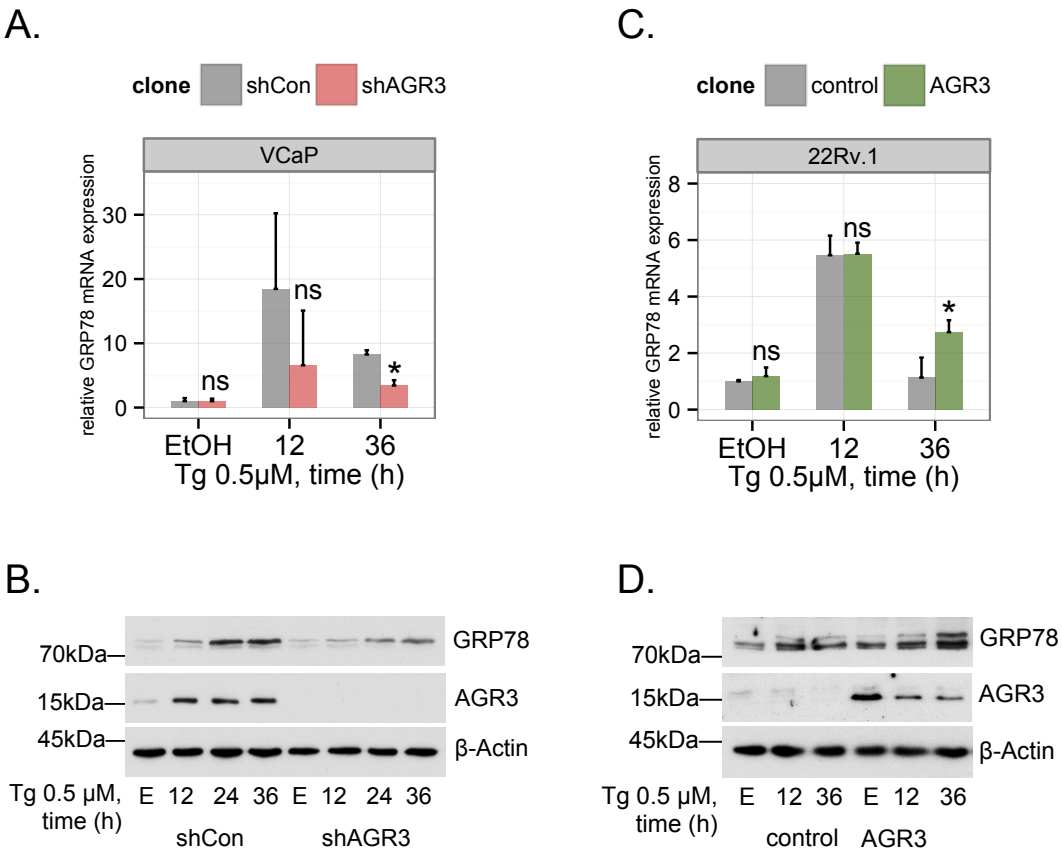

Figure 17. AGR3 enhances the expression of GRP78 at both protein and mRNA level in VCaP and 22R.v1 cells.

(A) Effect of AGR3 suppression on the expression of GRP78 mRNA during ER stress in VCaP cells. Control (shCon) and AGR3-knockdown (shAGR3) VCaP cells were treated with 0.5 µM Tg for 12 and 36 h or with EtOH (E) for 36 h as control. cDNA reverse transcribed from total RNA of each of these samples was used as template in qPCR reactions with GRP78 and RiBP0 primers as control. GRP78 expression was computed relative to RibP0 expression. (* $p<0.05$, mean ± SD, ns = not significant, n = 3)

(B) Effect of AGR3 suppression on the expression of GRP78 protein during ER stress in VCaP cells. Control and AGR3-knockdown VCaP cells were treated with 0.5 µM Tg for 12, 24

and 36 h or with EtOH for 36 h as control. Whole-cell lysates collected at these time points were immunoblotted with AGR3, GRP78, and ß-actin antibody as control.
(C) Effect of AGR3 overexpression on GRP78 mRNA levels during ER stress in 22Rv.1 cells. control and AGR3-expressing 22Rv.1 clones were treated with 0.5 µM Tg for 12 and 36 h or with EtOH (E) for 36 h as control. Relative GRP78 expression was computed by normalizing expression to RibP0 values. (* $p<0.05$, mean + SD, ns = not significant, n = 3)
(D) Effect of AGR3 overexpression on GRP78 protein levels during ER stress in 22Rv.1 cells. control and AGR3-expressing 22Rv.1 clones were treated with 0.5 µM Tg for 12 and 36 h or with EtOH (E) for 36 h as control. Whole-cell lysates collected at these time points were immunoblotted with AGR3, GRP78, and ß-actin antibody as control.

Basal GRP78 expression did not differ between control and AGR3-expressing 22Rv.1 cells (Figure 17C). Upon ER stress, maximal GRP78 mRNA induction was observed at 12 h after treatment with 0.5 µM Tg, however at this time point, GRP78 mRNA induction did not differ between AGR3-overexpression and control cells. After 36 h of Tg exposure, GRP78 mRNA expression was significantly higher in AGR3-expressing than control 22Rv.1 cells (Figure 17C). At the protein level, basal expression of GRP78 was also not altered by AGR3 overexpression. However, by 36 h of treatment, GRP78 protein level was higher in AGR3-expressing than control 22Rv.1 cells, suggesting enhanced cellular response to ER stress (Figure 17D).

Taken together, these results indicate that AGR3 expression enhances prostate cancer cell response to ER stress.

4.11 AGR3 enhances prostate cancer cell viability during ER stress

The positive influence of AGR3 on GRP78 expression during ER stress suggests enhanced cellular viability, which is defined as the ability of cells to retain and recover cellular function under normal or stress conditions.

Viable cells are able to carry out the metabolic reactions necessary to produce energy and maintain synthesis of cellular components. Therefore, in in the present study, cell viability under ER stress was estimated by

monitoring the number of metabolically active cells using the Celltiter-Blue reagent.

To determine the impact of AGR3 on cell viability, control (shCon) and AGR3-knockdown (shAGR3) VCaP cells, as well as control and AGR3-expressing 22Rv.1 cells were exposed to 0.5 µM Tg or EtOH for 12 and 36 h. At each of these time points, the viability of Tg treated cells was assayed and reported as a percentage of the viability of EtOH treated cells.

After 12 h of Tg treatment, the viability of AGR3-knockdown cells was significantly reduced when compared to the viability of control VCaP cells (Figure 18A). However, at 36 h, the viability of these cells did not differ. In 22Rv.1 cells, after 12 h of Tg treatment, the difference in viability of control and AGR3-expressing clones did not reach statistical significance (Figure 18B). After 36 h of treatment, a small, but statistically significant difference in the viability of AGR3-expressing cells was detected.

Together, these experiments suggest that the presence of AGR3 exerts a positive influence on the viability of prostate cancer cells during physiological stress.

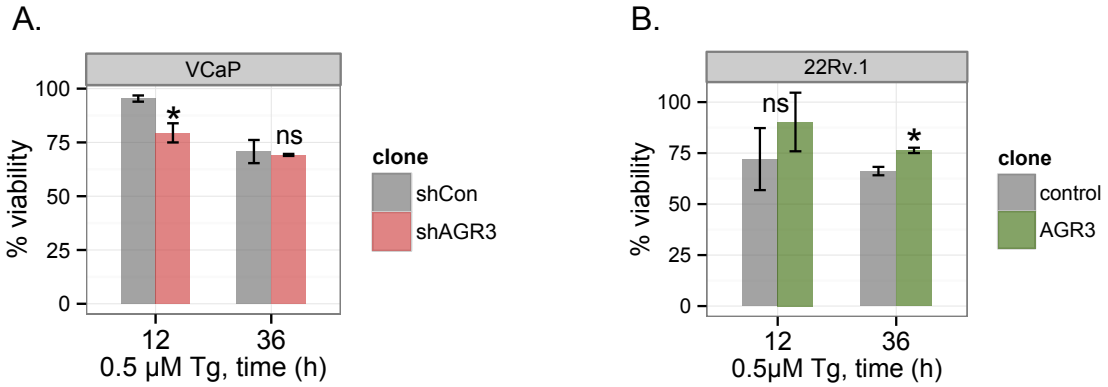

Figure 18. AGR3 enhances the viability of prostate cancer cells during ER stress.
(A) Effect of AGR3 suppression on the viability of control (shCon) and AGR3-knockdown (shAGR3) VCaP cells. shCon and shAGR3 cells were seeded in 96-well cell culture plates, and treated with either EtOH or 0.5 µM Tg for 12 and 36 h. At each of these time points, 20 µl of Celltiter-Blue reagent was added to the cells and metabolized over 1 h before measuring fluorescence at 590 nm. % Viability was calculated by expressing fluorescence values of Tg treated as a percentage of corresponding EtOH treated cells at each time point. (* $p<0.05$, mean ± SD, ns = not significant, n = 3)

(B) Effect of AGR3 suppression on the viability of control and AGR3 overexpressing 22Rv.1 cells. Control and AGR3-expressing 22Rv.1 cells were seeded in quadruplicate in 96 well cell culture plates, and treated using the same conditions described in (A). (* $p<0.05$, mean ± SD, ns = not significant, n = 3)

5. DISCUSSION

Tumor markers reduce mortality by enhancing diagnosis and prognosis of cancer. Prostate cancer benefits from a number of diagnostic (e.g. PSA, prostate specific antigen) and prognostic markers (e.g. the TMPRSS2-ERG gene fusion, Transmembrane protease, serine 2 – v-Ets erythroblastosis virus E26 oncogene related). The discovery and characterization of additional markers holds promise in reducing the mortality associated with this disease.

AGR3 is a member of the PDI (protein disulfide isomerase) family that contains an atypical thioredoxin catalytic motif and N and C-terminal ER (endoplasmic reticulum) localization signals. Within the PDI family, AGR3 has a closely related homolog (~64% protein sequence homology) called AGR2, and both genes show increased expression in prostate cancer [31, 37, 85]. AGR2 is involved in multiple facets of prostate cancer progression [32, 34, 103]. To date, the function AGR3 in prostate cancer has not been investigated.

The present study sought to characterize the expression and function of AGR3 in prostate cancer. Analysis of AGR3 expression in patients confirmed its upregulation in prostate cancer and revealed a possible association with aggressive disease. In prostate cancer cell lines, knockdown of endogenous AGR3 resulted in reduced proliferation while overexpression studies in three different prostate cancer cell lines showed that AGR3 could enhance cell proliferation. Proliferation could also be enhanced by extracellular AGR3, suggesting the possibility of autocrine action. AGR3 knockdown reduced adhesion and migration, with the latter mediated in part by upregulation of Lumican, a small leucine-rich proteoglycan. Furthermore, the AGR3 expression is induced during ER stress, where it associated with enhanced cell viability. Together, these results support a role for AGR3 as a possible marker of prostate cancer progression.

5.1 AGR3 is associated with advanced prostate cancer

The expression of AGR3 in prostate cancer has been previously reported [85]. The present study confirmed the upregulation of AGR3 mRNA in prostate cancer patients, and found an association between AGR3 expression and the Gleason scores 8-10 (Figure 3A) in Oncomine datasets. In addition, the pattern of AGR3 expression differed from that of its close homolog AGR2, which is reported to be overexpressed in primary prostate tumors [76]. In the Oncomine datasets analyzed here, the expression of AGR2 was significantly upregulated only in the Gleason 1-7 category, consistent with its reported upregulation in primary tumors. These findings suggest an inverse correlation between AGR2 and AGR3 expression in prostate cancer progression. This notion is supported by a study carried out in our lab, which found mutual regulation of these genes: knockdown of AGR3 lead to upregulation of AGR2, while knockdown of AGR2 resulted in increased AGR3 expression in VCaP cells [104]. Together, these results suggest that the inverse correlation of AGR2 and AGR3 expression in prostate cancer progression may depend in part on their mutual regulation.

How this interaction is mediated remains unclear, although clues are offered by reports characterizing AGR2 and AGR3 expression in prostate cancer. For example, both AGR2 and AGR3 are AR (androgen receptor) regulated genes, and in prostate cancer, AR-dependent gene expression is controlled by the activity of FOXA1 (forkhead box A1) [68]. FOXA1 has been shown to control the promoter activity of AGR2 [40], and evidence suggests that AGR2 may in turn affect FOXA1 expression [104]. In addition, chip-seq data in LNCaP and VCaP cells reveal FOXA1 binding of the AGR3 promoter at several sites [30]. It is therefore conceivable that FOXA1 plays a role in the regulation of AGR3, and that AGR2 may indirectly affect AGR3 levels by altering FOXA1 expression.

Nevertheless, AGR2 and AGR3 are also found co-expressed in some tissue types (e.g. ovarian cancer [57]). Therefore, the conditions that favor co-expression, or a mutually exclusive pattern of expression may relate to the

cancer type, and could depend on any of the tumor-related functions of these genes.

5.2 AGR3 enhances prostate cancer cell proliferation

Increased expression in prostate cancer suggests a possible role for AGR3 in prostate cancer cell proliferation. In line with this view, suppression of endogenous AGR3 protein in pooled VCaP clones resulted in reduced cell proliferation, while AGR3 expression enhanced proliferation in the AGR3-negative 22Rv.1, LNCaP and PC-3 cells, but did so at only moderate levels of expression. Higher amounts of AGR3 protein expression abrogated this effect (LNCaP and PC-3) and even inhibited proliferation (22Rv.1), indicating the possibility that forcing an artificially high level of expression has a detrimental effect on cell proliferation.

Therefore, to eliminate the caveats associated with stable protein overexpression, the effect of AGR3 on cell proliferation was studied using an inducible-expression system in 22Rv.1 cells, the advantages of which include greater control of expression levels and genetic background (i.e. comparing induced to uninduced states of the same clone), as well as the absence of cell adaptation to stable gene expression overtime. Consistent with previous results, modulating AGR3 levels in the same cells (same clone) confirmed both enhanced proliferation (at moderate expression level) and reduced proliferation at high levels of AGR3 expression. Separately, inducing maximal expression in three different clones with varying maximal expression levels resulted in enhanced proliferation of the clone with the lowest expression level, and reduced proliferation in clones achieving a high level of AGR3 expression.

Taken together, these knockdown and overexpression studies suggest a positive role for AGR3 in prostate cancer cell proliferation. Since AGR3 expression is highest in advanced stages of the disease, these findings indicate that AGR3 may promote an aggressive phenotype by enhancing cell proliferation.

5.3 AGR3 is a secreted protein able to promote prostate cancer cell proliferation

Molecular chaperones are known to be secreted extracellular space where they play a diverse set of functions. One of the better-characterized functions of a secreted AGR protein is carried out by *n*AG, the newt homolog of human AGR2, the activity of which is crucial for limb regeneration. Extracellular *n*AG can strongly induce the proliferation of blastema cells in culture [46].

In the present study, secretion of AGR3 protein was confirmed in the medium of 22Rv.1 cells transfected with AGR3 cDNA, as well as in the medium of AGR3-inducible 22Rv.1 cells after induction. Subsequently, AGR3 conditioned media generated from inducible 22Rv.1 cells were used in proliferation assays. 22R.v1 (control, not AGR3-inducible) and DU145 cells showed enhanced proliferation in the presence of AGR3. DU145 cells showed a more pronounced effect in this experiment, which is likely explained by the individual differences between DU145 and 22Rv.1 cells.

Secreted *n*AG mediates its effect through interaction with Prod 1, which is a member of the LY6 cell-surface antigen family of proteins. In breast cancer, AGR3 was shown to interact with the extracellular domain of C4.4 (GPI-anchored metastasis-associated protein C4.4A homolog), which is also a member of the LY6 family [43]. If this interaction is proven functional, individual differences in C4.4 expression between cell lines could eventually account for the observed differences of extracellular AGR3 in different cell lines. Taken together these results suggest a role for extracellular AGR3 in prostate cancer development.

5.4 AGR3 enhances adhesion and migration in prostate cancer cells

In prostate cancer progression, disregulated cell proliferation is typically followed by changes in adhesive interactions with the extracellular

matrix that eventually develop into enhanced cell migration. Increased migration is an enabling step in the progression to advanced disease, and given the elevated expression of AGR3 in advanced prostate cancer patients, a role was hypothesized for this gene in cell migration and adhesion.

VCaP cells with a stable AGR3 knockdown showed reduced migration (using the Boyden chamber assay) and adhesion to substrate (collagen I and fibronectin). To confirm this result, similar migration and adhesion experiments were carried out using 22Rv.1 cells with stable AGR3 expression, which yielded enhanced migration and adhesion to substrate. Together these results, suggest a positive effect of AGR3 on prostate cancer cell migration and adhesion.

To understand how AGR3 accomplishes these effects, data from a genome-wide expression experiment of VCaP cells with a stable AGR3 knockdown was analyzed for GO gene set enrichment. The expression changes induced by the knockdown of AGR3 were enriched with GO terms in development and extracellular matrix-related categories.

Enrichment of development-related GO terms is consistent with the reported functions of AGR3 homologs in *X. laevis* development, and suggests human AGR3 involvement in prostate morphogenesis [38, 39]. At present, there are no knockout mice models of AGR3 available and the effect of this gene in prostate development remains unknown. Moreover, the effect of the highly related AGR2 in prostate development has not been studied in knockout mice either. A clue as to how development-related functions of AGR2 and AGR3 could contribute to prostate cancer progression is held in a single report, which determined a function of AGR2 in establishing a neuroendocrine phenotype in prostate cancer cells, a finding made likely by the involvement of AGR2 and AGR3 homologs in neural patterning of the *X. Laevis* forebrain [38, 103]. The role of AGR3 in prostate development and prostate cancer cell phenotype (i.e. luminal v.s. basal v.s. neuroendocrine) could be further investigated.

The second category of GO enrichment includes five extracellular matrix-related terms related to cell migration and adhesion. Further analysis of these terms revealed a core group of genes driving enrichment, the expression of which was subsequently verified using qPCR. Significant

upregulation was confirmed for LUM (Lumican), KAL1 (Kallmann syndrome 1) and COL5A2 (Collagen V, subunit A2) gene expression, and of these, LUM exhibited high expression values in both microarray (high raw signal) and qPCR experiments suggesting its abundance in VCaP cells. A reciprocal reduction of LUM expression was observed in 22Rv.1 cells stably expressing AGR3. Given previous reports implicating LUM in cell migration and adhesion, the relationship between LUM and AGR3 was explored further in the context of VCaP cell migration and adhesion [93, 94, 96, 97].

LUM is a member of the SLRP (small leucine-rich proteoglycan) family of proteins involved in regulating collagenous matrix assembly. LUM shows opposite roles in non-cancer and cancer cell systems. For example, in the corneal epithelium of mice, it stimulates cell migration in an Erk1/2-dependent manner [105]. In contrast, in melanoma and prostate cancer cells (e.g. PC-3, DU145, and LNCaP) it was shown to inhibit both migration and invasion [93, 94, 97]. These reports imply a negative impact of LUM expression on cancer cell migration, and suggest that its upregulation in AGR3-depleted VCaP cells can help explain the reduced migration of these cells.

In the present study, upregulation of LUM in AGR3-depleted VCaP cells was confirmed at both mRNA and protein levels. In addition, transient suppression of LUM expression revealed that upregulation of LUM in VCaP cells with stable AGR3 suppression is in part responsible for the decreased migration, but not adhesion, observed. This result is consistent with the previously described function of LUM in prostate cancer cell migration [97].

How AGR3 suppression leads to LUM upregulation is currently unclear. The LUM gene promoter has been studied, and is reported to be under the influence of an Sp3 (specificity protein 3) enhancer and an upstream suppressor motif matching GATA (GATA binding protein) response elements [106]. However, out of the 6 known GATA transcription factors in *H. sapiens*, those mediating LUM suppression have not yet been identified. The transcriptome analysis carried out in the present study showed changes in expression of a large number of genes with GATA1 response elements in their promoter, indicating altered activity of this transcription factor in AGR3-depleted VCaP cells. GATA1 could therefore be responsible for the increase

in LUM expression in these cells. How AGR3 alters GATA1 activity is unclear.

5.5 AGR3 protein expression is enhanced during ER stress, and is required for full cellular response to ER stress and preservation of cell viability

In the tumor microenvironment, cells experience physiological stress under a variety of adverse conditions such as hypoxia, oxidative stress, lack of nutrients, or changes in physiological pH. Typically, exposure to these conditions generates a surplus of unfolded protein in the ER, which is accompanied by upregulation of ER-resident chaperones meant to alleviate the excess protein burden. AGR3 is part of the protein disulfide isomerase family, members of which act as chaperones of protein folding in the ER. The protein sequence of AGR3 codes for an ER localization signal, an ER retention signal, and a thioredoxin fold, suggesting a possible role for AGR3 in protein folding in the ER.

Two of the most common properties of molecular chaperones that deal with protein folding in the ER, are upregulation during ER stress and ER localization. ER localization of AGR3 was confirmed using immunofluorescence to track AGR3 and GRP78 (ER resident chaperone, marker of the ER organelle) in VCaP and AGR3-expressing 22Rv.1 cells. Overlap between AGR3 and GRP78 signals indicated ER localization of AGR3 in prostate cancer cells, and confirmed its previously reported localization the ER compartment [101]. In addition, AGR3 protein upregulation was detected after treatment with four different ER stress-inducing reagents: Ca^{2+}-depleting (thapsigargin), glycosylation-inhibiting (tunicamycin), reducing (dithiothreitol) and oxidizing (H_2O_2). Together, these experiments provide evidence for AGR3 involvement in processes that mitigate ER stress.

AGR3 protein reached maximal expression at 12 h after stress, and attenuated after that, until endogenous levels were reached again at 36 h. This pattern of expression differed from that of PDI, which maintained high levels even after prolonged (36 h) of ER stress. Loss of AGR3 protein after

prolonged stress suggests a role for AGR3 in the early moments of ER stress, when cells typically attempt to mount a pro-survival response. During ER stress, cells attenuate protein translation to prevent additional burden to the ER therefore indicate be a function of the protein stability of AGR3. Future studies determining protein stability (i.e. cycloheximide time course) could be used to determine the stability of AGR3 protein, and gain insight into its regulation.

The expression pattern of AGR3 was mirrored by cell viability during ER stress. VCaP cells with a stable AGR3 knockdown showed reduced viability at 12 h after the application of stress, but showed no difference from controls after 36 h. The opposite effect was observed in 22Rv.1 cells, where stable AGR3 expression provided no significantly enhanced viability in the early moments of ER stress (12 h), but did produce a statistically significant enhancement at 36 h after treatment. The absence of enhanced viability at 12 h in 22Rv.1 cells could be explained by the fact that these cells have no endogenous AGR3 expression and could have adapted to maximizing viability during the early stage of ER stress in its absence.

The influence of AGR3 during ER stress was additionally estimated by monitoring GRP78 expression, which is indicative of the cells response to ER stress. Inducing stress in VCaP cells with a stable AGR3 knockdown resulted in attenuated GRP78 expression at both mRNA (significant at 36 h) and protein levels, that when coupled to reduced cell viability suggests an attenuated response to ER stress. Conversely, in 22Rv.1 cells with a stable AGR3 expression, GRP78 levels were significantly increased at the both mRNA level and protein level after 36. Given that cell viability was also enhanced at this time point, this result suggests that the presence of AGR3 exerts a positive influence on the cells response to ER stress. Combined, these results suggest that AGR3 protein expression is enhanced during ER stress, and that its presence is required for maximal cell viability.

Given that AGR3 catalytic motif (CxxS), one possible reason for reduced viability in the absence of AGR3 may be the reduced folding capacity. The same catalytic motif is present in AGR2, and is implicated in the processing of mucin proteins in the ER. The possibility of AGR3 performing a similar function is reflected in its tissue expression pattern. AGR3, like AGR2,

is typically expressed in mucin-producing tissues (i.e. lungs, stomach, intestine, https://www.nextbio.com), as well as mucinous ovarian cancer [57]. Future studies could mutate the active residues of this catalytic motif before testing viability in VCaP cells (dominant negative experiments) or 22Rv.1 cells (overexpression experiments), to ascertain whether the thioredoxin motif of AGR3 plays a role in cell viability. Reduced viability in these experiments could suggest that AGR3 functions in part by interacting with client molecules, possibly by forming mixed disulfide bonds.

Taken together, these results suggest that AGR3 bears the classic features of a molecular chaperone (i.e. is upregulated during ER stress, and localizes in the ER), and possibly plays an important role in enhancing prostate cancer cell survival in the challenging conditions of the tumor microenvironment.

6. CONCLUSIONS

AGR3 is upregulated in the later stages of prostate cancer where tumors are typically aggressive (i.e. progress rapidly through subsequent stages) and metastatic. Similar to AGR2, the expression of AGR3 enhances the migration and adhesion of tumor cells. This finding is important when considering the inverse correlation between AGR2 and AGR3 expression in prostate cancer patients. It is possible that in the advanced stages of prostate malignancy, the migratory phenotype of aggressive disease is maintained by upregulated AGR3 in the absence of AGR2. Moreover, AGR3 appears to enhance cell migration in part through suppression of Lumican, which is another extracellular matrix protein and tumor suppressor. How AGR3 affects Lumican expression could be further investigated.

Consistent with its expression at advanced stages of prostate cancer, AGR3 appears to exert a positive effect on tumor growth by enhancing hallmark features of aggressive disease such as cell proliferation and cell viability. Importantly, AGR3 appears able to carry out these functions independent of cell type. In addition, the presence of extracellular AGR3 was confirmed, and its involvement in cell proliferation was demonstrated. Given its effect on tumor growth, this aspect of AGR3 biology is particularly relevant for two reasons: 1. AGR3 may act in a paracrine fashion to enhance proliferation of adjacent cells that do not express it, 2. an assay could be developed to detect extracellular AGR3 for use as a diagnostic or prognostic marker in prostate cancer.

Taken together, the findings of this study establish the importance of AGR3 in prostate cancer biology, and rationalize further consideration of this protein as a potential marker of prostate cancer progression.

7. **References**

1. Jemal, A., F. Bray, M.M. Center, J. Ferlay, E. Ward, and D. Forman, *Global cancer statistics.* CA Cancer J Clin, 2011. **61**(2): p. 69-90.

2. Cinar, B., N.K. Mukhopadhyay, G. Meng, and M.R. Freeman, *Phosphoinositide 3-kinase-independent non-genomic signals transit from the androgen receptor to Akt1 in membrane raft microdomains.* Journal of Biological Chemistry, 2007. **282**(40): p. 29584-29593.

3. Mabjeesh, N.J., M.T. Willard, C.E. Frederickson, H. Zhong, and J.W. Simons, *Androgens stimulate hypoxia-inducible factor 1 activation via autocrine loop of tyrosine kinase receptor/phosphatidylinositol 3'-kinase/protein kinase B in prostate cancer cells.* Clinical Cancer Research, 2003. **9**(7): p. 2416-2425.

4. Xu, Y., S.-Y. Chen, K.N. Ross, and S.P. Balk, *Androgens induce prostate cancer cell proliferation through mammalian target of rapamycin activation and post-transcriptional increases in cyclin D proteins.* Cancer research, 2006. **66**(15): p. 7783-7792.

5. Comstock, C.E. and K.E. Knudsen, *The complex role of AR signaling after cytotoxic insult: implications for cell-cycle-based chemotherapeutics.* Cell Cycle, 2007. **6**(11): p. 1307-13.

6. Denis, L.J. and K. Griffiths, *Endocrine treatment in prostate cancer.* Semin Surg Oncol, 2000. **18**(1): p. 52-74.

7. Buttyan, R., M.A. Ghafar, and A. Shabsigh, *The effects of androgen deprivation on the prostate gland: cell death mediated by vascular regression.* Curr Opin Urol, 2000. **10**(5): p. 415-20.

8. Buttyan, R., A. Shabsigh, H. Perlman, and M. Colombel, *Regulation of Apoptosis in the Prostate Gland by Androgenic Steroids.* Trends Endocrinol Metab, 1999. **10**(2): p. 47-54.

9. Edwards, J., N.S. Krishna, K.M. Grigor, and J.M. Bartlett, *Androgen receptor gene amplification and protein expression in hormone refractory prostate cancer.* Br J Cancer, 2003. **89**(3): p. 552-6.

10. Waltering, K.K., A. Urbanucci, and T. Visakorpi, *Androgen receptor (AR) aberrations in castration-resistant prostate cancer.* Mol Cell Endocrinol, 2012. **360**(1-2): p. 38-43.

11. Shiota, M., A. Yokomizo, N. Fujimoto, and S. Naito, *Androgen receptor cofactors in prostate cancer: potential therapeutic targets of castration-resistant prostate cancer.* Curr Cancer Drug Targets, 2011. **11**(7): p. 870-81.

12. Merseburger, A.S., J. Bellmunt, C. Jenkins, C. Parker, J.M. Fitzpatrick, and G. European Treatment Practices, *Perspectives on treatment of*

metastatic castration-resistant prostate cancer. Oncologist, 2013. **18**(6): p. 775.

13. Taylor, B.S., N. Schultz, H. Hieronymus, A. Gopalan, Y. Xiao, B.S. Carver, V.K. Arora, P. Kaushik, E. Cerami, B. Reva, Y. Antipin, N. Mitsiades, T. Landers, I. Dolgalev, J.E. Major, M. Wilson, N.D. Socci, A.E. Lash, A. Heguy, J.A. Eastham, H.I. Scher, V.E. Reuter, P.T. Scardino, C. Sander, C.L. Sawyers, and W.L. Gerald, *Integrative genomic profiling of human prostate cancer.* Cancer Cell, 2010. **18**(1): p. 11-22.

14. Dong, J.T., *Chromosomal deletions and tumor suppressor genes in prostate cancer.* Cancer Metastasis Rev, 2001. **20**(3-4): p. 173-93.

15. Conley-Lacomb, M.K., A. Saliganan, P. Kandagatla, Y.Q. Chen, M.L. Cher, and S.R. Chinni, *PTEN loss mediated Akt activation promotes prostate tumor growth and metastasis via CXCL12/CXCR4 signaling.* Mol Cancer, 2013. **12**(1): p. 85.

16. Mulholland, D.J., L.M. Tran, Y. Li, H. Cai, A. Morim, S. Wang, S. Plaisier, I.P. Garraway, J. Huang, T.G. Graeber, and H. Wu, *Cell autonomous role of PTEN in regulating castration-resistant prostate cancer growth.* Cancer Cell, 2011. **19**(6): p. 792-804.

17. Kim, J., I.E. Eltoum, M. Roh, J. Wang, and S.A. Abdulkadir, *Interactions between cells with distinct mutations in c-MYC and Pten in prostate cancer.* PLoS Genet, 2009. **5**(7): p. e1000542.

18. Ellwood-Yen, K., T.G. Graeber, J. Wongvipat, M.L. Iruela-Arispe, J. Zhang, R. Matusik, G.V. Thomas, and C.L. Sawyers, *Myc-driven murine prostate cancer shares molecular features with human prostate tumors.* Cancer Cell, 2003. **4**(3): p. 223-38.

19. Gartel, A.L. and K. Shchors, *Mechanisms of c-myc-mediated transcriptional repression of growth arrest genes.* Exp Cell Res, 2003. **283**(1): p. 17-21.

20. Iwata, T., D. Schultz, J. Hicks, G.K. Hubbard, L.N. Mutton, T.L. Lotan, C. Bethel, M.T. Lotz, S. Yegnasubramanian, W.G. Nelson, C.V. Dang, M. Xu, U. Anele, C.M. Koh, C.J. Bieberich, and A.M. De Marzo, *MYC overexpression induces prostatic intraepithelial neoplasia and loss of Nkx3.1 in mouse luminal epithelial cells.* PLoS One, 2010. **5**(2): p. e9427.

21. Emmert-Buck, M.R., C.D. Vocke, R.O. Pozzatti, P.H. Duray, S.B. Jennings, C.D. Florence, Z. Zhuang, D.G. Bostwick, L.A. Liotta, and W.M. Linehan, *Allelic loss on chromosome 8p12-21 in microdissected prostatic intraepithelial neoplasia.* Cancer Res, 1995. **55**(14): p. 2959-62.

22. Haggman, M.J., K.J. Wojno, C.P. Pearsall, and J.A. Macoska, *Allelic loss of 8p sequences in prostatic intraepithelial neoplasia and carcinoma.* Urology, 1997. **50**(4): p. 643-7.

23. He, W.W., P.J. Sciavolino, J. Wing, M. Augustus, P. Hudson, P.S. Meissner, R.T. Curtis, B.K. Shell, D.G. Bostwick, D.J. Tindall, E.P. Gelmann, C. Abate-Shen, and K.C. Carter, *A novel human prostate-specific, androgen-regulated homeobox gene (NKX3.1) that maps to 8p21, a region frequently deleted in prostate cancer.* Genomics, 1997. **43**(1): p. 69-77.

24. Bhatia-Gaur, R., A.A. Donjacour, P.J. Sciavolino, M. Kim, N. Desai, P. Young, C.R. Norton, T. Gridley, R.D. Cardiff, G.R. Cunha, C. Abate-Shen, and M.M. Shen, *Roles for Nkx3.1 in prostate development and cancer.* Genes Dev, 1999. **13**(8): p. 966-77.

25. Kunderfranco, P., M. Mello-Grand, R. Cangemi, S. Pellini, A. Mensah, V. Albertini, A. Malek, G. Chiorino, C.V. Catapano, and G.M. Carbone, *ETS transcription factors control transcription of EZH2 and epigenetic silencing of the tumor suppressor gene Nkx3.1 in prostate cancer.* PLoS One, 2010. **5**(5): p. e10547.

26. Varambally, S., S.M. Dhanasekaran, M. Zhou, T.R. Barrette, C. Kumar-Sinha, M.G. Sanda, D. Ghosh, K.J. Pienta, R.G. Sewalt, A.P. Otte, M.A. Rubin, and A.M. Chinnaiyan, *The polycomb group protein EZH2 is involved in progression of prostate cancer.* Nature, 2002. **419**(6907): p. 624-9.

27. Bachmann, I.M., O.J. Halvorsen, K. Collett, I.M. Stefansson, O. Straume, S.A. Haukaas, H.B. Salvesen, A.P. Otte, and L.A. Akslen, *EZH2 expression is associated with high proliferation rate and aggressive tumor subgroups in cutaneous melanoma and cancers of the endometrium, prostate, and breast.* J Clin Oncol, 2006. **24**(2): p. 268-73.

28. Tomlins, S.A., D.R. Rhodes, S. Perner, S.M. Dhanasekaran, R. Mehra, X.W. Sun, S. Varambally, X. Cao, J. Tchinda, R. Kuefer, C. Lee, J.E. Montie, R.B. Shah, K.J. Pienta, M.A. Rubin, and A.M. Chinnaiyan, *Recurrent fusion of TMPRSS2 and ETS transcription factor genes in prostate cancer.* Science, 2005. **310**(5748): p. 644-8.

29. Oikawa, T. and T. Yamada, *Molecular biology of the Ets family of transcription factors.* Gene, 2003. **303**: p. 11-34.

30. Yu, J., J. Yu, R.S. Mani, Q. Cao, C.J. Brenner, X. Cao, X. Wang, L. Wu, J. Li, M. Hu, Y. Gong, H. Cheng, B. Laxman, A. Vellaichamy, S. Shankar, Y. Li, S.M. Dhanasekaran, R. Morey, T. Barrette, R.J. Lonigro, S.A. Tomlins, S. Varambally, Z.S. Qin, and A.M. Chinnaiyan, *An integrated network of androgen receptor, polycomb, and TMPRSS2-ERG gene fusions in prostate cancer progression.* Cancer Cell, 2010. **17**(5): p. 443-54.

31. Zhang, J.S., A. Gong, J.C. Cheville, D.I. Smith, and C.Y. Young, *AGR2, an androgen-inducible secretory protein overexpressed in prostate cancer.* Genes Chromosomes Cancer, 2005. **43**(3): p. 249-59.

32. Bu, H., S. Bormann, G. Schafer, W. Horninger, P. Massoner, A. Neeb, V.K. Lakshmanan, D. Maddalo, A. Nestl, H. Sultmann, A.C. Cato, and H.

Klocker, *The anterior gradient 2 (AGR2) gene is overexpressed in prostate cancer and may be useful as a urine sediment marker for prostate cancer detection.* Prostate, 2011. **71**(6): p. 575-87.

33. Sharma, N.L., C.E. Massie, A. Ramos-Montoya, V. Zecchini, H.E. Scott, A.D. Lamb, S. MacArthur, R. Stark, A.Y. Warren, I.G. Mills, and D.E. Neal, *The androgen receptor induces a distinct transcriptional program in castration-resistant prostate cancer in man.* Cancer Cell, 2013. **23**(1): p. 35-47.

34. Hu, Z., Y. Gu, B. Han, J. Zhang, Z. Li, K. Tian, C.Y. Young, and H. Yuan, *Knockdown of AGR2 induces cellular senescence in prostate cancer cells.* Carcinogenesis, 2012. **33**(6): p. 1178-86.

35. Patel, P., C. Clarke, D.L. Barraclough, T.A. Jowitt, P.S. Rudland, R. Barraclough, and L.Y. Lian, *Metastasis-promoting anterior gradient 2 protein has a dimeric thioredoxin fold structure and a role in cell adhesion.* J Mol Biol, 2013. **425**(5): p. 929-43.

36. Petek, E., C. Windpassinger, H. Egger, P.M. Kroisel, and K. Wagner, *Localization of the human anterior gradient-2 gene (AGR2) to chromosome band 7p21.3 by radiation hybrid mapping and fluorescencein situ hybridisation.* Cytogenet Cell Genet, 2000. **89**(3-4): p. 141-2.

37. Bu, H., M.R. Schweiger, T. Manke, A. Wunderlich, B. Timmermann, M. Kerick, L. Pasqualini, E. Shehu, C. Fuchsberger, A.C. Cato, and H. Klocker, *Anterior gradient 2 and 3--two prototype androgen-responsive genes transcriptionally upregulated by androgens and by oestrogens in prostate cancer cells.* FEBS J, 2013. **280**(5): p. 1249-66.

38. Aberger, F., G. Weidinger, H. Grunz, and K. Richter, *Anterior specification of embryonic ectoderm: the role of the Xenopus cement gland-specific gene XAG-2.* Mech Dev, 1998. **72**(1-2): p. 115-30.

39. Ivanova, A.S., M.B. Tereshina, G.V. Ermakova, V.V. Belousov, and A.G. Zaraisky, *Agr genes, missing in amniotes, are involved in the body appendages regeneration in frog tadpoles.* Sci Rep, 2013. **3**: p. 1279.

40. Zheng, W., P. Rosenstiel, K. Huse, C. Sina, R. Valentonyte, N. Mah, L. Zeitlmann, J. Grosse, N. Ruf, P. Nurnberg, C.M. Costello, C. Onnie, C. Mathew, M. Platzer, S. Schreiber, and J. Hampe, *Evaluation of AGR2 and AGR3 as candidate genes for inflammatory bowel disease.* Genes Immun, 2006. **7**(1): p. 11-8.

41. Sive, H.L., K. Hattori, and H. Weintraub, *Progressive determination during formation of the anteroposterior axis in Xenopus laevis.* Cell, 1989. **58**(1): p. 171-80.

42. Novoselov, V.V., E.M. Alexandrova, G.V. Ermakova, and A.G. Zaraisky, *Expression zones of three novel genes abut the developing*

anterior neural plate of Xenopus embryo. Gene Expr Patterns, 2003. **3**(2): p. 225-30.

43. Fletcher, G.C., S. Patel, K. Tyson, P.J. Adam, M. Schenker, J.A. Loader, L. Daviet, P. Legrain, R. Parekh, A.L. Harris, and J.A. Terrett, *hAG-2 and hAG-3, human homologues of genes involved in differentiation, are associated with oestrogen receptor-positive breast tumours and interact with metastasis gene C4.4a and dystroglycan.* Br J Cancer, 2003. **88**(4): p. 579-85.

44. Shih, L.J., Y.F. Lu, Y.H. Chen, C.C. Lin, J.A. Chen, and S.P. Hwang, *Characterization of the agr2 gene, a homologue of X. laevis anterior gradient 2, from the zebrafish, Danio rerio.* Gene Expr Patterns, 2007. **7**(4): p. 452-60.

45. Kumar, A., P.B. Gates, and J.P. Brockes, *Positional identity of adult stem cells in salamander limb regeneration.* C R Biol, 2007. **330**(6-7): p. 485-90.

46. Kumar, A., J.W. Godwin, P.B. Gates, A.A. Garza-Garcia, and J.P. Brockes, *Molecular basis for the nerve dependence of limb regeneration in an adult vertebrate.* Science, 2007. **318**(5851): p. 772-7.

47. Kumar, A., J.P. Delgado, P.B. Gates, G. Neville, A. Forge, and J.P. Brockes, *The aneurogenic limb identifies developmental cell interactions underlying vertebrate limb regeneration.* Proc Natl Acad Sci U S A, 2011. **108**(33): p. 13588-93.

48. Thompson, D.A. and R.J. Weigel, *hAG-2, the human homologue of the Xenopus laevis cement gland gene XAG-2, is coexpressed with estrogen receptor in breast cancer cell lines.* Biochem Biophys Res Commun, 1998. **251**(1): p. 111-6.

49. Zhou, M., H.L. Chen, S. Cheng, L. Mei, H.L. Zhang, M. Xie, W.N. Xiong, and Y.J. Xu, *Effect of dexamethasone on expression of AGR2 protein in asthmatic mice.* J Huazhong Univ Sci Technolog Med Sci, 2013. **33**(1): p. 33-6.

50. Zhao, F., R. Edwards, D. Dizon, K. Afrasiabi, J.R. Mastroianni, M. Geyfman, A.J. Ouellette, B. Andersen, and S.M. Lipkin, *Disruption of Paneth and goblet cell homeostasis and increased endoplasmic reticulum stress in Agr2-/- mice.* Dev Biol, 2010. **338**(2): p. 270-9.

51. Park, S.W., G. Zhen, C. Verhaeghe, Y. Nakagami, L.T. Nguyenvu, A.J. Barczak, N. Killeen, and D.J. Erle, *The protein disulfide isomerase AGR2 is essential for production of intestinal mucus.* Proc Natl Acad Sci U S A, 2009. **106**(17): p. 6950-5.

52. Gupta, A., D. Wodziak, M. Tun, D.M. Bouley, and A.W. Lowe, *Loss of anterior gradient 2 (Agr2) expression results in hyperplasia and defective*

lineage maturation in the murine stomach. J Biol Chem, 2013. **288**(6): p. 4321-33.

53. Li, S., Y. Wang, Y. Zhang, M.M. Lu, F.J. DeMayo, J.D. Dekker, P.W. Tucker, and E.E. Morrisey, *Foxp1/4 control epithelial cell fate during lung development and regeneration through regulation of anterior gradient 2.* Development, 2012. **139**(14): p. 2500-9.

54. Norris, A.M., A. Gore, A. Balboni, A. Young, D.S. Longnecker, and M. Korc, *AGR2 is a SMAD4-suppressible gene that modulates MUC1 levels and promotes the initiation and progression of pancreatic intraepithelial neoplasia.* Oncogene, 2012.

55. Verma, S., M.L. Salmans, M. Geyfman, H. Wang, Z. Yu, Z. Lu, F. Zhao, S.M. Lipkin, and B. Andersen, *The estrogen-responsive Agr2 gene regulates mammary epithelial proliferation and facilitates lobuloalveolar development.* Dev Biol, 2012. **369**(2): p. 249-60.

56. Higa, A., A. Mulot, F. Delom, M. Bouchecareilh, D.T. Nguyen, D. Boismenu, M.J. Wise, and E. Chevet, *Role of pro-oncogenic protein disulfide isomerase (PDI) family member anterior gradient 2 (AGR2) in the control of endoplasmic reticulum homeostasis.* J Biol Chem, 2011. **286**(52): p. 44855-68.

57. Gray, T.A., N.J. MacLaine, C.O. Michie, P. Bouchalova, E. Murray, J. Howie, R. Hrstka, M.M. Maslon, R. Nenutil, B. Vojtesek, S. Langdon, L. Hayward, C. Gourley, and T.R. Hupp, *Anterior Gradient-3: a novel biomarker for ovarian cancer that mediates cisplatin resistance in xenograft models.* J Immunol Methods, 2012. **378**(1-2): p. 20-32.

58. Alanen, H.I., R.A. Williamson, M.J. Howard, A.K. Lappi, H.P. Jantti, S.M. Rautio, S. Kellokumpu, and L.W. Ruddock, *Functional characterization of ERp18, a new endoplasmic reticulum-located thioredoxin superfamily member.* J Biol Chem, 2003. **278**(31): p. 28912-20.

59. Gupta, A., A. Dong, and A.W. Lowe, *AGR2 gene function requires a unique endoplasmic reticulum localization motif.* J Biol Chem, 2012. **287**(7): p. 4773-82.

60. Rowe, M.L., L.W. Ruddock, G. Kelly, J.M. Schmidt, R.A. Williamson, and M.J. Howard, *Solution structure and dynamics of ERp18, a small endoplasmic reticulum resident oxidoreductase.* Biochemistry, 2009. **48**(21): p. 4596-606.

61. Norgaard, P. and J.R. Winther, *Mutation of yeast Eug1p CXXS active sites to CXXC results in a dramatic increase in protein disulphide isomerase activity.* Biochem J, 2001. **358**(Pt 1): p. 269-74.

62. Maslon, M.M., R. Hrstka, B. Vojtesek, and T.R. Hupp, *A divergent substrate-binding loop within the pro-oncogenic protein anterior gradient-2 forms a docking site for Reptin.* J Mol Biol, 2010. **404**(3): p. 418-38.

63. Ambolet-Camoit, A., L.C. Bui, S. Pierre, A. Chevallier, A. Marchand, X. Coumoul, M. Garlatti, K. Andreau, R. Barouki, and M. Aggerbeck, *2,3,7,8-tetrachlorodibenzo-p-dioxin counteracts the p53 response to a genotoxicant by upregulating expression of the metastasis marker agr2 in the hepatocarcinoma cell line HepG2.* Toxicol Sci, 2010. **115**(2): p. 501-12.

64. Zweitzig, D.R., D.A. Smirnov, M.C. Connelly, L.W. Terstappen, S.M. O'Hara, and E. Moran, *Physiological stress induces the metastasis marker AGR2 in breast cancer cells.* Mol Cell Biochem, 2007. **306**(1-2): p. 255-60.

65. Hong, X.Y., J. Wang, and Z. Li, *AGR2 Expression is Regulated by HIF-1 and Contributes to Growth and Angiogenesis of Glioblastoma.* Cell Biochem Biophys, 2013.

66. Vanderlaag, K.E., S. Hudak, L. Bald, L. Fayadat-Dilman, M. Sathe, J. Grein, and M.J. Janatpour, *Anterior gradient-2 plays a critical role in breast cancer cell growth and survival by modulating cyclin D1, estrogen receptor-alpha and survivin.* Breast Cancer Res, 2010. **12**(3): p. R32.

67. Hurtado, A., K.A. Holmes, C.S. Ross-Innes, D. Schmidt, and J.S. Carroll, *FOXA1 is a key determinant of estrogen receptor function and endocrine response.* Nat Genet, 2011. **43**(1): p. 27-33.

68. Sahu, B., M. Laakso, K. Ovaska, T. Mirtti, J. Lundin, A. Rannikko, A. Sankila, J.P. Turunen, M. Lundin, J. Konsti, T. Vesterinen, S. Nordling, O. Kallioniemi, S. Hautaniemi, and O.A. Janne, *Dual role of FoxA1 in androgen receptor binding to chromatin, androgen signalling and prostate cancer.* EMBO J, 2011. **30**(19): p. 3962-76.

69. Zhang, Y., T.Z. Ali, H. Zhou, D.R. D'Souza, Y. Lu, J. Jaffe, Z. Liu, A. Passaniti, and A.W. Hamburger, *ErbB3 binding protein 1 represses metastasis-promoting gene anterior gradient protein 2 in prostate cancer.* Cancer Res, 2010. **70**(1): p. 240-8.

70. Al Saleh, S., F. Al Mulla, and Y.A. Luqmani, *Estrogen receptor silencing induces epithelial to mesenchymal transition in human breast cancer cells.* PLoS One, 2011. **6**(6): p. e20610.

71. Innes, H.E., D. Liu, R. Barraclough, M.P. Davies, P.A. O'Neill, A. Platt-Higgins, S. de Silva Rudland, D.R. Sibson, and P.S. Rudland, *Significance of the metastasis-inducing protein AGR2 for outcome in hormonally treated breast cancer patients.* Br J Cancer, 2006. **94**(7): p. 1057-65.

72. Riener, M.O., C. Pilarsky, J. Gerhardt, R. Grutzmann, F.R. Fritzsche, M. Bahra, W. Weichert, and G. Kristiansen, *Prognostic significance of AGR2 in pancreatic ductal adenocarcinoma.* Histol Histopathol, 2009. **24**(9): p. 1121-8.

73. Fritzsche, F.R., E. Dahl, A. Dankof, M. Burkhardt, S. Pahl, I. Petersen, M. Dietel, and G. Kristiansen, *Expression of AGR2 in non small cell lung cancer.* Histol Histopathol, 2007. **22**(7): p. 703-8.

74. Valladares-Ayerbes, M., M. Blanco-Calvo, M. Reboredo, M.J. Lorenzo-Patino, P. Iglesias-Diaz, M. Haz, S. Diaz-Prado, V. Medina, I. Santamarina, S. Pertega, A. Figueroa, and L.M. Anton-Aparicio, *Evaluation of the Adenocarcinoma-Associated Gene AGR2 and the Intestinal Stem Cell Marker LGR5 as Biomarkers in Colorectal Cancer.* Int J Mol Sci, 2012. **13**(4): p. 4367-87.

75. Fritzsche, F.R., E. Dahl, S. Pahl, M. Burkhardt, J. Luo, E. Mayordomo, T. Gansukh, A. Dankof, R. Knuechel, C. Denkert, K.J. Winzer, M. Dietel, and G. Kristiansen, *Prognostic relevance of AGR2 expression in breast cancer.* Clin Cancer Res, 2006. **12**(6): p. 1728-34.

76. Maresh, E.L., V. Mah, M. Alavi, S. Horvath, L. Bagryanova, E.S. Liebeskind, L.A. Knutzen, Y. Zhou, D. Chia, A.Y. Liu, and L. Goodglick, *Differential expression of anterior gradient gene AGR2 in prostate cancer.* BMC Cancer, 2010. **10**: p. 680.

77. Darb-Esfahani, S., F. Fritzsche, G. Kristiansen, W. Weichert, J. Sehouli, I. Braicu, M. Dietel, and C. Denkert, *Anterior gradient protein 2 (AGR2) is an independent prognostic factor in ovarian high-grade serous carcinoma.* Virchows Arch, 2012. **461**(2): p. 109-16.

78. Wang, Z., Y. Hao, and A.W. Lowe, *The adenocarcinoma-associated antigen, AGR2, promotes tumor growth, cell migration, and cellular transformation.* Cancer Res, 2008. **68**(2): p. 492-7.

79. Pohler, E., A.L. Craig, J. Cotton, L. Lawrie, J.F. Dillon, P. Ross, N. Kernohan, and T.R. Hupp, *The Barrett's antigen anterior gradient-2 silences the p53 transcriptional response to DNA damage.* Mol Cell Proteomics, 2004. **3**(6): p. 534-47.

80. Hrstka, R., R. Nenutil, A. Fourtouna, M.M. Maslon, C. Naughton, S. Langdon, E. Murray, A. Larionov, K. Petrakova, P. Muller, M.J. Dixon, T.R. Hupp, and B. Vojtesek, *The pro-metastatic protein anterior gradient-2 predicts poor prognosis in tamoxifen-treated breast cancers.* Oncogene, 2010. **29**(34): p. 4838-47.

81. Park, K., Y.J. Chung, H. So, K. Kim, J. Park, M. Oh, M. Jo, K. Choi, E.J. Lee, Y.L. Choi, S.Y. Song, D.S. Bae, B.G. Kim, and J.H. Lee, *AGR2, a mucinous ovarian cancer marker, promotes cell proliferation and migration.* Exp Mol Med, 2011. **43**(2): p. 91-100.

82. Liu, D., P.S. Rudland, D.R. Sibson, A. Platt-Higgins, and R. Barraclough, *Human homologue of cement gland protein, a novel metastasis inducer associated with breast carcinomas.* Cancer Res, 2005. **65**(9): p. 3796-805.

83. Ramachandran, V., T. Arumugam, H. Wang, and C.D. Logsdon, *Anterior gradient 2 is expressed and secreted during the development of pancreatic cancer and promotes cancer cell survival.* Cancer Res, 2008. **68**(19): p. 7811-8.

84. King, E.R., C.S. Tung, Y.T. Tsang, Z. Zu, G.T. Lok, M.T. Deavers, A. Malpica, J.K. Wolf, K.H. Lu, M.J. Birrer, S.C. Mok, D.M. Gershenson, and K.K. Wong, *The anterior gradient homolog 3 (AGR3) gene is associated with differentiation and survival in ovarian cancer.* Am J Surg Pathol, 2011. **35**(6): p. 904-12.

85. Vaarala, M.H., P. Hirvikoski, S. Kauppila, and T.K. Paavonen, *Identification of androgen-regulated genes in human prostate.* Mol Med Rep, 2012. **6**(3): p. 466-72.

86. Agell, L., S. Hernandez, L. Nonell, M. Lorenzo, E. Puigdecanet, S. de Muga, N. Juanpere, R. Bermudo, P.L. Fernandez, J.A. Lorente, S. Serrano, and J. Lloreta, *A 12-gene expression signature is associated with aggressive histological in prostate cancer: SEC14L1 and TCEB1 genes are potential markers of progression.* Am J Pathol, 2012. **181**(5): p. 1585-94.

87. Olmos, D., D. Brewer, J. Clark, D.C. Danila, C. Parker, G. Attard, M. Fleisher, A.H. Reid, E. Castro, S.K. Sandhu, L. Barwell, N.B. Oommen, S. Carreira, C.G. Drake, R. Jones, C.S. Cooper, H.I. Scher, and J.S. de Bono, *Prognostic value of blood mRNA expression signatures in castration-resistant prostate cancer: a prospective, two-stage study.* Lancet Oncol, 2012. **13**(11): p. 1114-24.

88. Abate-Shen, C. and M.M. Shen, *Molecular genetics of prostate cancer.* Genes Dev, 2000. **14**(19): p. 2410-34.

89. Vanaja, D.K., J.C. Cheville, S.J. Iturria, and C.Y. Young, *Transcriptional silencing of zinc finger protein 185 identified by expression profiling is associated with prostate cancer progression.* Cancer Res, 2003. **63**(14): p. 3877-82.

90. Biolabs, N.E. *RheoSwitch Mammalian Inducible Expression System.* Instruction Manual 2007 [cited 2013 September, 2013]; Available from: http://66.155.211.155/nebecomm/ManualFiles/manualE3000.pdf.

91. Webb, D.J., J.T. Parsons, and A.F. Horwitz, *Adhesion assembly, disassembly and turnover in migrating cells -- over and over and over again.* Nat Cell Biol, 2002. **4**(4): p. E97-100.

92. Subramanian, A., P. Tamayo, V.K. Mootha, S. Mukherjee, B.L. Ebert, M.A. Gillette, A. Paulovich, S.L. Pomeroy, T.R. Golub, E.S. Lander, and J.P. Mesirov, *Gene set enrichment analysis: a knowledge-based approach for interpreting genome-wide expression profiles.* Proc Natl Acad Sci U S A, 2005. **102**(43): p. 15545-50.

93. Brezillon, S., A. Radwanska, C. Zeltz, A. Malkowski, D. Ploton, H. Bobichon, C. Perreau, M. Malicka-Blaszkiewicz, F.X. Maquart, and Y. Wegrowski, *Lumican core protein inhibits melanoma cell migration via alterations of focal adhesion complexes.* Cancer Lett, 2009. **283**(1): p. 92-100.

94. Zeltz, C., S. Brezillon, J. Kapyla, J.A. Eble, H. Bobichon, C. Terryn, C. Perreau, C.M. Franz, J. Heino, F.X. Maquart, and Y. Wegrowski, *Lumican inhibits cell migration through alpha2beta1 integrin.* Exp Cell Res, 2010. **316**(17): p. 2922-31.

95. Malinowski, M., K. Pietraszek, C. Perreau, M. Boguslawski, V. Decot, J.F. Stoltz, L. Vallar, J. Niewiarowska, C. Cierniewski, F.X. Maquart, Y. Wegrowski, and S. Brezillon, *Effect of lumican on the migration of human mesenchymal stem cells and endothelial progenitor cells: involvement of matrix metalloproteinase-14.* PLoS One, 2012. **7**(12): p. e50709.

96. Nikitovic, D., G. Chalkiadaki, A. Berdiaki, J. Aggelidakis, P. Katonis, N.K. Karamanos, and G.N. Tzanakakis, *Lumican regulates osteosarcoma cell adhesion by modulating TGFbeta2 activity.* Int J Biochem Cell Biol, 2011. **43**(6): p. 928-35.

97. Coulson-Thomas, V.J., Y.M. Coulson-Thomas, T.F. Gesteira, C.A. Andrade de Paula, C.R. Carneiro, V. Ortiz, L. Toma, W.W. Kao, and H.B. Nader, *Lumican expression, localization and antitumor activity in prostate cancer.* Exp Cell Res, 2013. **319**(7): p. 967-81.

98. Levine, C.G., D. Mitra, A. Sharma, C.L. Smith, and R.S. Hegde, *The efficiency of protein compartmentalization into the secretory pathway.* Mol Biol Cell, 2005. **16**(1): p. 279-91.

99. Kober, F.X., W. Koelmel, J. Kuper, J. Drechsler, C. Mais, H.M. Hermanns, and H. Schindelin, *The crystal structure of the protein-disulfide isomerase family member ERp27 provides insights into its substrate binding capabilities.* J Biol Chem, 2013. **288**(3): p. 2029-39.

100. Grek, C. and D. Townsend, *Protein Disulfide Isomerase Superfamily in Disease and the Regulation of Apoptosis.* Endoplasmic Reticulum Stress in Cancers. **1**: p. 4-17.

101. Raykhel, I., H. Alanen, K. Salo, J. Jurvansuu, V.D. Nguyen, M. Latva-Ranta, and L. Ruddock, *A molecular specificity code for the three mammalian KDEL receptors.* J Cell Biol, 2007. **179**(6): p. 1193-204.

102. Lee, A.S., *The ER chaperone and signaling regulator GRP78/BiP as a monitor of endoplasmic reticulum stress.* Methods, 2005. **35**(4): p. 373-81.

103. Kani, K., P.D. Malihi, Y. Jiang, H. Wang, Y. Wang, D.L. Ruderman, D.B. Agus, P. Mallick, and M.E. Gross, *Anterior gradient 2 (AGR2): blood-based biomarker elevated in metastatic prostate cancer associated with the neuroendocrine phenotype.* Prostate, 2013. **73**(3): p. 306-15.

104. Bormann, S., *Anterior Gradient 2 Genprodukte als Marker und Regulatoren der Prostatakrebsprogression*, 2012, Karlsruhe, Karlsruher Institut für Technologie (KIT), Diss., 2012.

105. Seomun, Y. and C.K. Joo, *Lumican induces human corneal epithelial cell migration and integrin expression via ERK 1/2 signaling.* Biochem Biophys Res Commun, 2008. **372**(1): p. 221-5.

106. Grover, J., C.Y. Liu, W.W. Kao, and P.J. Roughley, *Analysis of the human lumican gene promoter.* J Biol Chem, 2000. **275**(52): p. 40967-73.

ACKNOWLEDGEMENT

I would like to express my gratitude to Prof. Andrew Cato, my supervisor, for giving me the opportunity to carry out this work in his lab, the patient guidance through the years, and the vital critique of this work. Of the broad range of topics taught, I am particularly grateful for the in-depth knowledge received in the principles of gene expression, a trademark of all the alumni of his lab.

I would also like to thank Dr. Antje Neeb, my second supervisor, whose broad expertise enabled multiple aspects of this project. She has provided a constant supply of encouragement and a standard of scientific research to strive for.

I would also like to thank the members of my thesis advisory committee, especially Dr. Thomas Dickmeis, for the prompt and useful review of my work, as well as Prof. Jörg Kämper for agreeing to be my koreferent.

Over three years ago I set on a very long journey to characterize the function of a rather small protein. This document attempts to tell the tale of this long process. It cannot however duly account for that fact that I would not have come this far without help from the fantastic group of individuals populating labs 109 and 114 at IT*G* through the years. The following is a futile attempt to convey the true extent my gratitude to my fellow lab members.

For the copious and free-flowing help with all things “lab”, including the frequent and generous application of delicious pastries, cookies, and fruit to the neglecting student, I would like to extend a special thanks Rebecca Seeger.

In the same spirit, I would like thank my other partners in crime, Katja, Jutta, Anne, Steffi, Manu, Tobi, Emml, Danilo, and David. Remember guys, I know where the bodies are buried.

I would also like to acknowledge the help of Christoph Dittus who masterfully fixed my favorite protein electrophoresis equipment. Keep up the good work. I owe you beer.

Last but NOT least, I would like to extend a special thanks and acknowledge the constant support coming from the lovely producers, directors, and support cast of my show: Mira, Agron, Eriola, and Marie. I intend to spend the rest of my days showing you just how much you mean to me. Prepare to be seriously annoyed.

In a change of pace, I would like to apologize to the 4 am cleaning lady, who received multiple heart-attacks from finding me still in the lab every now and then. Its over, but stay insured anyway.

This work is dedicated to those who find pleasure in discovery.

PUBLICATIONS

Articles

Bu H, Schweiger MR, Manke T, Wunderlich A, Timmermann B, Kerick M, Pasqualini L, **Shehu E**, Fuchsberger C, Cato AC *et al*: Anterior gradient 2 and 3--two prototype androgen-responsive genes transcriptionally upregulated by androgens and by oestrogens in prostate cancer cells. *The FEBS journal* 2013, **280**(5):1249-1266.

Book chapters

Harvey A: **Cancer Cell Signalling**: John Wiley & Sons; 2013.
"Insulin and the insulin-like growth factor (IGF) family"
Maria Thorpe, **Erald Shehu** and Amanda Harvey

Abstracts (poster of the same title presented in conference)

20th Meeting of the EAU (European Association of Eurology) Section of Urological Research (ESUR)
"Regulation of the pioneer factor FoxA1 by anterior gradient 2 protein in androgen receptor-mediated gene expression in prostate cancer cells."
Shehu E.[1], Saha D.[1], Bormann S.[1], Bu H.[2], Klocker H.[2], Neeb A.[1], Cato, A.C.B[1]
[1] Karlsruhe Institute of Technology, Institute of Toxicology and Genetics, Eggenstein-Leopoldshafen, Germany
[2]Department of Urology, Division of Experimental Urology, Innsbruck Medical University, Innsbruck, Austria

9th World Congress on Urological Research, 15-17th of September 2011 in Innsbruck, Austria
"Expression levels of Anterior Gradient homologue 3 protein distinguish between proliferative and migratory properties of prostate cancer cells."
Shehu E., Bormann S., Sperlich J., Neeb A., Cato A.C.B. Karlsruhe Institute of Technology, Institute of Toxicology and Genetics, Eggenstein-Leopoldshafen, Germany